# A MODEL FOR THE SHORT RANGE NUCLEAR FORCE

Melinda Swift B.Sc.(Hons.)

A thesis submitted in fulfillment of the
requirements for the degree of
Doctor of Philosophy
at the
University of Adelaide

Department of Physics and Mathematical Physics
University of Adelaide
South Australia

October 1992

# Contents

# List of Figures

# List of Tables

# Abstract

It has long been believed that meson exchange processes are responsible for the long distance part of the nucleon-nucleon (N-N) interaction. However, at short range the theoretical origin of the interaction is still unclear. Attempts have been made to understand the short range part of the interaction using quark dynamics. Most of these have assumed a One Gluon Exchange (OGE) mechanism to produce the force. This has not been entirely successful, especially in the tensor case, where it gives rise to a smaller force than observed.

In our approach we study the N-N interaction assuming the quarks couple directly to the pion. We use a Born-Oppenheimer approximation for the N-N force and treat the two nucleons as a six quark non-relativistic wave function. The six quark wave function is obtained by antisymmetrisation of the product of two single nucleon wave functions. Due to the short distances involved it is also possible to get quark exchange between the nucleons. There are no free parameters used in this model, they are fixed either by N-N scattering (coupling constant) or hadron spectroscopy (nucleon size).

In presenting our results we find that the Quark Pion Coupling Potential (QPCP) has a more complicated structure than the standard One Pion Exchange Potential at short range. We find that at short range there is repulsion whereas at intermediate range there is attraction. We examine these results and give a detailed picture of the contributions arising in each of the spin-isospin channels .

# Declaration

Except as stated herein this thesis contains no material which has been accepted for the award of any other degree or diploma in any University. To the best of my knowledge and belief, this thesis contains no copy or paraphrase of previous material previously published or written by any other person, except where due reference is made in the text of this thesis.

I give consent to this copy of my thesis, when deposited in the University Library, being available for loan and photocopying.

Melinda Swift

# Acknowledgements

I would like to firstly thank my supervisor Prof A. W. Thomas without whose encouragement and support I would never have undertaken this work. I would also like to thank all my colleagues who, over the years contributed to this work, especially Dr K. Holinde, Dr G. Liu for his help, collaboration and for supplying me with much of the data for the plots shown, Dr A. Rawlinson for his proofreading and everyone at the Physics department too numerous to mention. I would like to especially thank my parents for their love and support and a very special thanks to my husband John without whom I would never have made it through, not only with his love and support but also for the diagrams contained in this thesis.

# Chapter 1

# Introduction

The history of quarks and their role in the modelling of nucleon structure is explored. We look at Quantum Chromo Dynamics (QCD) and its relationship to our understanding of nuclear structure. In particular, from QCD one can motivate a non-relativistic quark model which can be applied to the problem of short range nuclear structure. Many other models exist, for example the bag model and soliton models, but for the purpose of our work we are interested in the model defined as the constituent quark model (CQM).

## 1.1 History

In 1964-5 Gell-Mann [Gel64] and Zweig [Zwe64] proposed the idea of quarks to simplify the bookkeeping of elementary particles. Quarks are the fundamental spin $\frac{1}{2}$ particles which are thought to be the building blocks of all strongly interacting particles. The quote from James Joyce's Finnegans Wake " The palpitant, piping, chirrup, crook and quark" inspired Gell-Mann to choose the name quark for the fundamental fields that he had put forward.

The eightfold way was one of the first steps in understanding particle physics. Gell-Mann [Gel64] and Zweig [Zwe64] proposed the existence of the fundamental representation of the symmetry group SU(3) - flavour. From this comes Quantum Chromodynamics

(QCD) which is considered by most as the theory of strong interactions. Colour was assigned as a quantum number when it seemed the Pauli principle would be violated in the $\Delta^{++}$ - three identical up quarks with spin up in the same spatial orbit.

Within the framework of QCD the apparently arbitrary addition of colour as a property of quarks becomes an essential element. By demanding that the theory should be invariant under arbitrary transformations amongst the colours at each point in space-time, one arrives at a very powerful dynamical theory. Just as in electromagnetism the gauge principle based on U(1) demands the existence of massless vector photons, QCD based on SU(3), has eight massless gluons which mediate the strong interaction [MaPa78] [AbLe73].

An acceptable microscopic description of nuclear physics should involve quarks explicitly. This means we have to use a phenomenological model of hadron structure. This model should incorporate as much as possible of the properties of QCD.

## 1.2 Quantum Chromodynamics

QCD has three major properties. The first is asymptotic freedom, which means that the fine stucture constant $\alpha(Q^2)$ decreases logarithmically. At the one loop level

$$\alpha(Q^2) = \frac{4\pi}{(11 - \frac{2}{3}n_f)ln(\frac{Q^2}{\Lambda^2})} \tag{1.1}$$

with $n_f$ the number of quark flavours and $\Lambda$ the scale parameter. The proof relies on renormalisation group arguments. The weak decrease of the coupling constant at high energy is the main justification of the success of the quark- parton description of Deep Inelastic Scattering (DIS). This implies that for very high energies it is a good approximation to treat the quarks inside hadrons as free particles.

The second property which is widely accepted but not rigourously proven is that the quarks are confined to colour singlet configurations only. That is, if we start with a bound

q-$\bar{q}$ pair and try to move them apart the energy of the system rises approximately linearly. The pair can only be free of each other at finite energy by making another q-$\bar{q}$ pair in between and hence two colour singlet pairs. The ground state of a gauge theory can have three possible modes, the coulomb mode, the Higgs mode and the confinement mode. The ground state of QCD is in the confinement mode. This is characterised by confined quarks and screened, zero mass gluons. An indication of permanent quark confinement comes from the fact that the running coupling constant of QCD (1.1) becomes infinite as the momentum transfer approaches the scale parameter $\lambda^2$, but in this region the renormalisation group treatment is not valid as it is not in the perturbative regime.

The third and last property is that at least for the first three flavours, the quark masses seem to be very light [Pa75, GaLe] . In fact, with $(m_u + m_d)/2$ less than 10 MeV, which is very small compared to typical hadronic masses, QCD has an almost exact chiral symmetry. That is, in the limit $m_d = m_u = 0$ there is no interaction which can mix left-handed with right-handed fermions hence the notation $SU(2)_L \times SU(2)_R$. In such a theory the Goldstone theorem says there are two choices. One is that for every eigenstate of the theory there is a degenerate partner of opposite parity. The other is that the symmetry of the vacuum is broken and massless pseudoscalar bosons appear. For $SU(2)_L \times SU(2)_R$ this Goldstone boson is the pion.

In a non Abelian gauge theory such as QCD the gluons also carry colour charge. As a consequence, a virtual gluon emitted from a quark not only sees the colour charge of another quark, diagram (a) in Fig 1.1 and of a virtual quark-antiquark pair (b) but also the colour charge of the gluons (c). The combined effect of the Feynman diagrams in Fig 1.1 yields the effective quark-quark coupling constant

$$\begin{aligned} \alpha_s(Q^2) &= \frac{g_s^2(Q^2)}{4\pi} \\ &= \alpha_s^{(0)}\left[1 - \frac{2}{3} f \frac{\alpha_s^{(0)}}{4\pi} ln\frac{\Lambda^2}{Q^2} + 11\frac{\alpha_s^{(0)}}{4\pi} ln\frac{\Lambda^2}{Q^2}\right] \end{aligned} \tag{1.2}$$

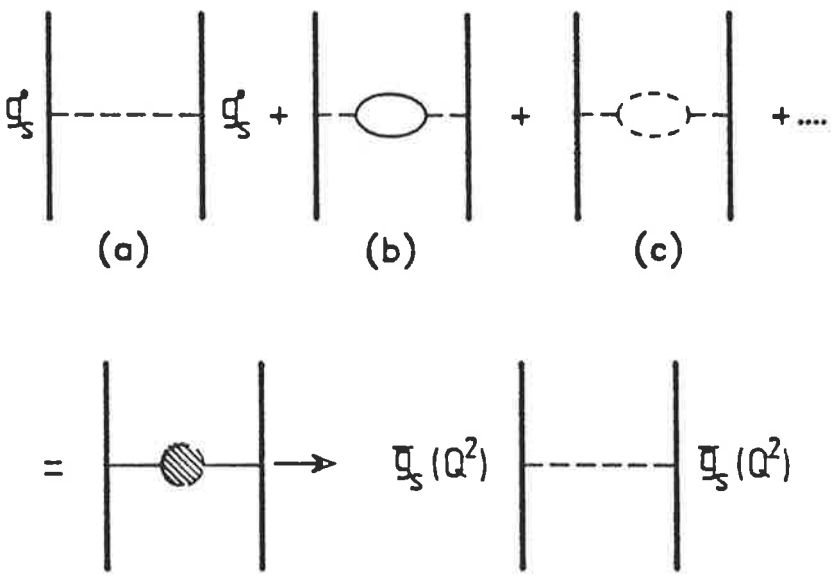


Figure 1.1: Diagrams which contribute to second order in $g_s^0$ to the running coupling constant $g_s(Q^2)$. The virtual gluon emitted from a quark see the colour charge of another quark (a), the quark- antiquark pair (b) and the colour charge of the virtual gluon (c). [Fla82]

where

$$\alpha_s^{(0)} = \frac{(g_s^0)^2}{4\pi} \tag{1.3}$$

and $g_s^0$ is the bare quark-gluon coupling constant, f is the number of quark flavours which contribute at the corresponding energy; $Q^2$ is the space like momentum transfer carried by the virtual gluon and L is the cutoff parameter. The second term is the contribution of the virtual quark-antiquark pairs. This term is negative and leads to charge screening. The third term comes from the virtual gluon loop. It is positive and gives antiscreening. The appearance of these two competing terms of opposite sign is a peculiarity of nonAbelian gauge theories. In an Abelian gauge theory like QED the gauge boson carries no charge and there is no trilinear coupling of the gauge boson.

Due to its complexity we do not actually use QCD, but rather models which incorporate its main features, namely :

- confinement
- asymptotic freedom
- chiral symmetry

## 1.3 The Non-Relativistic Quark Model

One of the earliest and probably most widely successful QCD motivated models is the non-relativistic quark model (NRQM) [DeR+75] [Is80]. This model is an "effective" theory, once removed from QCD, in that the u and d masses are of the order of 300 MeV. This means the quarks are considered to be dressed by higher order processes. Confinement is incorporated through a phenomenological potential and the hyperfine q-q interaction arising from the one gluon exchange is then obtained as an expansion in powers of v/c. By the nature of the construction of the model it is not intended to include asymptotic freedom, neither does the notion of chiral symmetry appear as a natural consequence. Through asymptotic freedom, the effective quark-gluon coupling of colour dynamics becomes weaker at short distances. This property is expected to make the NN interaction accesible to a perturbative treatment at short range. At larger distances when the nucleons no longer overlap the quark-gluon degrees of freedom are effectively frozen in by colour confinement. Here meson exchange gives a good parameterisation of the low and medium energy phenomenology.

Liberman [Lib77] introduces the idea of the non- relativistic quark model (NRQM) (although it wasn't labelled this way until later). The model was brought about to describe the short range nuclear force. There was already the idea that the nuclear forces arose directly from the interaction of quarks and the forces which confine them in the nucleons. This idea was also advocated by Johnson [Jo75] and others who developed the bag model. The only drawback with this model was that it didn't provide a simple treatment for the

two body problem.

The model of Schnitzer [Schn75] was used to construct a wave function according to the prescriptions given by Feynman, Kislinger and Ravndal [Fey71]. The colour wave function is antisymmetric, the spin-unitary-spin wave functions are symmetric and the space wave function is a gaussian or simple harmonic oscillator.

In describing the interactions of the two nucleons close together by using space wave functions for the quarks which are localised about two fixed centers, errors are introduced in not allowing for center of mass corrections. The worst of these are subtracted out of the final result and the rest can be minimised by using a non-variational wave function. Antisymmetric six quark wave functions are then constructed from the three quark wave functions. The space part is

$$G(1..6) = g(123, \frac{R}{2})g(456, -\frac{R}{2}) \pm g(123, -\frac{R}{2})g(456, \frac{R}{2}) \tag{1.4}$$

where

$$g(123, \frac{R}{2}) = exp\{-\frac{\beta^2}{2}[(r_1 - \frac{R}{2})^2 + (r_2 - \frac{R}{2})^2 + (r_3 - \frac{R}{2})^2]\} \tag{1.5}$$

and R is the distance between the centers of the two nucleons and $r_i$ are the co-ordinates of the individual quarks.

In early developments of the quark model, the colour property permitted the necessary antisymmetry in the ground state of the baryon species to conserve the Fermi character of the quarks. This is described in the Young tableau as $[f] = [111]$. All baryons thus belong to the singlet representation of the SU(3) colour group. It is considered that it is through the colour property that quarks interact strongly. The resulting two-body, effective quark-quark interaction is expected to have the form [DeR+75, DeG+75]

$$V_{qq} = \sum_{i<j} \hat{\lambda}_i \cdot \hat{\lambda}_j v(r_{ij}) \tag{1.6}$$

Here $\hat{\lambda}_i$ is the vector of generating operators for the SU(3) colour group operating on the $i^{th}$ particle with the properties

$$< \lambda_i \cdot \lambda_j >= \begin{cases} -\frac{16}{3} & \text{colour antisymmetric pairs } [f]_c = [11] \\ +\frac{8}{3} & \text{colour symmetric pairs } [f]_c = [2] \end{cases} \tag{1.7}$$

Due to the lack of experimental evidence for the support of free quarks it suggests that within a baryon having only antisymmetric pairs of colour states, the quarks are strongly confined i.e. $-\frac{16}{3}v(r_{ij})$ increases (positively) with distance similar to a harmonic oscillator. It follows that quarks in symmetric colour states are repelled with a strength that grows with distance. According to QCD we have objects with colour (like quarks) which will interact strongly and objects without colour (like leptons) that will not. As all observed baryons are colour singlets they behave at long distances like colourless objects. At intermediate distances the colour distribution within the baryons is revealed and a remnant of the strong interaction between the constituent quarks emerges as an effective interaction between baryons.

# Chapter 2

# The model

In this chapter we will discuss the Born-Oppenheimer approximation from the original idea in 1927 to how it has been incorporated in modern day models. We examine the short range force and the different potentials used to explain it. Previous work in this area includes Oka and Yazaki [Oka84], Holinde [Hol84], Faessler et al. [Faes+82, FaFer83, Faes+83] using One Gluon Exchange, and Fernandez [Fern87] using One Pion Exchange at the quark level. We will consider some of these papers in more detail before advancing to our own work.

## 2.1 Born-Oppenheimer Approximation

It has been shown that the motion of an electron in a field of fixed nuclei leads to energy levels which are functions of the internuclear separation R. These energy levels can be used as potential energy curves to discuss the motion of the nuclei. According to quantum mechanics these curves, Fig 2.1, are an approximate treatment of the problem consisting of a nuclei and electron; or nuclei and electrons in a more complicated case. The Born-Oppenheimer model was introduced in the 1920's as an explanation for the potential curve in the hydrogen molecule ion $H_2^+$.

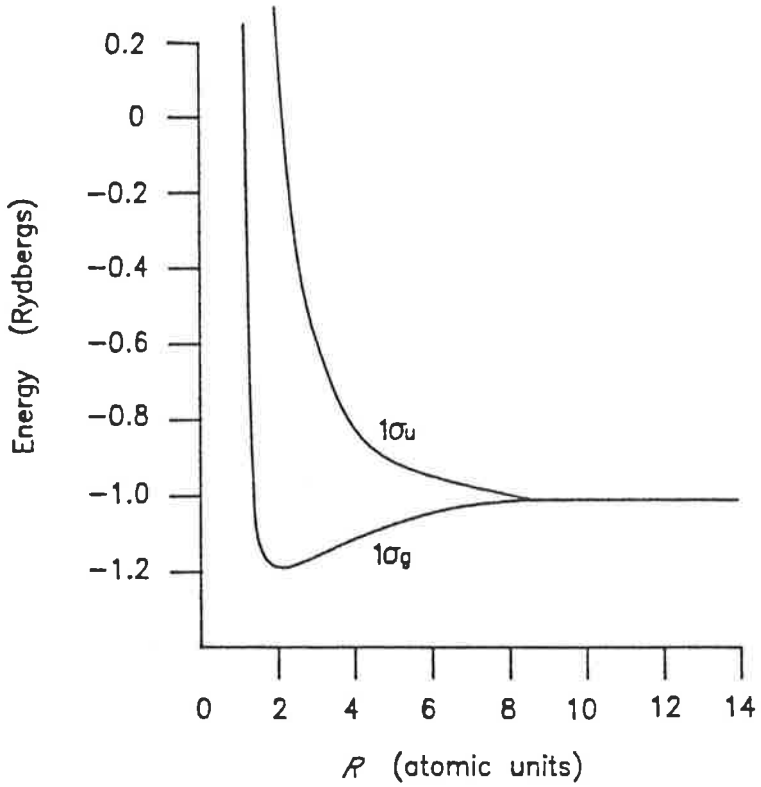


Figure 2.1: The energy curve for the lowest energy levels of $H_2^+$ as a function of internuclear repulsive energy. Figure taken from [Slat63] page 8.

As the name suggests it was put forward by Born and Oppenheimer [BoOp27] and the idea, following the description given by Slater [Slat63] is put forward below. We start with a $H_2^+$ molecule in the 1s (even) state at an internuclear separation corresponding to the minimum of the energy curve Fig 2.1. Now slowly increase the internuclear separation. The electrons move very rapidly about the nuclei, so if the rate of increase of R is slow enough then the electrons will rearrange themselves at each instant as if the nuclear separation was constant. However, as R increases the energy of the system gradually increases. This is from having forces act upon the nuclei doing work on the molecule equal to the force times the displacement. To maintain the nuclei at fixed distances or increasing the distance between them very slowly requires an external force acting on them. This force is equivalent to $\frac{dE}{dR}$ where E is the energy given in Fig 2.1 in order that the force times the displacement $\left(\frac{dE}{dR}\right) dR$ is equal to the increase in energy dE.

If it requires a force of $\frac{dE}{dR}$ from external sources to hold the nuclei in equilibrium then in the absence of such an external force, there is an equal and opposite force $-\frac{dE}{dR}$ acting on the nuclei arising from the electrostatics of the system itself. If there is an attraction between the nuclei as in this case, then it comes about indirectly; without the electron the nuclei would repel each other but with the electronic charge concentrated in the region between the two nuclei, it will attract each nucleus. This attraction can be calculated and more than balances the repulsion between the bare nuclei, resulting in a net attraction. This attraction will set the nuclei into motion, as if the energy E(R) were a potential energy curve for the internuclear motion. Treating this motion according to quantum mechanics implies that we use the energy E(R) as a potential energy function in a Schrödinger equation for the nuclear motion. We must remember that E(R) is really not just a potential energy, it also includes the kinetic energy of the electronic motion which automatically changes as the distance R changes, just as the potential energy does.

### 2.1.1 The Heitler-London Method

Shortly after Heisenberg wrote his paper [He26, He26, He26] on the two electron problem Heitler and London proposed their method for treating the hydrogen molecule [HeLo26]. They used the idea of starting with atomic orbitals in setting up an approximate solution for the hydrogen molecule. The following description [Slat63] outlines the method proposed by them. Let A represent a hydrogen 1s wave function about atom A and B a hydrogen 1s wave function about atom B. Let the coordinates of the two electrons be denoted by 1 and 2. When the atoms are widely separated, the ground state will correspond to the situation where 1 electron is on one atom and the other on the other atom. Thus it can be represented by the wave function A(1)B(2). This could easily be written as A(2)B(1), as Heisenberg pointed out; these two wave functions will be degenerate with each other. When we solve a perturbation problem between these two functions we find that the

suitable linear combinations are the sum and the difference; $A(1)B(2) \pm A(2)B(1)$ which are symmetric and antisymmetric respectively in the coordinates of the electrons. We find that the symmetric function has an energy curve similar to the attractive potential curve $1\sigma_g$ of Fig 2.1 while the antisymmetric function indicates repulsion between the atoms, as in the repulsive curve $1\sigma_u$ of Fig 2.1. The attractive curve has an energy minimum agreeing roughly with that observed in the hydrogen molecule. By arguments similar to those used by Heisenberg, Heitler and London identified the symmetric function with a singlet state and the antisymmetric state with a triplet. This fitted the experimental fact that the ground state of the hydrogen molecule is a singlet.

## 2.2 The Born-Oppenheimer Approximation Applied to N-N Interactions

In this section we will look at how the Born-Oppenheimer approximation has been incorporated into models of the nuclear force used today. We describe the adiabatic approach as used for a molecule and then extend it to the bag model. The Non Relativistic Quark model is looked at, and using the procedure in Oka and Yazaki [Oka84], we compare the two models.

### 2.2.1 At the Molecular Level

The Born-Oppenheimer approximation as described in the previous sections is basically an adiabatic approach. We now consider this using a modern example [HaKu78].

Consider a molecule which consists of a given number of electrons with mass m and of atomic nuclei with mass M. The Hamiltonian is written in the form

$$H = K_R + K_r + V(r, R) \tag{2.1}$$

where

$$K_r = \frac{\hbar^2}{2m} \sum_i \vec{\nabla}^2_{r_i} \tag{2.2}$$

is the operator for the kinetic energy of the electrons (light particles) and

$$K_R = \frac{\hbar^2}{2m} \sum_i \vec{\nabla}^2_{R_i} \tag{2.3}$$

the kinetic energy of the nuclei (heavy particles). The electron coordinates with respect to the centre of mass are designated by $r_i$ and R is the relative coordinates of the nuclei. V(r,R) is the potential energy of the interaction.

In molecular physics, due to the large ratio M/m of nuclear mass to electron mass, the molecular periods are much longer than the electronic periods. We can then use the approximation of regarding the nuclei as fixed in calculating the electronic motion. In the second step the nuclear motion can be calculated under the assumption that the electrons have their steady motion for each instantaneous arrangement of the nuclei.

### 2.2.2 In the Bag Model

This idea can be extended to incorporate the idea of a bag. The bag model requires, even when there are only a few constituents, a minimal number of degrees of freedom. These collective bag variables are regarded as the slowly moving part of the system in comparison with the massless quarks and gluons considered later. The bag equations are solved so that the energy levels of the quarks and gluons are in analogy with the Schrödinger equation for fixed positions of the nuclei. The correspondence with the original model is :

- nuclei → collective bag variables
- electrons → light quarks and massless gluons.

### 2.2.3 In the NRQM

Meson theory was originally developed to explain nuclear forces. It is believed that the short range part of the nuclear force is dominated by the exchange of heavy mesons and more complicated processes, than the single meson exchange. Another point of view is that the short range part of the nuclear force arises directly from the interaction of quarks and the forces which confine them in the nucleons. This was advocated by Johnson [Jo75] and others who developed the bag model. This model however doesn't lend itself to a simple treatment of the two centre problem, which the interaction of the two nucleons involves. The model adopted by Schnitzer [Schn75] is a simple phenomenological description of the forces between two quarks.

The choice of the force assumed to act between quarks is essentially dictated by the requirements of explaining quark confinement and saturation in both baryons and mesons. This force is supposed to have a long range as in Hookes law, to explain the permanent binding of quarks in hadrons. To explain the absence of similar long range forces between the observed mesons and baryons (saturation), an appropriate combination of attractive and repulsive forces is needed. This is given in the colour hypothesis and an interaction between quarks by means of a colour octet of vector bosons. The vector character of the interaction means that the forces between quarks will be spin dependent, and the spin dependent forces are related in a straightforward way to the central force. This does not entail any additional assumptions or parameters.

The adiabatic approach used in the non relativistic quark model has been successfully used by several different groups [Lib77, Ba77, WaSh80, Hol84, Rob81, CvGo83].

There has also been success in using the NRQM to describe the low lying states of the baryon [DeR+75, Jo+77, Cel77, IsKa78, IsKa79, IsKa79a, OnSch82, Ca+83]

The antisymmetriser used in describing the six quark wave function in terms of two nucleon wave functions is the form assumed in the resonating group method and, as a

form of the six quark wave function, is valid for any separation although the identity of the baryons B B' becomes ambiguous for small separations [Whe37, Wil+58, Shi+62, Kan77].

The hamiltonian consists of a kinetic energy term K and an interaction term V

$$H = K + V \tag{2.4}$$

where K is the sum of kinetic energies including rest masses for quarks minus the kinetic energy for the centre of mass motion of the total system

$$\begin{aligned} K &= \sum_i K_i - K_G \qquad K_i = m_i + \frac{\vec{p}_i^2}{2m_i} \\ K_G &= \frac{\vec{p}_G^2}{2m_G} \\ \vec{p}_G &= \sum_i \vec{p}_i \qquad m_G = \sum_i m_i \end{aligned} \tag{2.5}$$

and $m_i, \vec{p}_i$ are the mass and momentum of the $i^{th}$ quark respectively. V is the sum of the two body interactions, the confinement term $V_{ij}^{conf}$ and the residual term $V_{ij}^{res}$.

$$\begin{aligned} V &= \sum_{i<j} V_{ij} \\ V_{ij} &= V_{ij}^{conf} + V_{ij}^{res} \end{aligned} \tag{2.6}$$

The confinement term represents the non perturbative effects of QCD and is responsible for confining quarks within colour singlet hadrons. The commonly used form [DeR+75, Jo+77, Cel77, IsKa78, IsKa79, IsKa79a, OnSch82, Ca+83] for this is

$$\begin{aligned} V_{ij}^{conf} &= -(\lambda_i \cdot \lambda_j) a_n r_{ij}^n \qquad (n = 1, 2) \\ (\lambda_i \cdot \lambda_j) &= \sum_\alpha \lambda_i^\alpha \lambda_j^\alpha \end{aligned} \tag{2.7}$$

with $\lambda_i^\alpha$ the $\alpha^{th}$ generator of the colour SU(3) group for the $i^{th}$ quark and is normalised

as

$$(\lambda_i \cdot \lambda_i) = \sum_{\alpha} \lambda_i^{\alpha} \lambda_i^{\alpha} = \frac{16}{3} \tag{2.8}$$

The colour factor $(\lambda_i \cdot \lambda_j)$ is necessary to eliminate the direct confining interactions between colour singlet hadrons and is unique within the range of two body operators.

The momentum-independent part of the OGE Fermi Breit potential [DeR+75, Jo+77, Cel77, IsKa78, IsKa79, IsKa79a, OnSch82, Ca+83] gives $V^{res}$. The tensor term is responsible for mixing the S and D states but not considered important. The $\delta$-function piece of the interaction needs to be treated with care, an attractive $\delta$ interaction leads to instability of the system if higher order effects are fully taken into account. This can be avoided by introducing finite range effects which may arise as higher order effects of QCD. The calculations of 3 quark systems , [DeR+75, Jo+77, Cel77, IsKa78, IsKa79, IsKa79a, OnSch82, Ca+83, Bh+80] use the finite range versions. The $\delta$-function interaction is an approximation which is effective only within the limited space of relatively simple configurations.

### 2.2.4 Comparison of MIT Bag and NRQM in an Adiabatic Approach

In comparing the two models we follow the arguments used by Oka and Yazaki [Oka84]. They take the NRQM from [Lib77] and the MIT bag model from [DeT78]. A Born-Oppenheimer approximation is used to compare the two models. In both, the adiabatic potential at zero separation $V_{ad}(0)$ is determined by the expectation values of energy for the $(Os)^n (n = 3, 6)$ configuration. The "mass formula" for the potential model is

$$m(n, \alpha) = < (Os)^n, \alpha | H | (Os)^n, \alpha >$$

$$= n\varepsilon - \frac{3}{4m_q b^2} + \frac{< \Gamma_{cm} >_{n,\alpha}}{16}(m_\Delta - m_N) \ , \tag{2.9}$$

where $\alpha$ denotes all the necessary quantum numbers and $\varepsilon$ is given by

$$\varepsilon = m_q + \frac{3}{4m_q b^2} - \frac{4\alpha_s}{\sqrt{2\pi}b} + \frac{2}{3\sqrt{2\pi}}\frac{\alpha_s}{m_q^2 b^3} + \begin{cases} 16\sqrt{\frac{2}{\pi}}a_1 b & \text{linear confinement} \\ 24a_3 b^2 & \text{quadratic confinement} \ . \end{cases} \tag{2.10}$$

Here $\Gamma_{cm}$ is the colour magnetic operator given by

$$\Gamma_{cm} = -\sum_{i>j}(\lambda_i \cdot \lambda_j)(\sigma_i \cdot \sigma_j) \ , \tag{2.11}$$

and the colour magnetic part has been expressed by the $\Delta - N$ mass difference by the use of the relation

$$M_\Delta - M_N = \frac{4}{3\sqrt{2\pi}}\frac{\alpha_s}{m_q^2 b^3} \ . \tag{2.12}$$

$V_{AD}(0)$ for the N-N interaction can now be written as

$$\begin{aligned} V_{AD}^{pot}(0) &= m(6,\alpha) - 2m(3,N) - < K_{rel} > \\ &= \frac{< \Gamma_{cm} >_{6\alpha} + 16}{16}(M_\Delta - M_N) \ , \end{aligned} \tag{2.13}$$

$< K_{rel} >$ is the average kinetic energy for the relative motion between the two nucleons which is included in $< H >_\alpha$ of

$$V_{AD}(R) = \frac{< H >_R}{< N >_R} - \frac{< H >_\infty}{< N >_\infty} \tag{2.14}$$

and is equal to $\frac{3}{4m_q b^2}$. Equation (2.14) is the basis of the estimate given in the previous section.

The "mass formula" for the MIT bag model is [DeG+75]

$$m(n,\alpha) = \frac{n2.07}{R} + \frac{4\pi}{3}R^3 - \frac{Z_0}{R} + \frac{< \Gamma_{cm} >_{n,\alpha}}{16}(M_\Delta - M_N) \tag{2.15}$$

and $V_{AD}(0)$ is given by

$$\begin{aligned} V_{AD}^{bag}(0) &= m(6,\alpha) - 2m(3,N) - < K_{rel} > \\ &= \frac{< \Gamma_{cm} >_{6,\alpha} + 16}{16}(M_\Delta - M_N) - \frac{4\pi}{3}BR^3 + \frac{Z_0}{R} - < K_{rel} > \end{aligned} \tag{2.16}$$

There is no reliable estimate for $< K_{rel} >$ and it is assumed that the main contribution to $Z_0$ comes from the centre of mass correction and approximately cancels with $< K_{rel} >$ [DoJo80, LiWo82, Wo82].

In the bag model the volume energy represents the confinement whereas in the potential model the corresponding confinement term doesn't contribute to the NN interaction. So in general, the MIT bag model predicts a weaker repulsion or stronger attraction than the potential model, which can be ascribed to the confinement mechanism.

## 2.3 Effective Meson Exchange Potential

Oka and Yazaki [Oka84] investigated the short range nuclear force within a model involving quark and gluon exchange. They found that short range repulsion of the nuclear force is explained as the quark exchange interaction between nucleons which is (a) short ranged, (b) non-local and (c) state dependent. The two questions which arise from their work are [OkYa83]:

(1) How is the short range repulsion due to the quark exchange interaction affected by the longer range attraction due to meson exchange?

(2) What is the two body correlation in the quark model as compared with that of the conventional models with a local repulsive core?

To look at these they used a superposition of the cluster model and an effective meson exchange potential to construct a realistic model of the nuclear force which they labelled the Effective Meson Exchange Potential (EMEP) between two nucleons. It consists of central and tensor parts

$$V(R) = V^c(R) + V^t(R)R^2 S_{12} \tag{2.17}$$

and $S_{12}$ is the tensor operator

$$S_{ij} = \frac{3(\sigma_i \cdot r_{ij})(\sigma_j \cdot r_{ij})}{r_{ij}^2} - (\sigma_i \cdot \sigma_j) \tag{2.18}$$

Each part is chosen so as to (1) simulate the OPE potential at $R > 2fm$ and, (2) reproduce experimental data such as scattering phase shifts for $R < 2fm$. To incorporate the EMEP into the RGM equation for NN system they introduced the kernel V(R,R") by

$$V(\vec{R}, \vec{R}") = \int d\vec{R}" N^{\frac{1}{2}}(\vec{R}, \vec{R}") V(\vec{R}") N^{\frac{1}{2}}(\vec{R}", \vec{R}') \tag{2.19}$$

which is added to the hamiltonian kernel.

$$N_{\beta\beta'}(\vec{R}\vec{R}') = \int d\tau \Psi_\beta^+(123,456)\delta(\vec{R} - \vec{R}_{123,456}) \begin{pmatrix} 1 \\ H \end{pmatrix} A[\Psi_{\beta'}(123,456)\delta(\vec{R}' - \vec{R}_{123,456})] \tag{2.20}$$

and $N^{\frac{1}{2}}$ denotes the square root operator of the normalisation kernel.

Values for the parameters are given in Table 2.1. As the mass in the kinetic energy term for a nucleon is $3m_q$, they take $m_q = \frac{m_N}{3} \equiv 313MeV$ to have a correct relation between the momentum and energy. The Gaussian size parameter b is related to the rms

| | $m_q$ (MeV) | b (fm) | $\alpha_s$ | $a_1$ (MeV/fm) |
|---|---|---|---|---|
| I | 313 | .5 | .878 | 234.0 |
| II | 313 | .6 | 1.517 | 135.3 |
| III | 313 | .7 | 2.409 | 85.2 |

Table 2.1: Three sets of the quark model parameters used in the realistic model. Taken from Oka and Yazaki [Oka84].

radius of the quark core in the nucleon by

$$b = (< r^2 >_N)^{\frac{1}{2}} \tag{2.21}$$

They show that the quark cluster model gives definite predictions on the baryon baryon interaction at short distances. Important aspects of the model are the Pauli principle for quarks and the colour magnetic interaction (CMI).

The quark exchange mechanism supplemented by meson exchange is found to reproduce the observed NN phase shifts and deuteron properties. The short range part of the deuteron wave function is different from conventional models due to the strong non-locality of the quark exchange interaction.

It is shown that the resonating group method (RGM) with two colour singlet three quark clusters (baryons) gives a complete (even over complete) set of states for a colour singlet six quark system, and the six-body Schrödinger equation is reduced to a set of coupled integral equations with an infinite number of discrete channels. Convergence with respect to the number of channels seems to be intimately connected with the confining interaction and the problem of the colour van der waals force is discussed in this context.

## 2.4 OGE as described by Holinde

Holinde [Hol84] looked at the one gluon exchange potential in the NN interaction using an adiabatic or Born-Oppenheimer approximation. The possible ways in which a gluon can be exchanged between quarks is shown in Fig 2.2

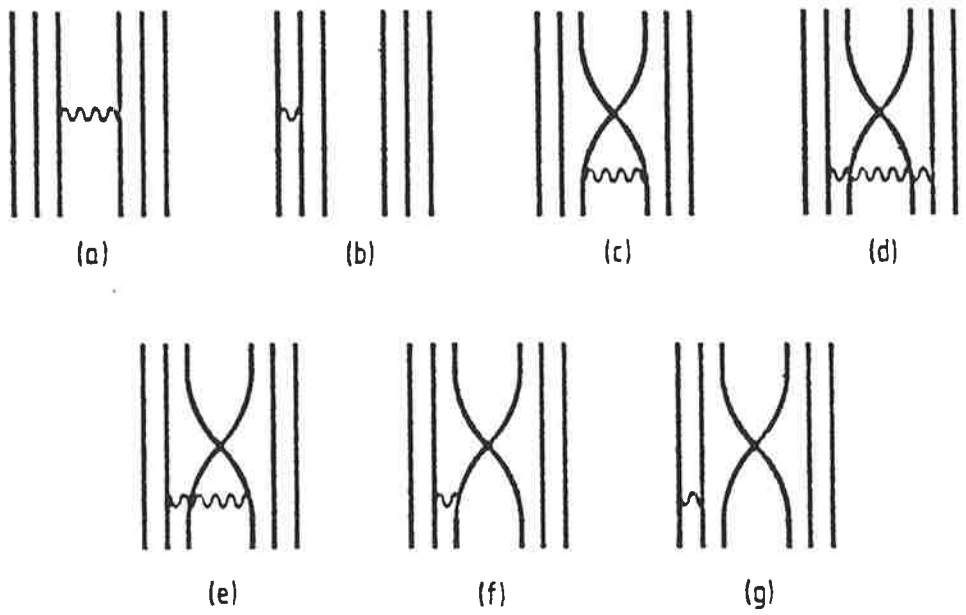


Figure 2.2: the one gluon exchange processes in the NN problem (b) contributes to the nucleon self energy, (a) vanishes, and the others contribute to the NN interaction energy.

To obtain the potential he starts with a quark gluon interaction lagrangian

$$L_{int} = \tfrac{1}{2} g \bar{\psi}(x) \lambda^{(i)} \gamma^{\mu} \psi(x) G_{\mu}^{(i)}(x) \tag{2.22}$$

with $g$ the quark-gluon coupling constant, $\psi(x)$ the quark field, $G_{\mu}^{(i)} (i = 1..8, \mu = 0,1,2,3)$ are the eight (massless) vector gluon fields, $\gamma^{\mu}$ the Dirac matrices and $\lambda^{(i)}$ the colour matrices.

A potential between quarks i and j can be derived which is similar to the Fermi-Breit

interaction used in QED. This gives

$$V_{OGE}(ij) = \frac{1}{4}\alpha_s \lambda_i \cdot \lambda_j \left[ \frac{1}{r_{ij}} 1_i 1_j - \frac{2}{3}\frac{\pi}{m^2}\delta(r_{ij})\sigma_i \cdot \sigma_j - \frac{3}{2m^2}\frac{1}{r_{ij}^3} l_{ij} \cdot s \right.$$
$$\left. + \frac{1}{4m^2}\frac{1}{r_{ij}^3}\left( \sigma_i \cdot \sigma_j - \frac{3\sigma_i \cdot r_{ij}\, \sigma_j \cdot r_{ij}}{r_{ij}^2} \right) \right] \qquad (2.23)$$

$l_{ij}$ is the (relative) angular momentum operator, $r_{ij}$ is the distance between the interacting quarks , m is the quark mass, $s \equiv \frac{1}{2}(\sigma_i + \sigma_j)$ and $\alpha_s \equiv \frac{g^2}{4\pi}$.

To this he adds the confining term

$$V_{conf}(ij) = -\lambda_i \cdot \lambda_j a r_{ij}^2 \qquad (2.24)$$

to give a total inter-quark potential of the form

$$V(ij) = V_{OGE}(ij) + V_{conf}(ij) \ . \qquad (2.25)$$

Within the Born-Oppenheimer approximation this leads to a NN potential :

$$V_{NN} = \frac{< \psi | H_A + H_B + \sum_{i=1}^{3}\sum_{j=4}^{6} V(ij) | \psi >}{< \psi | \psi >} - 2 < \phi_A | H_A | \phi_A > \qquad (2.26)$$

with

$$|\psi >= A|\phi_A \phi_B > \qquad (2.27)$$

and

$$\phi_N = \varphi(\xi)\chi(\sigma\tau)\zeta(c)$$
$$H_A = \sum_{i=1}^{3} t_i + \sum_{i>j=1}^{3} V(ij) - T_A^{cm} \ . \qquad (2.28)$$

Here $t_i$ is the kinetic energy operator for quark $i$ and $T_A^{cm}$ the center of mass energy of

cluster A.

Following Holinde we write the potential as

$$V_{NN} = V^1_{NN} + V^2_{NN} + V^3_{NN} \tag{2.29}$$

where

$$\begin{aligned}
V^1_{NN} &= V^{AC}_{NN} + V^B_{NN} \\
V^{AC}_{NN} &= -16\left[\frac{1}{4}\alpha_s\left(\sqrt{\frac{2}{\pi}}\beta - \frac{4}{R}erf(x) + \frac{1}{R}erf(x')\right) - \frac{1}{2}aR^2\right] c_{ST} e^{-\frac{1}{2}\beta^2R^2} \\
&\quad (1-(-)^{S+T}e^{-\frac{1}{2}\beta^2R^2})/N \\
V^B_{NN} &= 16\frac{\alpha_s}{4}\frac{2}{3}\frac{\pi}{m^2}\left(\frac{\beta^2}{2\pi}\right)^{\frac{3}{2}} e^{-\frac{1}{2}\beta^2R^2}/N\left\{d^{36}_{ST} + d^{25}_{ST}e^{-\frac{1}{2}\beta^2R^2}\right. \\
&\quad \left. -2d^{26}_{ST}e^{-\frac{1}{8}\beta^2R^2} - (-)^{S+T}(d^{36}_{ST}e^{-\frac{1}{2}\beta^2R^2} + d^{25}_{ST} - 2d^{26}_{ST}e^{-\frac{1}{8}\beta^2R^2})e^{-\frac{1}{2}\beta^2R^2}\right\} \\
V^2_{NN} &= -16\left\{2\left[\frac{1}{4}\alpha_s\left(\sqrt{\frac{2}{\pi}}\beta - \frac{2}{R}erf(x)\right) + \frac{1}{4}aR^2\right] c_{ST} + \frac{1}{4}\alpha_s\frac{2}{3}\frac{\pi}{m^2}\left(\frac{\beta^2}{2\pi}\right)^{\frac{3}{2}}\right. \\
&\quad \left.[3c_{ST} + d^{12}_{ST} + 2d^{26}_{ST}e^{-\frac{1}{8}\beta^2R^2}]\right\} e^{-\frac{1}{2}\beta^2R^2}(1-(-)^{S+T}e^{-\frac{1}{2}\beta^2R^2})/N \\
V^3_{NN} &= \frac{1}{2}\frac{\beta^2}{m}\beta^2R^2e^{-\frac{1}{2}\beta^2R^2}c_{ST}(1-(-)^{S+T}e^{-\frac{1}{2}\beta^2R^2})/N
\end{aligned} \tag{2.30}$$

where the $d^{ij}_{ST}$ are the matrix elements of the spin-isospin operators, $erf(x)$ is the error function.

$$\begin{aligned}
erf(x) &= \frac{2}{\sqrt{\pi}}\int_0^x e^{-t^2}dt \\
x &= \frac{1}{4}\sqrt{2}\beta R
\end{aligned}$$

$$x' = 2x \tag{2.31}$$

A few comments can be made concerning the structure of $V^i_{NN}$.

(i) The colour-magnetic (spin-spin) term builds up the dominant repulsive contribution in $V^1_{NN}$ and appears as a small correction in $V^2_{NN}$ which vanishes at R=0.

(ii) The contributions from the confinement term cancel whereas the total colour Coulomb term vanishes only at R=0. At R $\neq$ 0 it gives a repulsive contribution for even parity states and an attractive contribution for odd-parity states.

Two parameter sets were used for the potential. One is given by Faessler, Fernandez, Lübeck, Shimizu [Faes+82] denoted FFLS with parameters :

$m = 355MeV, \beta^{-1} = .475fm, a = 34.5MeV \cdot fm^{-2}, \alpha_s = .97.$

The other is given by Oka and Yazaki [Oka84] with parameters :

$m = 300MeV, \beta^{-1} = .6fm, a = 62.5MeV \cdot fm^{-2}, \alpha_s = 1.39.$

The choice of FFLS ensures that the nucleon mass is a minimum. The importance of using wave functions at variational equilibrium was underlined by Liu [Liu82].

At R=0 the NN interaction due to the colour-magnetic term is the same for both parameter sets since $\alpha_s\beta^3 m^{-2}$, which determines the $N\Delta$ splitting, has the same value. They also give essentially the same behaviour.

For FFLS, the colour-magnetic contribution to $V^1_{NN}$ agrees roughly with vector meson exchange around $1fm$, whereas it is sizeably weaker in odd-parity states. The results for the OY set is larger than $\rho-$ and $\omega-$ exchange in even-parity states. It agrees reasonably in odd-triplet states and is too small in odd-singlet states. The inconsistency between the different channels is due to the negative sign of the spin-spin term in the resulting NN interaction. By including the kinetic energy term $V^3_{NN}$ it improves the FFLS to the point where there is good agreement with vector meson exchange around $R = 1fm$ in all channels - where the OY result is consistently too large.

In summary Holinde derived the short range part of the NN interaction predicted

by quark-gluon exchange processes, in a Born-Oppenheimer approximation. Concerning the spin-isospin part of the central and spin-spin part, the dominant colour magnetic contribution shows a characteristic discrepancy from predictions provided by conventional $\omega$ and $\rho$ meson exchange ; namely the resulting spin-spin contributions have the opposite sign. This leads to a relatively weak repulsion in odd-parity states. The inconsistency between the different channels is removed when the kinetic energy correction is included.

Around $R = 1fm$ FFLS provides reasonable agreement with meson theoretic results, whereas OY are consistently too large due to the larger size parameter $\beta$. The inconsistency shows again when the contribution from the central (colour-Coulomb and confining) terms are included. The effect on even-parity is negligibly small, there is a sizeable attractive contribution in odd-parity states. From this it appears that a consistent agreement with vector meson exchange in all channels requires a model for the quark-gluon interaction, which has a rather small central part. This model, apart from giving the wrong isospin dependence provides a result which is much too small compared to the realistic meson exchange picture. The results for these are given in chapter 5 in comparison with the Quark One Pion Exchange Potential (QOPEP) that we have used.

## 2.5 QOPEP as desribed by Fernandez *et al.*

In their description Fernandez et al. [FerOs86] use a non relativistic contituent quark model of the nucleon, incorporating pion exchange between quarks, to calculate a modified OPE NN potential which includes effects of quark exchange between nucleons [Fern87, FerOs86] . Within this framework they explained the OPE $\delta$ procedure (or Poorman's absorption model). The latter yields a qualitative description of the double spin-flip helicity amplitude, $\phi_2$, for elastic nucleon-nucleon scattering [Ge81].

The aim of the paper is to show that the modifications produced in the OPE potential by quark exchange provide a qualitative understanding of this phenomenon. They obtain an

explanation for the modification of the OPE $(\sigma \cdot \sigma)(\tau \cdot \tau)$ dependent term provided by the Poorman's absorption model. A non relativistic quark model is used, where the quarks are not the current quarks of the QCD lagrangian but some sort of dressed constituent quarks. The philosophy behind the NRQM is to incorporate aysmptotic freedom and confinement by means of a two body potential between quarks. The OGE calculations are done by others [Hol84, Oka84, Faes+82, FaFer83, Faes+83].

In QCD, the pion must appear as a consequence of the dynamical breaking of chiral symmetry. Within the Cloudy Bag Model [AWT83, Theb+80, Theb+81]this led initially to the introduction of quark-pion coupling at the bag surface. Later, the equivalence to pseudo-vector quark-pion coupling throughout the confinement region was demonstrated (at least at the level of the Yukawa pion-nucleon coupling). It is the latter realisation of chiral symmetry that we adopt in our NRQM by adding a Yukawa-type coupling between the quarks and the pion field.

# Chapter 3

# The Quark-Pion Coupling Potential

In this chapter we formulate the Quark One Pion Exchange Potential (QOPEP) using the Born-Oppenheimer or adiabatic approximation as described in the previous chapter. This is used in a Non Relativistic Quark Model (NRQM), where we introduce the idea of quark exchange between nucleons at short distances. The potential is split into direct and exchange terms; direct being those without quark exchange between nucleons and exchange those in which quarks are exchanged between the nucleons. Our One Pion Exchange Potential is calculated in momentum space and separated into scalar and tensor terms at a later stage.

## 3.1 Born-Oppenheimer Model

In the cluster model approach the nucleon is taken as a function of three quarks. Its antisymmetric and normalized wave function can be written as

$$\phi_N = \varphi^x \varphi^{\sigma\tau} \varphi^c \tag{3.1}$$

where $\varphi^x$ is the symmetric spatial wave function for three quarks, $\varphi^{\sigma\tau}$ is the symmetric spin-isospin wave function and $\varphi^c$ is the antisymmetric state in colour space.

In an adiabatic cluster model, the interaction energy between two nucleons is the expectation of the energy of the six quark system minus the energy at infinite separation of the two clusters, namely

$$V_{NN} = \frac{<\psi|H_{\mathbf{a}} + H_{\mathbf{b}} + \sum_{i=1}^{3}\sum_{j=4}^{6} V(ij)|\psi>}{<\psi|\psi>} - 2<\phi_{\mathbf{a}}|H_{\mathbf{a}}|\phi_{\mathbf{a}}> \tag{3.2}$$

with $|\psi>$ the antisymmetric six quark state given by

$$|\psi> = A|\phi_{\mathbf{a}}\phi_{\mathbf{b}}> \tag{3.3}$$

where $\phi_{\mathbf{a}}$ and $\phi_{\mathbf{b}}$ are the wave functions for nucleons **a**, **b** respectively.

$H_{\mathbf{a}}$ is the internal Hamiltonian of the cluster **a**,

$$H_{\mathbf{a}} = \sum_{i=1}^{3} t_i \quad + \quad \sum_{\substack{i,j=1 \\ j>i}}^{3} V(ij) - T_{\mathbf{a}}^{cm} \tag{3.4}$$

with $t_i$ being the kinetic energy of quark $i$ and $T_{\mathbf{a}}^{cm}$ the corresponding center of mass (cm) energy of cluster **a** and and similarly for $H_{\mathbf{b}}$ .

Since each $\phi_{\mathbf{a}}$,$\phi_{\mathbf{b}}$ is totally antisymmetrised, A is given by

$$A = 1 - \sum_{i=1}^{3}\sum_{j=4}^{6} P_{ij} + \sum_{\substack{m,k=1 n,l=4 \\ m>k \quad n>l}}^{3\quad 6} P_{kl}\, P_{mn} - P_{14}P_{25}P_{36} \tag{3.5}$$

where $P_{ij}$ is the exchange operator interchanging quarks $i$ and $j$. After manipulation (see Appendix A), (3.5) can be written as

$$A \;=\; \left(1 - \sum_{i=1}^{3}\sum_{j=4}^{6} P_{ij}\right)(1 - P)$$

$$= (1 - 9P_{36})(1 - P) \tag{3.6}$$

with $P \equiv P_{14}P_{25}P_{36}$ the nucleon exchange operator.

We have shown in Appendix A that the normalisation can be written as

$$< \psi|\psi >= 20 < \phi_{\mathbf{a}}\phi_{\mathbf{b}}|(1 - 9P_{36})(1 - P)|\phi_{\mathbf{a}}\phi_{\mathbf{b}} > \quad . \tag{3.7}$$

We use a Born-Oppenheimer cluster approximation where

$$V(ij) = V^{conf}(ij) + V^{OPE}(ij) + V^{OGE}(ij) \tag{3.8}$$

and the confining term is

$$V^{conf}(ij) = -\lambda_i \cdot \lambda_j a\, r_{ij}^2 \tag{3.9}$$

with $\lambda_{i,j}$ the Gell-Mann matrices, $a$ the colour constant and $r_{ij}$ the distance between the quarks $i$ and $j$ . The One Gluon Exchange (OGE) Potential as used by Holinde [Hol84] is :

$$V^{OGE}(ij) = \frac{1}{4}\alpha_s \lambda_i \cdot \lambda_j \left[ \frac{1}{r_{ij}} \mathbf{1}_i \mathbf{1}_j - \frac{2}{3}\frac{\pi}{m^2}\delta(r_{ij})\sigma_i \cdot \sigma_j - \frac{3}{2m^2}\frac{1}{r_{ij}^3} l_{ij} \cdot s_{ij} \right.$$
$$\left. + \frac{1}{4m^2}\frac{1}{r_{ij}^3}\left( \sigma_i \cdot \sigma_j - 3\frac{\sigma_i \cdot r_{ij}\ \sigma_j \cdot r_{ij}}{r_{ij}^2} \right) \right] \quad , \tag{3.10}$$

where $l_{ij}$ is the relative angular momentum operator, $s_{ij} \equiv \frac{1}{2}(\sigma_i + \sigma_j)$, $m$ is the quark mass and $\alpha_s \equiv g^2/4\pi$. We write the One Pion Exchange (OPE) Potential in momentum space as

$$V^{OPE}(ij) = 4\pi \frac{f_{\pi qq}^2}{m_\pi^2} \vec{\tau_i} \cdot \vec{\tau_j} \int \frac{d^3q}{(2\pi)^3} \frac{\vec{\sigma_i} \cdot \vec{q} \vec{\sigma_j} \cdot \vec{q}}{q^2 + m_\pi^2} e^{iq \cdot (r_i - r_j)} \quad , \tag{3.11}$$

with $f_{\pi qq}^2$ the pion-quark-quark coupling constant and $m_\pi$ the mass of the pion .

In the previous chapter we discussed the confining potential and the One Gluon Exchange

Potential calculated by other people [Hol84, ElHol84, ElHol84a, Oka84]. The work done for the One Pion Exchange Potential was also discussed, in particular that of Fernandez and Shimizu [FerOs86, Shim84]. We concentrate on the QOPEP and look at its properties in detail. This will be generated by the pionic piece of the potential given in equation (3.8), viz :

$$V_{NN}^{OPE}(ij) = < \phi_{\mathbf{a}}\phi_{\mathbf{b}}|V^{OPE}(ij)|\phi_{\mathbf{a}}\phi_{\mathbf{b}} > \tag{3.12}$$

Following the formalism of Holinde [Hol84] we can rewrite (3.12) in terms of (3.2) and separate as

$$V_{NN}^{OPE} = V_1 + V_2 + V_3 \tag{3.13}$$

with

$$V_1 = \frac{1}{N} < \phi_{\mathbf{a}}\phi_{\mathbf{b}}| \sum_{i=1}^{3}\sum_{j=4}^{6} v_{ij}(1 - 9P_{36})(1 - P)|\phi_{\mathbf{a}}\phi_{\mathbf{b}} > \tag{3.14}$$

$$\begin{aligned} V_2 = \quad & \frac{1}{N} < \phi_{\mathbf{a}}\phi_{\mathbf{b}}|\frac{1}{2}\left(\sum_{i\neq j=1}^{3} v_{ij} + \sum_{k\neq l=4}^{6} v_{kl}\right)(1 - 9P_{36})(1 - P)|\phi_{\mathbf{a}}\phi_{\mathbf{b}} > \\ & -2 < \phi_{\mathbf{a}}| \sum_{i\neq j=1}^{3} v_{ij}|\phi_{\mathbf{a}} > \end{aligned} \tag{3.15}$$

$$\begin{aligned} V_3 \quad = \quad & \frac{1}{N} < \phi_{\mathbf{a}}\phi_{\mathbf{b}}|\frac{1}{2}\left(\sum_{i=1}^{6} t_i - T_{\mathbf{a}}^{CM} - T_{\mathbf{b}}^{CM}\right)(1 - 9P_{36})(1 - P)|\phi_{\mathbf{a}}\phi_{\mathbf{b}} > \\ & -2 < \phi_{\mathbf{a}}| \sum_{i=1}^{6} t_i - T_{\mathbf{a}}^{CM}|\phi_{\mathbf{a}} > \end{aligned} \tag{3.16}$$

where N is the normalisation and is given by (3.7)

$V_1$ is the main contributing term, describing the interaction between the clusters. $V_2$ is the non-negligible correction term which takes the difference of the potential inside the six quark system compared with two separate three quark systems ( ie the nucleons at

infinite separation). $V_3$ is the kinetic energy term which is the same for gluonic and pionic calculations and is given by Holinde [Hol84].

## 3.2 The Quark One Pion Exchange Potential

We will now look at the individual terms which make up the Quark One Pion Exchange Potential (QOPEP). There are seven topologically different possibilities in which a pion can be exchanged between quarks as shown in Fig 3.1. These diagrams represent the structure of the matrix elements involved and should not be interpreted as Feynman diagrams. In referring to the potentials created by the diagrams, they are labelled as shown in Table 3.1:

| Diagram | Potential Term | Pion Exchanged Between Quarks | Quark Exchange Between Nucleons |
|---|---|---|---|
| (a) | $v_{36}^{nqe}$ | 3 and 6 | no |
| (b) | $v_{12}^{nqe}$ | 1 and 2 | no |
| (c) | $v_{36}^{qe}$ | 3 and 6 | yes |
| (d) | $v_{25}^{qe}$ | 2 and 5 | yes |
| (e) | $v_{26}^{qe}$ | 2 and 6 | yes |
| (f) | $v_{23}^{qe}$ | 2 and 3 | yes |
| (g) | $v_{12}^{qe}$ | 1 and 2 | yes |

Table 3.1: Table listing the properties of the diagrams given in Fig.3.1

We also have the contribution when the nucleons are at infinite separation. This is labelled $v^s$.

The potentials are divided into two main parts, quark exchange $v^{qe}$ and non quark

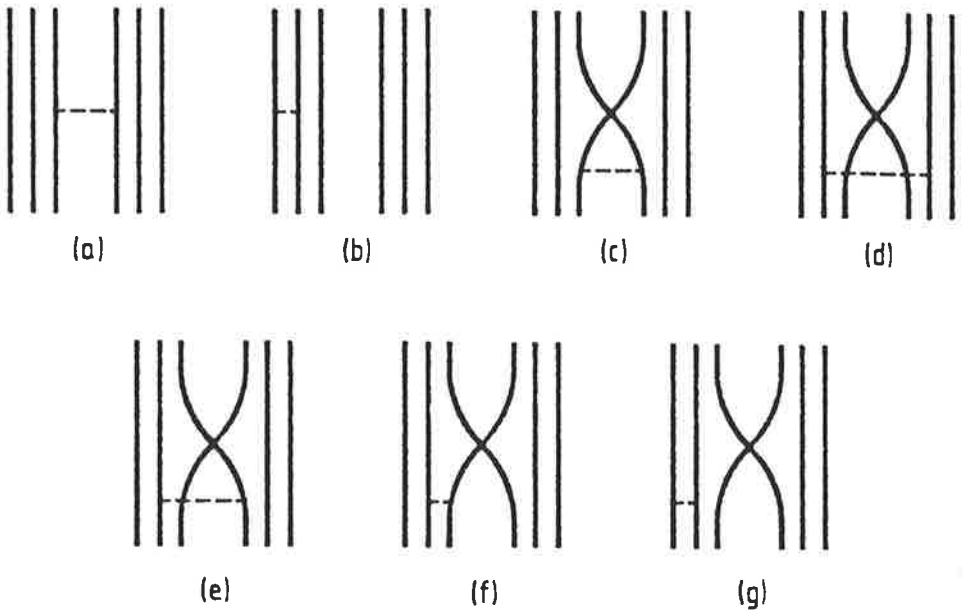


Figure 3.1: The quark-pion coupling contributions which make up the QOPEP

exchange $v^{nqe}$ terms. The potentials $V_1$ and $V_2$ can now be written in terms of the individual quark potentials

$$V_1 = 9v_{36}^{(nqe)} + v_{36}^{(qe)} + 4v_{25}^{(qe)} + 4v_{26}^{(qe)}$$
$$V_2 = 4v_{12}^{(qe)} + 4v_{23}^{(qe)} + 6(v_{12}^{(nqe)} - v_{12}^{(s)}) \tag{3.17}$$

The numerical coefficients come from counting the number of topologically equivalent diagrams.

The nucleon space wave functions are just the simple harmonic wave functions :

$$\varphi_a = \left(\frac{\beta^2}{\pi}\right)^{\frac{9}{4}} exp\left\{-\frac{\beta^2}{2}\left(\sum_{i=1}^{3}(r_i - \frac{R}{2})^2\right)\right\}$$
$$\varphi_b = \left(\frac{\beta^2}{\pi}\right)^{\frac{9}{4}} exp\left\{-\frac{\beta^2}{2}\left(\sum_{i=4}^{6}(r_i + \frac{R}{2})^2\right)\right\} \tag{3.18}$$

where R as shown in Fig 3.2 is the fixed distance between the origins of the two harmonic

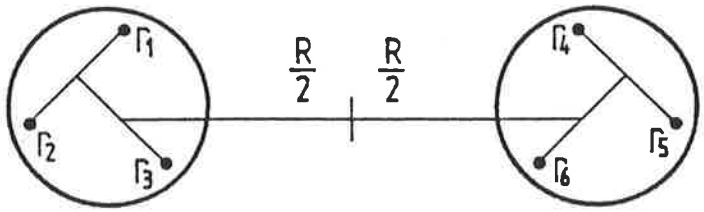


Figure 3.2: schematic diagram of the two nucleons at R separation

oscillator potentials building up clusters **a** and **b** and $r_i$ is the position of quark $i$. $\beta$ is the nucleon length constant related to the root mean square radius by

$$\beta^{-1} = b = < r_{rms}^2 >^{\frac{1}{2}} \tag{3.19}$$

We can now write the potentials in terms of matrix elements. Writing them individually gives

$$v_{36}^{nge} = \frac{< \phi_{\mathbf{a}}\phi_{\mathbf{b}}|V^{OPE}(36)(1-P)|\phi_{\mathbf{a}}\phi_{\mathbf{b}} >}{< \phi_{\mathbf{a}}\phi_{\mathbf{b}}|(1-9P_{36}^{\sigma\tau xc})(1-P)|\phi_{\mathbf{a}}\phi_{\mathbf{b}} >}$$

$$v_{12}^{nge} = \frac{< \phi_{\mathbf{a}}\phi_{\mathbf{b}}|V^{OPE}(12)(1-P)|\phi_{\mathbf{a}}\phi_{\mathbf{b}} >}{< \phi_{\mathbf{a}}\phi_{\mathbf{b}}|(1-9P_{36}^{\sigma\tau xc})(1-P)|\phi_{\mathbf{a}}\phi_{\mathbf{b}} >}$$

$$v_{36}^{qe} = -9\frac{< \phi_{\mathbf{a}}\phi_{\mathbf{b}}|V^{OPE}(36)P_{36}^{\sigma\tau xc}(1-P)|\phi_{\mathbf{a}}\phi_{\mathbf{b}} >}{< \phi_{\mathbf{a}}\phi_{\mathbf{b}}|(1-9P_{36}^{\sigma\tau xc})(1-P)|\phi_{\mathbf{a}}\phi_{\mathbf{b}} >}$$

$$v_{25}^{qe} = -9\frac{< \phi_{\mathbf{a}}\phi_{\mathbf{b}}|V^{OPE}(25)P_{36}^{\sigma\tau xc}(1-P)|\phi_{\mathbf{a}}\phi_{\mathbf{b}} >}{< \phi_{\mathbf{a}}\phi_{\mathbf{b}}|(1-9P_{36}^{\sigma\tau xc})(1-P)|\phi_{\mathbf{a}}\phi_{\mathbf{b}} >}$$

$$v_{26}^{qe} = -9\frac{<\phi_a\phi_b|V^{OPE}(26)P_{36}^{\sigma\tau xc}(1-P)|\phi_a\phi_b>}{<\phi_a\phi_b|(1-9P_{36}^{\sigma\tau xc})(1-P)|\phi_a\phi_b>}$$

$$v_{23}^{qe} = -9\frac{<\phi_a\phi_b|V^{OPE}(23)P_{36}^{\sigma\tau xc}(1-P)|\phi_a\phi_b>}{<\phi_a\phi_b|(1-9P_{36}^{\sigma\tau xc})(1-P)|\phi_a\phi_b>}$$

$$v_{12}^{qe} = -9\frac{<\phi_a\phi_b|V^{OPE}(12)P_{36}^{\sigma\tau xc}(1-P)|\phi_a\phi_b>}{<\phi_a\phi_b|(1-9P_{36}^{\sigma\tau xc})(1-P)|\phi_a\phi_b>}$$

$$v^s = <\phi_a|V^{OPE}(12)|\phi_a> \tag{3.20}$$

We will now look at $v_{36}^{qe}$ of (3.20) as an example. We can write this explicitly by expanding the nucleon wave functions using (3.1) and substituting in the potential (3.11). This gives

$$v_{36}^{qe} = -\frac{9}{N}\int\frac{d^3q}{(2\pi)^3} <(\varphi_a^{\sigma\tau}\varphi_a^x\varphi_a^c)\,(\varphi_b^{\sigma\tau}\varphi_b^x\varphi_b^c)\,|\vec{\tau}_3\cdot\vec{\tau}_6\frac{\vec{\sigma}_3\cdot q\vec{\sigma}_6\cdot q}{q^2+m_\pi^2}e^{iq\cdot(r_3-r_6)}$$
$$P_{36}^{\sigma\tau xc}(1-P^{\sigma\tau xc})|(\varphi_a^{\sigma\tau}\varphi_a^x\varphi_a^c)\,(\varphi_b^{\sigma\tau}\varphi_b^x\varphi_b^c)> \tag{3.21}$$

The contributions from the colour terms are :

$$<\varphi_a^c\varphi_b^c|P_{36}^c|\varphi_a^c\varphi_b^c> = \frac{1}{3}$$
$$<\varphi_a^c\varphi_b^c|P^c|\varphi_a^c\varphi_b^c> = 1\ . \tag{3.22}$$

The term $P^{\sigma\tau}$ will give an overall phase factor of $(-)^{S+T}$ which is independent of the quarks' spin and isospin. To simplify the calculations we keep this term with the radial matrix element. The radial matrix element and the spin-isospin matrix element can be calculated independently and then put back together to evaluate the potential. Equation (3.20) can be written as

$$v_{36}^{qe} = -\frac{3}{N}\int\frac{d^3q}{(2\pi)^3}\frac{1}{q^2+m_\pi^2} <\varphi_a^x\varphi_b^x|e^{iq\cdot(r_3-r_6)}P_{36}^x(1-(-)^{(S+T)}P^x)|\varphi_a^x\varphi_b^x>$$

$$< \varphi_{\mathbf{a}}^{\sigma\tau}\varphi_{\mathbf{b}}^{\sigma\tau}|\vec{\tau}_3\cdot\vec{\tau}_6\vec{\sigma}_3\cdot q\vec{\sigma}_6\cdot qP_{36}^{\sigma\tau}|\varphi_{\mathbf{a}}^{\sigma\tau}\varphi_{\mathbf{b}}^{\sigma\tau} > \quad (3.23)$$

where the radial matrix element is

$$\eta_R^{36(nqe)} =< \varphi_{\mathbf{a}}^{x}\varphi_{\mathbf{b}}^{x}|e^{iq\cdot(r_3-r_6)}P_{36}^{x}(1-(-)^{(S+T)}P^{x})|\varphi_{\mathbf{a}}^{x}\varphi_{\mathbf{b}}^{x} > \quad (3.24)$$

and the spin-isospin matrix element is

$$M^{36(nqe)}(\hat{O}(\sigma)\hat{O}(\tau)) =< \varphi_{\mathbf{a}}^{\sigma\tau}\varphi_{\mathbf{b}}^{\sigma\tau}|\vec{\tau}_3\cdot\vec{\tau}_6\vec{\sigma}_3\cdot q\vec{\sigma}_6\cdot qP_{36}^{\sigma\tau}|\varphi_{\mathbf{a}}^{\sigma\tau}\varphi_{\mathbf{b}}^{\sigma\tau} > \quad (3.25)$$

In chapter 4 we show the steps involved in solving the matrix elements and arriving at the final form of the quark- pion potentials.

# Chapter 4

# The Matrix Elements

In this chapter the matrix elements required to evaluate the N-N force are examined in detail and the solutions calculated. The first section is concerned with breaking down the spin-isospin matrix elements into separate spin and isospin components. We then need to reduce the spin operator into its scalar and tensor forms. Once this is done the matrix elements are evaluated and the solutions given in nucleon operator form. We then examine the radial matrix element and calculate the integrals. Finally the sections are brought together and the quark potentials are written explicitly.

## 4.1 Spin-Isospin Matrix Elements

There are two methods by which we can evaluate the spin-isospin matrix elements. The first is the method used by Holinde [Hol84] for the One Gluon Exchange case and Liu [Liu+92] for the One Pion Exchange. They convert the quark spin and isospin operators to nucleon operators directly and then solve for each spin, isospin channel. The rules used for this method are given in Appendix B.

The method used here is an extension of the method used by Warke & Shanker

[WaSh80]. The matrix elements are written in terms of partial waves. This allows us to calculate the spin and isospin dependent parts separately. The matrix elements can be written in the form

$$M(\hat{O}(\sigma)\hat{O}(\tau)) =< \varphi_{\mathbf{a}}^{\sigma\tau}\varphi_{\mathbf{b}}^{\sigma\tau}|\hat{O}(\sigma)\hat{O}(\tau)|\varphi_{\mathbf{a}}^{\sigma\tau}\varphi_{\mathbf{b}}^{\sigma\tau} > \tag{4.1}$$

where $\hat{O}(\sigma)$ is the spin operator, and $\hat{O}(\tau)$ is the isospin operator, and $|\varphi_{\mathbf{a}}^{\sigma\tau}\varphi_{\mathbf{b}}^{\sigma\tau} >$ can be treated as a six quark state of total spin (S) and isospin (T). The wavefunctions $\varphi_{\mathbf{a}}^{\sigma\tau}$ and $\varphi_{\mathbf{b}}^{\sigma\tau}$ represent nucleons **a** and **b**, namely two three quark states with total spin $\frac{1}{2}$ and total isospin $\frac{1}{2}$. The structure of the three quark states which have mixed symmetry in both spin and isospin but are totally symmetric overall :

$$\varphi_{\mathbf{a}}^{\sigma\tau} = \frac{1}{\sqrt{2}}[\chi_S^{\sigma}(\tfrac{1}{2})\chi_S^{\tau}(\tfrac{1}{2}) + \chi_A^{\sigma}(\tfrac{1}{2})\chi_A^{\tau}(\tfrac{1}{2})] \tag{4.2}$$

where

$$\begin{aligned} \chi_S &= |(1\,\tfrac{1}{2})\tfrac{1}{2} > \\ \chi_A &= |(0\,\tfrac{1}{2})\tfrac{1}{2} > \end{aligned} \tag{4.3}$$

If the state is symmetric (antisymmetric) in the first two quark coordinates, then the total spin or isospin of the first two quarks will be 1 (0). The structure can then be :

$$|\varphi_{\mathbf{a}}^{\sigma\tau}\varphi_{\mathbf{b}}^{\sigma\tau}; SMTM_T >= \tfrac{1}{2}\sum_{ll'}\ |(l\tfrac{1}{2})\tfrac{1}{2}(l'\tfrac{1}{2})\tfrac{1}{2}; SM > |(l\tfrac{1}{2})\tfrac{1}{2}(l'\tfrac{1}{2})\tfrac{1}{2}; TM_T > \tag{4.4}$$

where the $l$'s are the sum of the first two quarks,$M$ the projection of the spin and$M_T$ the projection of the isospin. We can use this formalism to rewrite the spin-isospin matrix

elements such that the spin and isospin terms are separated. This will then give us

$$\begin{aligned} M^{ij}(\hat{O}(\sigma)\hat{O}(\tau)) &= \frac{1}{4}\sum_{ll'l_1l_1'} < (l_1\tfrac{1}{2})\tfrac{1}{2}(l_1'\tfrac{1}{2})\tfrac{1}{2}; SM|\hat{O}(\sigma)|(l_2\tfrac{1}{2})\tfrac{1}{2}(l'\tfrac{1}{2})\tfrac{1}{2}; SM > \\ &\quad \times < (l_1\tfrac{1}{2})\tfrac{1}{2}(l_1'\tfrac{1}{2})\tfrac{1}{2}; TM_T|\hat{O}(\tau)|(l_2\tfrac{1}{2})\tfrac{1}{2}(l'\tfrac{1}{2})\tfrac{1}{2}; TM_T > \\ &= \frac{1}{4}\sum_{ll'l_1l_1'} \eta_S^{ij}(ll'l_1l_1')\eta_T^{ij}(ll'l_1l_1') \end{aligned} \tag{4.5}$$

$\eta_S^{ij}(ll'l_1l_1')$ is the spin matrix element and $\eta_T^{ij}(ll'l_1l_1')$ is the isospin matrix element.

## 4.2 Spin-Isospin Operators

We now consider the operators $\hat{O}(\tau)$ and $\hat{O}(\sigma)$ . In the formalism being used here we have for the isospin operator

$$\hat{O}(\tau) = \vec{\tau}_i \cdot \vec{\tau}_j \tag{4.6}$$

and for the spin operator

$$\hat{O}(\sigma) = \vec{\sigma}_i \cdot \vec{q}\,\vec{\sigma}_j \cdot \vec{q} \tag{4.7}$$

The isospin operator is a straight forward case, all that is to be done is to substitute the operator into the appropriate matrix element and evaluate. With the spin case, however, it needs first to be manipulated to factor out the spin dependent term.

Consider equation (4.7). From deShalit & Talmi page 521 [DeshTal] we have the formula converting the dot product of vectors rank $k$ to the cross product of the same vectors

$$(T^{(k)} \cdot U^{(k)}) = (-)^k\sqrt{2k+1}\,[T^{(k)} \times U^{(k)}]_0^0\,, \tag{4.8}$$

where

$$[T^{k_1} \times T^{k_2}]^{k_3}_{n_3} = \sum_{n_1 n_2} C^{k_1 k_2 k_3}_{n_1 n_2 n_3}\ T^{k_1}_{n_1}\, T^{k_2}_{n_2}\ , \tag{4.9}$$

and $C^{k_1 k_2 k_3}_{n_1 n_2 n_3}$ is a Clebsch-Gordon coefficient. Substituting (4.8) into the right hand side (RHS) of (4.7)

$$\begin{aligned} \vec{\sigma}_i \cdot \vec{q}\, \vec{\sigma}_j \cdot \vec{q} &= (-)^1\sqrt{3}\,[\vec{\sigma}_i \times \vec{q}]^0_0\,(-)^1\sqrt{3}\,[\vec{\sigma}_j \times \vec{q}]^0_0 \\ &= 3\,[\vec{\sigma}_i \times \vec{q}]^0_0\,[\vec{\sigma}_j \times \vec{q}]^0_0 \\ &= 3\left[[\vec{\sigma}_i \times \vec{q}]^0_0 \times [\vec{\sigma}_j \times \vec{q}]^0_0\right]^0_0 \end{aligned} \tag{4.10}$$

Using the recoupling scheme along the lines of the recoupling of four angular momenta [Ed57, eqn 6.4.2] we can rearrange the RHS of (4.10) into

$$3\sum_{\lambda m}(2\lambda+1)^{\frac{1}{2}}\left[[\vec{\sigma}_i \times \vec{\sigma}_j]^\lambda_m \times [\vec{q} \times \vec{q}]^\lambda_m\right]^0_0 \tag{4.11}$$

Now concentrate on just the $\vec{q} \times \vec{q}$ term. Using equation 5.1.4 of Edmonds [Ed57], namely

$$\begin{aligned} \vec{q}_m &= \left(\frac{4\pi}{3}\right)^{\frac{1}{2}} \mathcal{Y}_{1m}(\vec{q}) \\ &= q\left(\frac{4\pi}{3}\right)^{\frac{1}{2}} Y_{1m}(\hat{q}) \end{aligned} \tag{4.12}$$

with the $Y_{1m}(\hat{q})$ a spherical harmonic. Substituting this into $[\vec{q} \times \vec{q}]^\lambda_m$ gives

$$[\vec{q} \times \vec{q}]^\lambda_m = q^2 \sum_{m_1 m_2} \frac{4\pi}{3}[Y_{1m_1}(\hat{q}) \times Y_{1m_2}(\hat{q})]^\lambda_m\ . \tag{4.13}$$

Using (4.9) we find that (4.13) can be rewritten as

$$\sum_{m_1 m_2} \frac{4\pi}{3} q^2 C^{1\ 1\ \lambda}_{m_1 m_2 m}\, Y_{1m_1}(\hat{q})\, Y_{1m_2}(\hat{q})\ . \tag{4.14}$$

From equation 5.1.6 of ([Ed57]) we have

$$\mathcal{Y}_{l_1 m_1}(r)\,\mathcal{Y}_{l_2 m_2}(r) = \sum_{lm}\left[\frac{(2l_1+1)(2l_2+1)}{4\pi(2l+1)}\right]^{\frac{1}{2}} C^{l_1\ l_2\ l}_{m_1 m_2 m} C^{l_1 l_2 l}_{0\,0\,0}\, r^{l_1+l_2-l}\,\mathcal{Y}_{lm}(r)\,. \tag{4.15}$$

Rewriting this in terms of $Y_{lm}(\hat{r})$ gives

$$Y_{l_1 m_1}(\hat{r})\,Y_{l_2 m_2}(\hat{r}) = \sum_{lm}\left[\frac{(2l_1+1)(2l_2+1)}{4\pi(2l+1)}\right]^{\frac{1}{2}} C^{l_1\ l_2\ l}_{m_1 m_2 m}\, C^{l_1 l_2 l}_{0\,0\,0}\, Y_{lm}(\hat{r})\,, \tag{4.16}$$

and if we substitute (4.16) into (4.14) we find that the RHS of (4.13) can be written as

$$\sum_{m_1 m_2 \lambda' \mu} \frac{4\pi}{3} q^2 C^{1\ 1\ \lambda}_{m_1 m_2 m}\left[\frac{3.3}{4\pi(2\lambda'+1)}\right]^{\frac{1}{2}} C^{1\ 1\ \lambda'}_{m_1 m_2 \mu} C^{1\,1\,\lambda'}_{0\,0\,0}\, Y_{\lambda'\mu}(\hat{q})\,. \tag{4.17}$$

Converting the Clebsch-Gordon coefficients in (4.17) into 3-j symbols using the relation

$$C^{j_1\ j_2\ j_3}_{m_1 m_2 m_3} = (-)^{-m_3}(2j_3+1)^{\frac{1}{2}}\begin{pmatrix} j_1 & j_2 & j_3 \\ m_1 & m_2 & m_3 \end{pmatrix} \tag{4.18}$$

gives, after some manipulation

$$\begin{aligned}
[\vec{q}\times\vec{q}]^{\lambda}_{m} &= \sum_{m_1 m_2 \lambda' \mu} \frac{\sqrt{4\pi}\,q^2}{(2\lambda'+1)^{\frac{1}{2}}}(-)^{-m}(2\lambda+1)^{\frac{1}{2}}\begin{pmatrix} 1 & 1 & \lambda \\ m_1 & m_2 & m \end{pmatrix}(-)^{-\mu}(2\lambda'+1)^{\frac{1}{2}} \\
&\qquad \times \begin{pmatrix} 1 & 1 & \lambda \\ m_1 & m_2 & \mu \end{pmatrix}(-)^{0}(2\lambda'+1)^{\frac{1}{2}}\begin{pmatrix} 1\,1\,\lambda' \\ 0\,0\,0 \end{pmatrix} Y_{\lambda'\mu}(\hat{q}) \\
&= \sum_{m_1 m_2 \lambda' \mu} \sqrt{4\pi}\,q^2(-)^{m+\mu}(2\lambda+1)^{\frac{1}{2}}(2\lambda'+1)^{\frac{1}{2}}\begin{pmatrix} 1 & 1 & \lambda \\ m_1 & m_2 & m \end{pmatrix} \\
&\qquad \times \begin{pmatrix} 1 & 1 & \lambda' \\ m_1 & m_2 & \mu \end{pmatrix}\begin{pmatrix} 1\,1\,\lambda \\ 0\,0\,0 \end{pmatrix} Y_{\lambda'\mu}(\hat{q})
\end{aligned} \tag{4.19}$$

From [Ed57, eqn 3.7.8] we have the relationship

$$\sum_{m_1 m_2} \begin{pmatrix} j_1 & j_2 & j_3 \\ m_1 & m_2 & m_3 \end{pmatrix} \begin{pmatrix} j_1 & j_2 & j_3' \\ m_1 & m_2 & m_3' \end{pmatrix} = (2j_3+1)^{-1} \delta(j_3' j_3)\, \delta(m_3' m_3)\, \delta(j_1 j_2 j_3)\,. \tag{4.20}$$

Using this in (4.19) gives

$$[\vec{q} \times \vec{q}]^{\lambda}_{m} = \sqrt{4\pi}\, q^2 (-)^{2m} (2\lambda+1)(2\lambda+1)^{-1} \begin{pmatrix} 1 & 1 & \lambda \\ 0 & 0 & 0 \end{pmatrix} Y_{\lambda\mu}(\hat{q})\, \delta(11\lambda)\,. \tag{4.21}$$

This will only hold when $\lambda$ is even and only for the values $\lambda = 0, 2$. Using the above we find that (4.13) reduces to

$$[\vec{q} \times \vec{q}]^{\lambda}_{m} = \sqrt{4\pi}\, q^2 \begin{pmatrix} 1 & 1 & \lambda \\ 0 & 0 & 0 \end{pmatrix} Y_{\lambda m}(\hat{q})\,, \tag{4.22}$$

which we substitute into (4.11) to give

$$\vec{\sigma}_i \cdot \vec{q} \vec{\sigma}_j \cdot \vec{q} = \sum_{\lambda m} \sqrt{4\pi} q^2 (2\lambda+1)^{\frac{1}{2}} \begin{pmatrix} 1 & 1 & \lambda \\ 0 & 0 & 0 \end{pmatrix} \left[ [\vec{\sigma}_i \times \vec{\sigma}_j]^{\lambda}_{m} \times Y_{\lambda m}(\hat{q}) \right]^{0}_{0}\,. \tag{4.23}$$

This gives both the scalar ($\lambda = 0$) and tensor ($\lambda = 2$) terms.

### 4.2.1 Scalar Spin-Isospin Matrix Element

For $\lambda = 0$, (4.23) reduces to

$$(\vec{\sigma}_i \cdot \vec{q}\, \vec{\sigma}_j \cdot \vec{q})_{\lambda=0} = \frac{1}{3} q^2 \vec{\sigma}_i \cdot \vec{\sigma}_j \tag{4.24}$$

We will now look at one example in particular to show the method applied to evaluate the matrix elements. The potential we shall consider is $v^{qe}_{36}$ from equation (3.23). In this case the only spin dependent part of the operator is $\vec{\sigma}_i \cdot \vec{\sigma}_j$. Going back to the expression

used for the spin isospin matrix element in (4.5) we find :

$$M^{ij}(\hat{O}(\sigma)\hat{O}(\tau)) =< \varphi_{\mathbf{a}}^{\sigma\tau}\varphi_{\mathbf{b}}^{\sigma\tau}|\vec{\tau}_i\cdot\vec{\tau}_j\vec{\sigma}_i\cdot\vec{\sigma}_j 9P_{36}^{\sigma\tau}|\varphi_{\mathbf{a}}^{\sigma\tau}\varphi_{\mathbf{b}}^{\sigma\tau} > \tag{4.25}$$

If we substitute this into the spin-isospin matrix element written using equ. (4.5) and use the isospin operator $\vec{\tau}_i\cdot\vec{\tau}_j$ this will give us, up to a constant factor

$$M^{ij}(\hat{O}(\sigma)\hat{O}(\tau)) = \frac{1}{4}\sum_{ll'l_1l_1'}\eta_S^{ij}(ll'l_1l_1')\eta_T^{ij}(ll'l_1l_1') \tag{4.26}$$

with

$$\begin{aligned}\eta_S^{ij}(ll'l_1l_1') &= < (l\tfrac{1}{2})\tfrac{1}{2}(l'\tfrac{1}{2})\tfrac{1}{2};SM|\vec{\sigma}_i\cdot\vec{\sigma}_j P_{36}^{\sigma}|(l_1\tfrac{1}{2})\tfrac{1}{2}(l_1'\tfrac{1}{2})\tfrac{1}{2};SM > \\ \eta_T^{ij}(ll'l_1l_1') &= < (l\tfrac{1}{2})\tfrac{1}{2}(l'\tfrac{1}{2})\tfrac{1}{2};TM_T|\vec{\tau}_i\cdot\vec{\tau}_j P_{36}^{\tau}|(l_1\tfrac{1}{2})\tfrac{1}{2}(l_1'\tfrac{1}{2})\tfrac{1}{2};TM_T >\end{aligned} \tag{4.27}$$

As both the spin and isospin have the same structure only one equation of (4.27) needs to be solved. As an example the term $\eta_S^{36}(ll'l_1l_1')$ for diagram (c) of Fig 3.1 will be calculated below. We have

$$\eta_S^{36}(ll'l_1l_1') =< (l\tfrac{1}{2})\tfrac{1}{2}(l'\tfrac{1}{2})\tfrac{1}{2};SM|\vec{\sigma}_3\cdot\vec{\sigma}_6 P_{36}^{\sigma}P^{\sigma}|(l_1\tfrac{1}{2})\tfrac{1}{2}(l_1'\tfrac{1}{2})\tfrac{1}{2};SM > \tag{4.28}$$

Recoupling this so that we have the quarks on which the operators will act coupled together yields :

$$\begin{aligned}\eta_S^{36}(ll'l_1l_1') = \sum_{l_{1245},l_{36}} 2[(2l_{1245}+1)(2l_{36}+1)]^{\frac{1}{2}} \begin{Bmatrix} l_1 & l_1' & l_{1245} \\ \frac{1}{2} & \frac{1}{2} & l_{36} \\ \frac{1}{2} & \frac{1}{2} & 1 \end{Bmatrix} \\ \times < (l\tfrac{1}{2})\tfrac{1}{2}(l'\tfrac{1}{2})\tfrac{1}{2};SM|\vec{\sigma}_3\cdot\vec{\sigma}_6 P_{36}^{\sigma}|(l_1l_1')l_{1245}(\tfrac{1}{2}\tfrac{1}{2})l_{36};SM >\end{aligned} \tag{4.29}$$

| $M^{ij}_{scal}$ | Spin-Isospin Operators |
|---|---|
| $M^{36(qe)}_{scal}$ | $\frac{9}{4}\left[(1-\frac{1}{27}\vec{\tau}^{\mathbf{a}}_N\cdot\vec{\tau}^{\mathbf{b}}_N)\mathbf{1}^{\mathbf{a}}_N\cdot\mathbf{1}^{\mathbf{b}}_N-\frac{1}{27}(1-\frac{25}{27}\vec{\tau}^{\mathbf{a}}_N\cdot\vec{\tau}^{\mathbf{b}}_N)\vec{\sigma}^{\mathbf{a}}_N\cdot\vec{\sigma}^{\mathbf{b}}_N\right]$ |
| $M^{25(qe)}_{scal}$ | $\frac{25}{36}\left[(1+\frac{1}{75}\vec{\tau}^{\mathbf{a}}_N\cdot\vec{\tau}^{\mathbf{b}}_N)\mathbf{1}^{\mathbf{a}}_N\cdot\mathbf{1}^{\mathbf{b}}_N+\frac{1}{75}(1+\frac{61}{3}\vec{\tau}^{\mathbf{a}}_N\cdot\vec{\tau}^{\mathbf{b}}_N)\vec{\sigma}^{\mathbf{a}}_N\cdot\vec{\sigma}^{\mathbf{b}}_N\right]$ |
| $M^{26(qe)}_{scal}$ | $\frac{239}{216}\left[(1+\frac{37}{239}\vec{\tau}^{\mathbf{a}}_N\cdot\vec{\tau}^{\mathbf{b}}_N)\mathbf{1}^{\mathbf{a}}_N\cdot\mathbf{1}^{\mathbf{b}}_N+\frac{37}{239}(1+\frac{77}{111}\vec{\tau}^{\mathbf{a}}_N\cdot\vec{\tau}^{\mathbf{b}}_N)\vec{\sigma}^{\mathbf{a}}_N\cdot\vec{\sigma}^{\mathbf{b}}_N\right]$ |
| $M^{23(qe)}_{scal}$ | $\frac{239}{216}\left[(1+\frac{37}{239}\vec{\tau}^{\mathbf{a}}_N\cdot\vec{\tau}^{\mathbf{b}}_N)\mathbf{1}^{\mathbf{a}}_N\cdot\mathbf{1}^{\mathbf{b}}_N+\frac{37}{239}(1+\frac{77}{111}\vec{\tau}^{\mathbf{a}}_N\cdot\vec{\tau}^{\mathbf{b}}_N)\vec{\sigma}^{\mathbf{a}}_N\cdot\vec{\sigma}^{\mathbf{b}}_N\right]$ |
| $M^{12(qe)}_{scal}$ | $\frac{5}{4}\left[(1+\frac{13}{45}\vec{\tau}^{\mathbf{a}}_N\cdot\vec{\tau}^{\mathbf{b}}_N)\mathbf{1}^{\mathbf{a}}_N\cdot\mathbf{1}^{\mathbf{b}}_N+\frac{13}{45}(1+\frac{205}{117}\vec{\tau}^{\mathbf{a}}_N\cdot\vec{\tau}^{\mathbf{b}}_N)\vec{\sigma}^{\mathbf{a}}_N\cdot\vec{\sigma}^{\mathbf{b}}_N\right]$ |

Table 4.1: **The spin-isospin matrix elements for the scalar term which have quark exchange**

If we let $\vec{\sigma}_3\cdot\vec{\sigma}_6 P^{\sigma}_{36}$ act to the right and then recouple we find :

$$\eta^{36}_S(ll'l_1l'_1)=\sum_{l_{1245},l_{36}}4(2l_{1245}+1)(2l_{36}+1)(-)^{l_{36}+1}(2(-)^{l_{36}+1}-1)\left\{\begin{array}{ccc} l_1 & l'_1 & l_{1245}\\ \frac{1}{2} & \frac{1}{2} & l_{36}\\ \frac{1}{2} & \frac{1}{2} & 1\end{array}\right\}^2 \quad (4.30)$$

This can now be substituted back into the spin-isospin matrix element to give us

$$M^{36}(\hat{O}(\sigma)\hat{O}(\tau)) \;=\; \frac{1}{4}\sum_{l,l',l_1,l'_1}\eta^{36}_S(ll'l_1l'_1)\eta^{36}_T(ll'l_1l'_1) \quad (4.31)$$

| $M^{ij}_{scal}$ | Spin-Isospin Operators |
|---|---|
| $M^{36(nqe)}_{scal}$ | $\frac{25}{81}\vec{\tau}^{\mathbf{a}}_N \cdot \vec{\tau}^{\mathbf{b}}_N \vec{\sigma}^{\mathbf{a}}_N \cdot \vec{\sigma}^{\mathbf{b}}_N$ |
| $M^{cen}_{scal}$ | $\frac{1}{4}\left[(1+\frac{1}{9}\vec{\tau}^{\mathbf{a}}_N \cdot \vec{\tau}^{\mathbf{b}}_N)\mathbf{1}^{\mathbf{a}}_N \cdot \mathbf{1}^{\mathbf{b}}_N + \frac{1}{9}(1+\frac{25}{9}\vec{\tau}^{\mathbf{a}}_N \cdot \vec{\tau}^{\mathbf{b}}_N)\vec{\sigma}^{\mathbf{a}}_N \cdot \vec{\sigma}^{\mathbf{b}}_N\right]$ |
| $M^{(s)}_{scal}$ | 5 |
| $M^{12(qe)}_{scal}$ | 5 |

Table 4.2: The spin-isospin matrix elements for the scalar terms which have no quark exchange

where

$$\eta^{36}_S(ll'l_1l'_1) = \sum_{l_{1245},l_{36}} 4(2l_{1245}+1)(2l_{36}+1)(-)^{l_{36}+1}(2(-)^{l_{36}+1}-1)\begin{Bmatrix} l_1 & l'_1 & l_{1245} \\ \frac{1}{2} & \frac{1}{2} & l_{36} \\ \frac{1}{2} & \frac{1}{2} & 1 \end{Bmatrix}^2$$

$$\eta^{36}_T(ll'l_1l'_1) = \sum_{\mu_{1245},\mu_{36}} 4(2\mu_{1245}+1)(2\mu_{36}+1)(-)^{\mu_{36}+1}(2(-)^{\mu_{36}+1}-1)\begin{Bmatrix} l_1 & l'_1 & \mu_{1245} \\ \frac{1}{2} & \frac{1}{2} & \mu_{36} \\ \frac{1}{2} & \frac{1}{2} & 1 \end{Bmatrix}^2 \tag{4.32}$$

This can be solved for each value of S and T, which is what we require. The format for the solutions to the matrix elements is to write them in terms of nucleon spin and isospin operators. These are given in Table 4.1 and Table 4.2. In Appendix C we give the steps taken to get from (4.31) to the form listed in the Tables 4.1, 4.2.

### 4.2.2 Tensor Spin-Isospin Matrix Element

The tensor term occurs when we have $\lambda = 2$ . This then gives for the spin operator in (4.23)

$$(\vec{\sigma}_i \cdot \vec{q}\,\vec{\sigma}_j \cdot \vec{q})_{\lambda=2} = \sum_m \sqrt{4\pi}\, q^2 \sqrt{\frac{2}{15}}\, [\vec{\sigma}_i \times \vec{\sigma}_j]^2_m \cdot Y_{2m}(\hat{q}) \tag{4.33}$$

Our spin-isospin matrix element now becomes

$$M^{ij}_{tens}(\hat{O}(\sigma)\hat{O}(\tau)) \\ =< \varphi^{\sigma\tau}_{\mathbf{a}}\varphi^{\sigma\tau}_{\mathbf{b}}|\vec{\tau}_i \cdot \vec{\tau}_j \sum_m \sqrt{4\pi}\, q^2 \sqrt{\frac{2}{15}}\, [\vec{\sigma}_i \times \vec{\sigma}_j]^2_m \cdot Y_{2m}(\hat{q})(1 - 9P^{\sigma\tau}_{36})|\varphi^{\sigma\tau}_{\mathbf{a}}\varphi^{\sigma\tau}_{\mathbf{b}} > \tag{4.34}$$

We now need to evaluate the spin-isospin matrix elements for the tensor case. The isospin matrix element is the same as for the scalar term, the only change being for the spin matrix element. We will leave out the constants to make the presentation more transparent and do the more complicated case as an example. This is the case with the quark exchange operator $P^{\sigma\tau}_{36}$ included.

We know that

$$[\vec{\sigma}_i \times \vec{\sigma}_j]^2_m \cdot Y_{2m}(\hat{q}) = \frac{\sqrt{5}}{\sqrt{24\pi}} S_{ij}(\hat{q})\,, \tag{4.35}$$

and substituting this into equation (4.33) gives us the relationship

$$(\vec{\sigma}_i \cdot \vec{q}\,\vec{\sigma}_j \cdot \vec{q})_{\lambda=2} = \frac{q^2}{3} S_{ij}(\hat{q})\,, \tag{4.36}$$

which we will later be able to relate to the nucleon tensor operator $S_{\mathbf{ab}}(\hat{q})$

We can now calculate the matrix element $M^{ij}_{tens}(\hat{O}(\sigma)\hat{O}(\tau))$ for the quark exchange case.

$$M^{ij}_{tens}(\hat{O}(\sigma)\hat{O}(\tau)) =< \varphi^{\sigma\tau}_{\mathbf{a}}\varphi^{\sigma\tau}_{\mathbf{b}}|\vec{\tau}_i \cdot \vec{\tau}_j \sum_m [\vec{\sigma}_i \times \vec{\sigma}_j]^2_m \cdot Y_{2m}(\hat{q}) P^{\sigma\tau}_{36}|\varphi^{\sigma\tau}_{\mathbf{a}}\varphi^{\sigma\tau}_{\mathbf{b}} > \tag{4.37}$$

Using the rule from Warke and Shanker [WaSh80] we can separate the spin and isospin components, as was done for the scalar case. This gives us an isospin term which is the same as for the scalar case and leaving the spin term $\eta_S(ll'l_1l_1')$ to be evaluated.

$$
\begin{aligned}
&M^{ij}_{tens}(\hat{O}(\sigma)\hat{O}(\tau)) \\
&\quad = \frac{1}{4}\sum_{ll'l_1l_1';m} < (l\tfrac{1}{2})\tfrac{1}{2}(l'\tfrac{1}{2})\tfrac{1}{2}; SM|[\vec{\sigma}_i \times \vec{\sigma}_j]^2_m \cdot Y_{2m}(\hat{q})P^{\sigma}_{36}|(l_1\tfrac{1}{2})\tfrac{1}{2}(l_1'\tfrac{1}{2})\tfrac{1}{2}; SM > \\
&\qquad \times < (l\tfrac{1}{2})\tfrac{1}{2}(l'\tfrac{1}{2})\tfrac{1}{2}; TM_T|\vec{\tau}_i \cdot \vec{\tau}_j P^{\tau}_{36}|(l_1\tfrac{1}{2})\tfrac{1}{2}(l_1'\tfrac{1}{2})\tfrac{1}{2}; TM_T > , \\
&\quad = \frac{1}{4}\sum_{ll'l_1l_1'} \eta^{ij}_S(ll'l_1l_1')\eta^{ij}_T(ll'l_1l_1') \, . \qquad (4.38)
\end{aligned}
$$

We now concentrate on the spin term

$$
\begin{aligned}
\eta^{ij}_S(ll'l_1l_1') &= < (l\tfrac{1}{2})\tfrac{1}{2}(l'\tfrac{1}{2})\tfrac{1}{2}; SM|\sum_m [\vec{\sigma}_i \times \vec{\sigma}_j]^2_m \cdot Y_{2m}(\hat{q})P^{\sigma}_{36}|(l_1\tfrac{1}{2})\tfrac{1}{2}(l_1'\tfrac{1}{2})\tfrac{1}{2}; SM > \\
&= \sum_m Y_{2m}(\hat{q}) < (l\tfrac{1}{2})\tfrac{1}{2}(l'\tfrac{1}{2})\tfrac{1}{2}; SM|[\vec{\sigma}_i \times \vec{\sigma}_j]^2_m P^{\sigma}_{36}|(l_1\tfrac{1}{2})\tfrac{1}{2}(l_1'\tfrac{1}{2})\tfrac{1}{2}; SM > \, . \qquad (4.39)
\end{aligned}
$$

We need to recouple the RHS to get the quarks 3 and 6 coupled together to be able to operate to the right with $P^{\sigma}_{36}$ . This gives

$$
\begin{aligned}
\eta^{ij}_S(ll'l_1l_1') &= \sum_{m,l_{1245},l_{36}} Y_{2m}(\hat{q}) 2\left[(2l_{1245}+1)(2l_{36}+1)\right]^{\frac{1}{2}} \begin{Bmatrix} l_1 & l_1' & l_{1245} \\ \frac{1}{2} & \frac{1}{2} & l_{36} \\ \frac{1}{2} & \frac{1}{2} & 1 \end{Bmatrix} \\
&\qquad \times < (l\tfrac{1}{2})\tfrac{1}{2}(l'\tfrac{1}{2})\tfrac{1}{2}; SM|[\vec{\sigma}_i \times \vec{\sigma}_j]^2_m P^{\sigma}_{36}|(l_1l_1')l_{1245}(\tfrac{1}{2}\tfrac{1}{2})l_{36}; SM > , \qquad (4.40)
\end{aligned}
$$

and after operating to the right with $P^{\sigma}_{36}$ we get,

$$\eta_S^{ij}(ll'l_1l_1') = \sum_{m,l_{1245},l_{36}} Y_{2m}(\hat{q}) 2\,[(2l_{1245}+1)(2l_{36}+1)]^{\frac{1}{2}} \begin{Bmatrix} l_1 & l_1' & l_{1245} \\ \frac{1}{2} & \frac{1}{2} & l_{36} \\ \frac{1}{2} & \frac{1}{2} & 1 \end{Bmatrix} (-)^{l_{36}+1}$$
$$\times < (l\tfrac{1}{2})\tfrac{1}{2}(l'\tfrac{1}{2})\tfrac{1}{2}; SM|[\vec{\sigma}_i \times \vec{\sigma}_j]^2_m|(l_1l_1')l_{1245}(\tfrac{1}{2}\tfrac{1}{2})l_{36}; SM > \ . \qquad (4.41)$$

After recoupling this takes the form :

$$\eta_S^{ij}(ll'l_1l_1') = \sum_{m,l_{1245},l_{36},\lambda\kappa} Y_{2m}(\hat{q}) 2(2l_{1245}+1)(2l_{36}+1)[(2\lambda+1)(2\kappa+1)]^{\frac{1}{2}}(-)^{l_{36}+1}$$
$$\times \begin{Bmatrix} l_1 & l_1' & l_{1245} \\ \frac{1}{2} & \frac{1}{2} & l_{36} \\ \frac{1}{2} & \frac{1}{2} & 1 \end{Bmatrix} \begin{Bmatrix} l_1 & l_1' & l_{1245} \\ \frac{1}{2} & \frac{1}{2} & l_{36} \\ \lambda & \kappa & 1 \end{Bmatrix}$$
$$\times < (l\tfrac{1}{2})\tfrac{1}{2}(l'\tfrac{1}{2})\tfrac{1}{2}; SM|[\vec{\sigma}_i \times \vec{\sigma}_j]^2_m|(l_1\tfrac{1}{2})\lambda(l_1'\tfrac{1}{2})\kappa; SM > \ . \qquad (4.42)$$

Using the Wigner-Eckart theorem [Ed57, 5.4.1] to reduce the matrix element in (4.42) gives,

$$\eta_S^{ij}(ll'l_1l_1') = \sum_{m,l_{1245},l_{36},\lambda\kappa} Y_{2m}(\hat{q})\, 2\,(2l_{1245}+1)(2l_{36}+1)[(2\lambda+1)(2\kappa+1)]^{\frac{1}{2}}$$
$$\times \begin{Bmatrix} l_1 & l_1' & l_{1245} \\ \frac{1}{2} & \frac{1}{2} & l_{36} \\ \frac{1}{2} & \frac{1}{2} & 1 \end{Bmatrix} \begin{Bmatrix} l_1 & l_1' & l_{1245} \\ \frac{1}{2} & \frac{1}{2} & l_{36} \\ \lambda & \kappa & 1 \end{Bmatrix} (-)^{l_{36}+1}(-)^{S-M} \begin{pmatrix} S & 2 & S \\ -M & m & M \end{pmatrix}$$
$$\times < (l\tfrac{1}{2})\tfrac{1}{2}(l'\tfrac{1}{2})\tfrac{1}{2}; S \,||\, [\vec{\sigma}_i \times \vec{\sigma}_j]^2_m \,||\, (l_1\tfrac{1}{2})\lambda(l_1'\tfrac{1}{2})\kappa; S > \ . \qquad (4.43)$$

From deShalit & Feschbach [DeshTal, page 522] we use the rule for separating operators

to get

$$\eta_S^{ij}(ll'l_1l_1') = \sum_{m,l_{1245},l_{36},\lambda\kappa} Y_{2m}(\hat{q})\, 2\,(2l_{1245}+1)(2l_{36}+1)[(2\lambda+1)(2\kappa+1)]^{\frac{1}{2}}$$
$$\times \begin{Bmatrix} l_1 & l_1' & l_{1245} \\ \frac{1}{2} & \frac{1}{2} & l_{36} \\ \frac{1}{2} & \frac{1}{2} & 1 \end{Bmatrix} \begin{Bmatrix} l_1 & l_1' & l_{1245} \\ \frac{1}{2} & \frac{1}{2} & l_{36} \\ \lambda & \kappa & 1 \end{Bmatrix} \begin{Bmatrix} \frac{1}{2} & \frac{1}{2} & S \\ \lambda & \kappa & S \\ 1 & 1 & 2 \end{Bmatrix}$$
$$\times \begin{pmatrix} S & 2 & S \\ -M & m & M \end{pmatrix} \sqrt{5}(2S+1)(-)^{l_{36}+1}(-)^{S-M}$$
$$\times < (l_1\tfrac{1}{2})\tfrac{1}{2}||\vec{\sigma}_i||(l_1\tfrac{1}{2})\lambda >< (l_1'\tfrac{1}{2})\tfrac{1}{2}||\vec{\sigma}_j||(l_1'\tfrac{1}{2})\kappa > \ . \qquad (4.44)$$

To give a solution in terms of nucleon operators we need to first evaluate the spin matrix element at the nucleon level. The tensor operator is

$$S_{\mathbf{ab}}(\hat{q}) = Y_{2m}(\hat{q}) \cdot [\vec{\sigma}_{\mathbf{a}} \times \vec{\sigma}_{\mathbf{b}}]^2_m \ . \qquad (4.45)$$

The matrix element for the nucleon case is then

$$\eta^N(ll'l_1l_1') = < (l\tfrac{1}{2})\tfrac{1}{2}(l'\tfrac{1}{2})\tfrac{1}{2}; SM|Y_{2m}(\hat{q}) \cdot [\vec{\sigma}_{\mathbf{a}} \times \vec{\sigma}_{\mathbf{b}}]^2_m|(l_1\tfrac{1}{2})\tfrac{1}{2}(l_1'\tfrac{1}{2})\tfrac{1}{2}; SM >$$

$$= \sum_m Y_{2m}(\hat{q}) < (l\tfrac{1}{2})\tfrac{1}{2}(l'\tfrac{1}{2})\tfrac{1}{2}; SM|[\vec{\sigma}_{\mathbf{a}} \times \vec{\sigma}_{\mathbf{b}}]^2_m|(l_1\tfrac{1}{2})\tfrac{1}{2}(l_1'\tfrac{1}{2})\tfrac{1}{2}; SM > \qquad (4.46)$$

Using the Wigner-Eckart theorem [Ed57, 5.4.1] this becomes

$$\eta^N(ll'l_1l_1') = \sum_m Y_{2m}(\hat{q})(-)^{S-m} \begin{pmatrix} S & 2 & S \\ -M & m & M \end{pmatrix}$$
$$\times < (l\tfrac{1}{2})\tfrac{1}{2}(l'\tfrac{1}{2})\tfrac{1}{2}; S||[\vec{\sigma}_a \times \vec{\sigma}_b]^2_m||(l_1\tfrac{1}{2})\tfrac{1}{2}(l_1'\tfrac{1}{2})\tfrac{1}{2}; S > . \qquad (4.47)$$

From deShalit & Talmi [DeshTal, page 522] this can be written as

$$\eta^N(ll'l_1l_1') = \sum_m Y_{2m}(\hat{q})(-)^{S-m}\begin{pmatrix} S & 2 & S \\ -M & m & M \end{pmatrix}\sqrt{5}(2S+1)\begin{Bmatrix} \frac{1}{2} & \frac{1}{2} & S \\ \frac{1}{2} & \frac{1}{2} & S \\ 1 & 1 & 2 \end{Bmatrix}$$
$$\times < (l\tfrac{1}{2})\tfrac{1}{2}||\vec{\sigma}_{\mathbf{a}}||(l_1\tfrac{1}{2})\tfrac{1}{2} >< (l'\tfrac{1}{2})\tfrac{1}{2}||\vec{\sigma}_{\mathbf{b}}||(l_1'\tfrac{1}{2})\tfrac{1}{2} > . \qquad (4.48)$$

Substituting the results

$$< (l\tfrac{1}{2})\tfrac{1}{2}; S||\vec{\sigma}_{\mathbf{a}}||(l_1\tfrac{1}{2})\tfrac{1}{2}; S >= \sqrt{6}$$
$$< (l'\tfrac{1}{2})\tfrac{1}{2}; S||\vec{\sigma}_{\mathbf{b}}||(l_1'\tfrac{1}{2})\tfrac{1}{2}; S >= \sqrt{6} \qquad (4.49)$$

leads to

$$\eta^N = 6\sum_m Y_{2m}(\hat{q})(-)^{S-m}\begin{pmatrix} S & 2 & S \\ -M & m & M \end{pmatrix}\sqrt{5}(2S+1)\begin{Bmatrix} \frac{1}{2} & \frac{1}{2} & S \\ \frac{1}{2} & \frac{1}{2} & S \\ 1 & 1 & 2 \end{Bmatrix} \qquad (4.50)$$

We can use this to write the quark tensor operator in terms of the nucleon tensor operator.

Rewriting equation (4.48) gives us

$$\eta_S^{ij}(ll'l_1l_1') = \sum_{l_{1245},l_{36},\lambda,\kappa} 2(2l_{1245}+1)(2l_{36}+1)[(2\lambda+1)(2\kappa+1)]^{\frac{1}{2}}(-)^{l_{36}+1}$$
$$\times\begin{Bmatrix} l_1 & l_1' & l_{1245} \\ \frac{1}{2} & \frac{1}{2} & l_{36} \\ \frac{1}{2} & \frac{1}{2} & 1 \end{Bmatrix}\begin{Bmatrix} l_1 & l_1' & l_{1245} \\ \frac{1}{2} & \frac{1}{2} & l_{36} \\ \lambda & \kappa & 1 \end{Bmatrix}\begin{Bmatrix} \frac{1}{2} & \frac{1}{2} & S \\ \lambda & \kappa & S \\ 1 & 1 & 2 \end{Bmatrix}\begin{Bmatrix} \frac{1}{2} & \frac{1}{2} & S \\ \frac{1}{2} & \frac{1}{2} & S \\ 1 & 1 & 2 \end{Bmatrix}^{-1}$$
$$\times\frac{1}{6} < (l\tfrac{1}{2})\tfrac{1}{2}||\vec{\sigma}_i||(l_1\tfrac{1}{2})\tfrac{1}{2} >< (l'\tfrac{1}{2})\tfrac{1}{2}; S||\vec{\sigma}_j||(l_1'\tfrac{1}{2})\tfrac{1}{2}; S > S_{\mathbf{ab}}(\hat{q}) \qquad (4.51)$$

where for $S = 1$ :

$$\left\{ \begin{array}{ccc} \frac{1}{2} & \frac{1}{2} & S \\ \frac{1}{2} & \frac{1}{2} & S \\ 1 & 1 & 2 \end{array} \right\} = \frac{1}{9} \tag{4.52}$$

The solution to each of the quark exchange tensor cases is then done separately. Once we have a solution for the spin- isospin matrix elements we can write these in terms of nucleon operators. These are given in Table 4.3.

| $M_{tens}^{ij}$ | Tensor Spin-Isospin Operators |
|---|---|
| $M_{tens}^{36(nqe)}$ | $\frac{25}{81}\vec{\tau}_N^{\mathbf{a}} \cdot \vec{\tau}_N^{\mathbf{b}} S_{\mathbf{ab}}(\hat{R})$ |
| $M_{tens}^{36(qe)}$ | $\frac{1}{6}\left(1 - \frac{25}{162}\vec{\tau}_N^{\mathbf{a}} \cdot \vec{\tau}_N^{\mathbf{b}}\right) S_{\mathbf{ab}}(\hat{R})$ |
| $M_{tens}^{25(qe)}$ | $\frac{1}{108}\left(1 + \frac{7}{3}\vec{\tau}_N^{\mathbf{a}} \cdot \vec{\tau}_N^{\mathbf{b}}\right) S_{\mathbf{ab}}(\hat{R})$ |
| $M_{tens}^{26(qe)}$ | $\frac{1}{36}\left(1 - \frac{5}{9}\vec{\tau}_N^{\mathbf{a}} \cdot \vec{\tau}_N^{\mathbf{b}}\right) S_{\mathbf{ab}}(\hat{R})$ |
| $M_{tens}^{23(qe)}$ | $\frac{1}{36}\left(1 - \frac{5}{9}\vec{\tau}_N^{\mathbf{a}} \cdot \vec{\tau}_N^{\mathbf{b}}\right) S_{\mathbf{ab}}(\hat{R})$ |

Table 4.3: The solutions to the spin-isospin matrix elements for the tensor case in terms of nucleon operators.

## 4.3 The Radial Term

Going back to equation (3.20) we find that the radial matrix element is of the form

$$\eta_R^{ij} = < \varphi_{\mathbf{a}}^x \varphi_{\mathbf{b}}^x | e^{iq\cdot(r_i - r_j)} P_{36}^x (1 - (-)^{(S+T)} P^x) | \varphi_{\mathbf{a}}^x \varphi_{\mathbf{b}}^x > \tag{4.53}$$

where the wave functions are just simple harmonic oscillators given by (3.18).

Once the radial matrix elements have been calculated the radial integrals can be evaluated. The radial matrix elements have the same form for both the scalar and tensor cases. The radial matrix elements are given below.

To solve the radial integrals we need to go back to the original equations for the quark-pion potentials in (3.20).

For the scalar terms this will give us

$$M_{scal}^{ij}(R) = \int \frac{d^3q}{(2\pi)^3} \frac{q^2}{q^2 + m_\pi^2} \eta_R^{ij} \tag{4.54}$$

The tensor term will be of the form

$$M_{tens}^{ij}(R) = \int \frac{d^3q}{(2\pi)^3} \frac{q^2}{q^2 + m_\pi^2} \eta_R^{ij} S_{\mathbf{ab}}(\hat{q}) \tag{4.55}$$

An example of each of the above will be calculated below to give an idea of the method used to calculate the potentials. For simplicity we will choose the 36 exchange term. We calculate the scalar term first, and obtain the radial matrix element from Table 4.4

$$\begin{aligned} M_{scal}^{36(qe)}(R) &= \int \frac{d^3q}{(2\pi)^3} \frac{q^2}{q^2 + m_\pi^2} \eta_R^{36} \\ &= \int \frac{d^3q}{(2\pi)^3} \frac{q^2}{q^2 + m_\pi^2} e^{-\frac{\beta^2 R^2}{2}} e^{-\frac{q^2}{2\beta^2}} (1 - e^{iq\cdot R} e^{-\frac{\beta^2 R^2}{2}}) \end{aligned}$$

| $\eta_R^{ij}$ | Radial Matrix Element |
|---|---|
| $\eta_R^{36(qe)}$ | $e^{-\frac{\beta^2 R^2}{2}} e^{-\frac{q^2}{2\beta^2}} (1-(-)^{(S+T)} e^{iq\cdot R} e^{-\frac{\beta^2 R^2}{2}})$ |
| $\eta_R^{25(qe)}$ | $e^{-\frac{\beta^2 R^2}{2}} e^{-\frac{q^2}{2\beta^2}} (e^{iq\cdot R} - (-)^{(S+T)} e^{-\frac{\beta^2 R^2}{2}})$ |
| $\eta_R^{26(qe)}$ | $e^{-\frac{\beta^2 R^2}{2}} e^{-\frac{q^2}{2\beta^2}} e^{\frac{iq\cdot R}{2}} (1-(-)^{(S+T)} e^{-\frac{\beta^2 R^2}{2}})$ |
| $\eta_R^{23(qe)}$ | $e^{-\frac{\beta^2 R^2}{2}} e^{-\frac{q^2}{2\beta^2}} e^{\frac{iq\cdot R}{2}} (1-(-)^{(S+T)} e^{-\frac{\beta^2 R^2}{2}})$ |
| $\eta_R^{12(qe)}$ | $e^{-\frac{\beta^2 R^2}{2}} e^{-\frac{q^2}{2\beta^2}} (1-(-)^{(S+T)} e^{-\frac{\beta^2 R^2}{2}})$ |
| $\eta_R^{36(nqe)}$ | $e^{-\frac{q^2}{2\beta^2}} (e^{iq\cdot R} - (-)^{(S+T)} e^{-\frac{\beta^2 R^2}{2}})$ |
| $\eta_R^{12(nqe)}$ | $e^{-\frac{q^2}{2\beta^2}} (1-(-)^{(S+T)} e^{-\frac{\beta^2 R^2}{2}})$ |

Table 4.4: The radial matrix elements for all the cases, ie. quark and. non quark exchange terms.

$$= A^{36(qe)} - B^{36(qe)} \tag{4.56}$$

with

$$A^{36(qe)} = \int \frac{d^3q}{(2\pi)^3} \frac{q^2}{q^2+m_\pi^2} e^{-\frac{\beta^2 R^2}{2}} e^{-\frac{q^2}{2\beta^2}}$$

$$= 4\pi e^{-\frac{\beta^2 R^2}{2}} F \tag{4.57}$$

where

$$F = \int \frac{dq}{(2\pi)^3} q^2 \frac{q^2}{q^2 + m_\pi^2} e^{-\frac{q^2}{2\beta^2}} \tag{4.58}$$

and

$$\begin{aligned} B^{36(qe)} &= \int \frac{d^3q}{(2\pi)^3} \frac{q^2}{q^2 + m_\pi^2} e^{-\frac{\beta^2 R^2}{2}} e^{-\frac{q^2}{2\beta^2}} e^{iq\cdot R} \\ &= e^{-\frac{\beta^2 R^2}{2}} \int \frac{dq}{(2\pi)^3} q^2 \frac{q^2}{q^2 + m_\pi^2} e^{-\frac{q^2}{2\beta^2}} \int_0^{2\pi} d\phi \int_{-1}^{1} d(Cos\theta) e^{iqRCos\theta} \\ &= 4\pi e^{-\frac{\beta^2 R^2}{2}} I_s(R) \,. \end{aligned} \tag{4.59}$$

Here

$$I_s(R) = \int \frac{dq}{(2\pi)^3} q^2 \frac{q^2}{q^2 + m_\pi^2} e^{-\frac{q^2}{2\beta^2}} j_0(qR) \,, \tag{4.60}$$

and $j_0(qR)$ is the $0^{th}$ order spherical Bessel function

$$j_0(qR) = \frac{Sin(qR)}{qR} \,. \tag{4.61}$$

For the scalar case, this leads to

$$M_{scal}^{36(qe)}(R) = 4\pi e^{-\frac{\beta^2 R^2}{2}} (F - e^{-\frac{\beta^2 R^2}{2}} I_s(R)) \,. \tag{4.62}$$

Now consider the tensor case

$$\begin{aligned} M_{tens}^{36(qe)}(R) &= \int \frac{d^3q}{(2\pi)^3} \frac{q^2}{q^2 + m_\pi^2} \eta_R^{36} S_{\mathbf{ab}}(\hat{q}) \\ &= \int \frac{d^3q}{(2\pi)^3} \frac{q^2}{q^2 + m_\pi^2} e^{-\frac{\beta^2 R^2}{2}} e^{-\frac{q^2}{2\beta^2}} (1 - e^{iq\cdot R} e^{-\frac{\beta^2 R^2}{2}}) Y_{2m}(\hat{q}) \cdot [\vec{\sigma_{\mathbf{a}}} \times \vec{\sigma_{\mathbf{b}}}]_m^2 \end{aligned}$$

$$= A^{36(qe)} - B^{36(qe)} \tag{4.63}$$

with

$$\begin{aligned} A^{36(qe)} &= e^{-\frac{\beta^2 R^2}{2}} \int \frac{d^3q}{(2\pi)^3} \frac{q^2}{q^2+m_\pi^2} e^{-\frac{q^2}{2\beta^2}} Y_{2m}(\hat{q}) \cdot [\vec{\sigma_a} \times \vec{\sigma_b}]^2_m \\ &= e^{-\frac{\beta^2 R^2}{2}} \int \frac{dq}{(2\pi)^3} q^2 \frac{q^2}{q^2+m_\pi^2} \int_0^{2\pi} d\phi \int_{-1}^{1} d(\cos(\hat{q})) \\ &\quad \times \sqrt{\frac{5}{16\pi}} (3\cos^2(\hat{q}) - 1) \cdot [\vec{\sigma_a} \times \vec{\sigma_b}]^2_m \\ &= 0\,, \end{aligned} \tag{4.64}$$

and

$$B^{36(qe)} = e^{-\frac{\beta^2 R^2}{2}} \int \frac{d^3q}{(2\pi)^3} \frac{q^2}{q^2+m_\pi^2} e^{-\frac{q^2}{2\beta^2}} e^{iq\cdot R} Y_{2m}(\hat{q}) \cdot [\vec{\sigma_a} \times \vec{\sigma_b}]^2_m\,. \tag{4.65}$$

From [[Ed57] 5.8.3] we have

$$e^{iq\cdot R} = 4\pi \sum_{l=0}^{\infty} \sum_{m=-l}^{l} i^l j_l(qR) Y_{lm}(\hat{R}) Y^*_{lm}(\hat{q})\,. \tag{4.66}$$

Substituting this into (4.65) and using

$$\int d\hat{q} Y^*_{lm}(\hat{q}) Y_{lm}(\hat{q}) = 1\,, \tag{4.67}$$

gives

$$B^{36(qe)} = -4\pi e^{-\frac{\beta^2 R^2}{2}} \int \frac{dq}{(2\pi)^3} q^2 \frac{q^2}{q^2+m_\pi^2} e^{-\frac{q^2}{2\beta^2}} j_2(qR) Y_{lm}(\hat{R}) \cdot [\vec{\sigma_a} \times \vec{\sigma_b}]^2_m\,. \tag{4.68}$$

The final solution, for the tensor case, is then

$$M_{tens}^{36(qe)}(R) = 4\pi e^{-\frac{\beta^2 R^2}{2}} I_t(R) S_{\mathbf{ab}}(\hat{R}) \tag{4.69}$$

where

$$I_t(R) = \int \frac{dq}{(2\pi)^3}\, q^2\, \frac{q^2}{q^2 + m_\pi^2}\; j_2(qR) \tag{4.70}$$

and $j_2(qR)$ is the $2^{nd}$ order spherical Bessel function

$$j_2(qR) = \left(\frac{3}{(qR)^3} - \frac{1}{(qR)}\right) sin(qR) - \frac{3}{(qR)^2} cos(qR)\,. \tag{4.71}$$

From this it can be seen that only those terms which include a factor of $e^{iq\cdot R}$ contribute to the tensor force. Once all the matrix elements have been calculated we can put them together to give an expression for the potentials from the different diagrams from Fig 3.1. This gives us for our solutions

$$v^{36(nqe)} = -\frac{f_{\pi qq}^2}{3m_\pi^2}\frac{4\pi}{N}\left[M_{scal}^{36(nqe)}(I_s(R) - (-)^{(S+T)} e^{\frac{-3\beta^2 R^2}{2}} F) + M_{tens}^{36(nqe)} I_t(R)\right]$$

$$v^{12(nqe)} = -\frac{f_{\pi qq}^2}{3m_\pi^2}\frac{4\pi}{N}(1 - (-)^{(S+T)} e^{-\frac{\beta^2 R^2}{2}}) F M_{scal}^{12(nqe)}$$

$$v^{(s)} = -\frac{f_{\pi qq}^2}{3m_\pi^2} 4\pi F M^{(s)}$$

$$v^{36(qe)} = -\frac{f_{\pi qq}^2}{3m_\pi^2}\frac{4\pi}{N} e^{-\frac{\beta^2 R^2}{2}}\left[M_{scal}^{36(qe)}(F - (-)^{(S+T)} e^{-\frac{\beta^2 R^2}{2}} I_s(R)) - M_{tens}^{36(qe)}(-)^{(S+T)} e^{-\frac{\beta^2 R^2}{2}} I_t(R))\right]$$

$$v^{25(qe)} = -\frac{f_{\pi qq}^2}{3m_\pi^2}\frac{4\pi}{N}e^{-\frac{\beta^2R^2}{2}}\left[M_{scal}^{25(qe)}(I_s(R) - (-)^{(S+T)}e^{-\frac{\beta^2R^2}{2}}F) + M_{tens}^{25(qe)}I_t(R)\right]$$

$$v^{26(qe)} = -\frac{f_{\pi qq}^2}{3m_\pi^2}\frac{4\pi}{N}e^{-\frac{\beta^2R^2}{2}}(1 - (-)^{(S+T)}e^{-\frac{\beta^2R^2}{2}})\left[M_{scal}^{26(qe)}I_s(\tfrac{R}{2}) + M_{tens}^{26(qe)}I_t(\tfrac{R}{2})\right]$$

$$v^{23(qe)} = -\frac{f_{\pi qq}^2}{3m_\pi^2}\frac{4\pi}{N}e^{-\frac{\beta^2R^2}{2}}(1 - (-)^{(S+T)}e^{-\frac{\beta^2R^2}{2}})\left[M_{scal}^{23(qe)}I_s(\tfrac{R}{2}) + M_{tens}^{23(qe)}I_t(\tfrac{R}{2})\right]$$

$$v^{12(qe)} = -\frac{f_{\pi qq}^2}{3m_\pi^2}\frac{4\pi}{N}e^{-\frac{\beta^2R^2}{2}}M_{scal}^{12(qe)}F(1 - (-)^{(S+T)}e^{-\frac{\beta^2R^2}{2}}) \tag{4.72}$$

with N the overlap integral $<\psi|\psi>$ of (3.7):

$$N = 1 - 3M_{scal}^{cen}e^{-\frac{\beta^2R^2}{2}} + 3M_{scal}^{cen}(-)^{(S+T)}e^{-\frac{\beta^2R^2}{2}} - (-)^{(S+T)}e^{-\frac{3\beta^2R^2}{2}} \tag{4.73}$$

In Appendix D we have taken the quark potential $v^{25(qe)}$ and calculated it in explicit detail to outline the steps involved in obtaining the potential.

# Chapter 5

# Results

In this chapter we will present and analyse the numerical results of our calculations. The only two parameters that can be adjusted are the quark-pion coupling constant $f_{\pi qq}$ and the nucleon size parameter $\beta$. However, these can be derived from nucleon properties and cannot be varied a great deal. We will look at the effect varying $\beta$ has on the QOPEP. We will then examine closely the breakdown of the QOPEP and the contributions from all the terms involved. We will then compare the QOPEP with other models, including the OGEP, as calculated by Holinde [Hol84] and described in chapter 2.

## 5.1 Parameters $\beta$ and $f_{\pi qq}$

We have shown earlier in (3.19) how the nucleon size parameter $\beta$ relates to the root mean square radius of the bag. This will then limit the range of values that $\beta$ can assume. For our calculations we have used $\beta^{-1} = 0.5fm$, the median value used in most of the literature, [Bro79, AWT83, FaFer83, Faes+83, Brä85, Fern87, Brä90] . The effect of varying $\beta$ is illustrated in Figs 5.1 and 5.2 where the ranges used are the most extreme possible while still being acceptable as possible nucleon radii. As the plots in Fig 5.1 and Fig 5.2 show, the shapes of the potentials don't change very much, but there is about a 40% variation

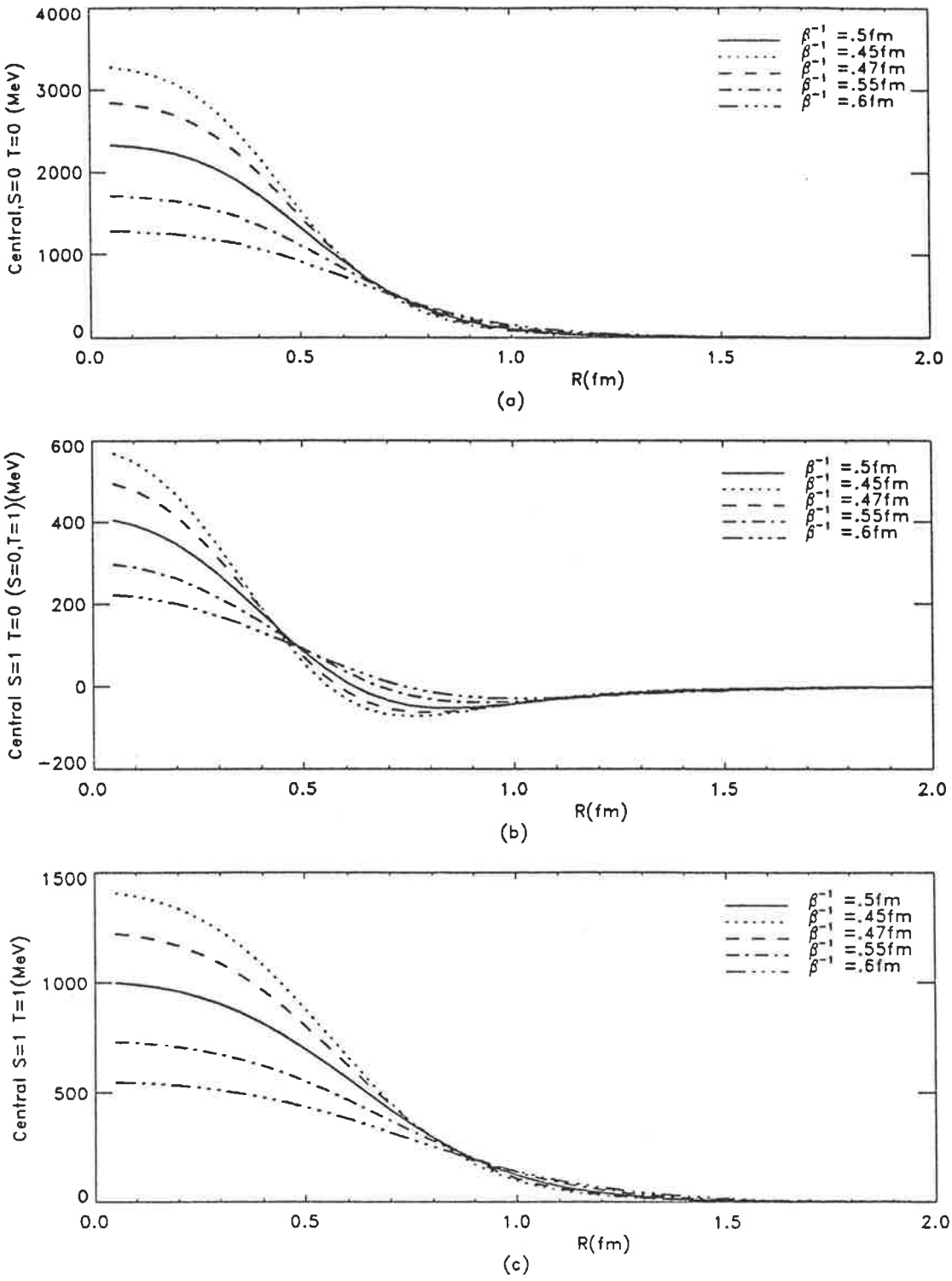


Figure 5.1: Plot of the total QOPEP in the central channels showing the effects of varying $\beta^{-1}$ from $\beta^{-1} = .45fm$ to $\beta^{-1} = .6fm$

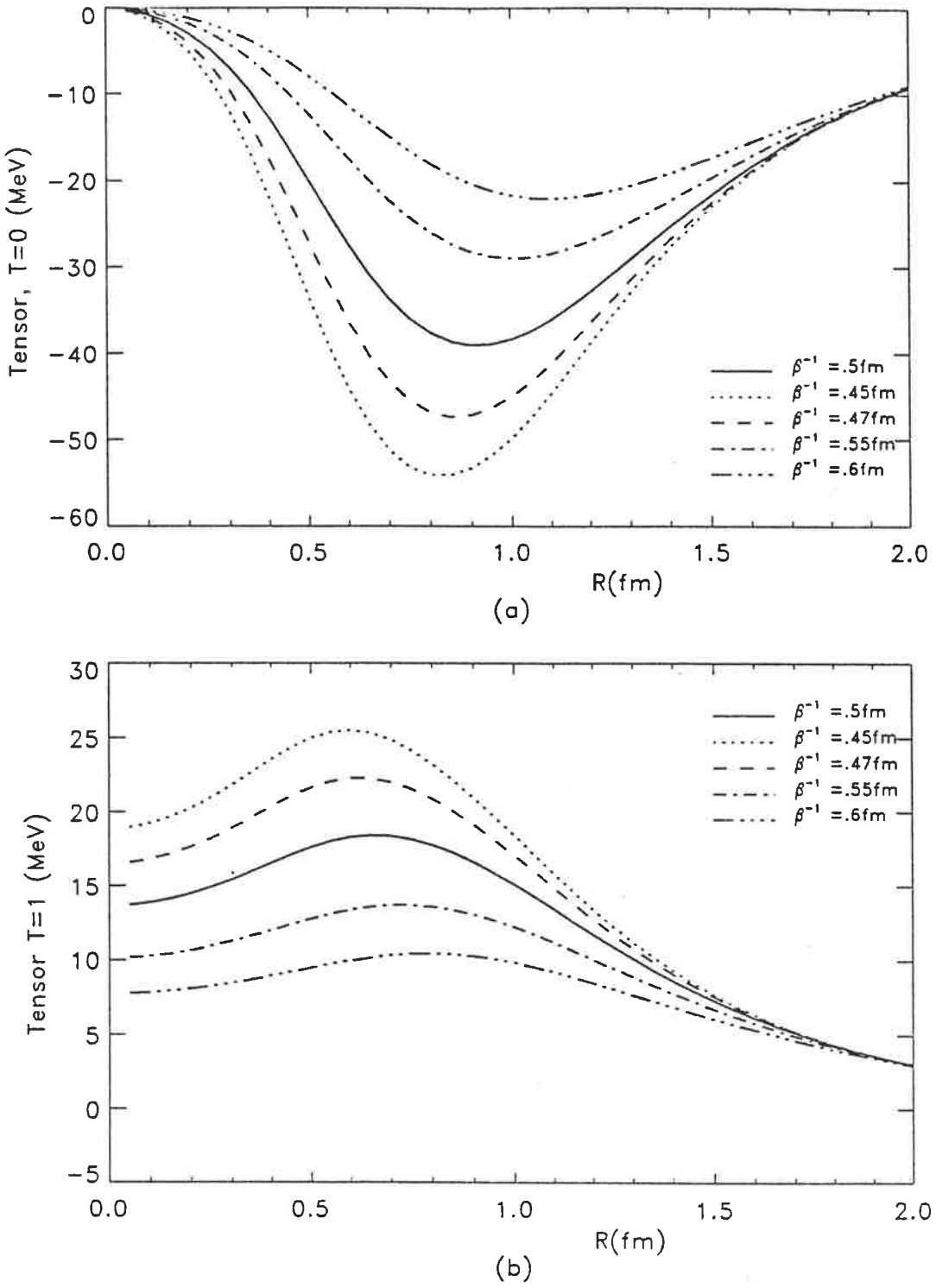


Figure 5.2: Plot of the sum of the exchange terms only in the QOPEP in the tensor channels with the effects of varying $\beta$.

from the mean maximum value. This is consistent in both Fig 5.1 and Fig 5.2. Since this model is somewhat similar to the chiral bag model picture, we would expect the value of $\beta^{-1}$ to be smaller than that used in the naive quark model. However, here we are more concerned with the general behaviour of the QOPEP and a slight variation of $\beta$ doesn't alter the main features of the QOPEP.

Corresponding to the choice of spatial wave functions for the nucleon in (3.18) the quark-pion coupling constant $f_{\pi qq}$ can be related to the nucleon-pion coupling constant $f_{\pi NN}$ by examining the asymptotic behaviour of the QOPEP and OPEP for point nucleons. At large R, the only term which dominates in the QOPEP is $v_{36}^{nqe}$, given by (4.72). In Appendix E we have shown in detail how the two coupling constants can be related by

$$f_{\pi qq}^2 = \frac{9}{25} e^{\frac{-m_\pi^2}{2\beta^2}} f_{\pi NN}^2, \tag{5.1}$$

where $f_{\pi NN}^2 = 0.082$ and $m_\pi$ is the pion mass.

## 5.2 QOPEP in Detail

We now take a closer look at the terms which contribute to the QOPEP. These are given explicitly in (4.72). In Fig 5.3 and Fig 5.4 we show the contributions from all the diagrams given in Fig 3.1. The contributions to the short range repulsion in the central potentials mainly come from the quark exchange terms. From Fig 5.4 we can see that the exchange terms contribute only to a minor degree in the tensor channels and that it is the non quark exchange term $v_{36}^{nqe}$ which gives the bulk of the potential. This gives rise to the similarity of the QOPEP tensor force to that of the OPE with a form factor.

The two factors causing the suppression of the tensor force in the quark exchange terms are the cancellation in the spin/isospin coefficients and the structure of the radial integrals. The function $I_{tens}(R)$ peaks around 0.8fm and goes to zero for R=0. Cut-off

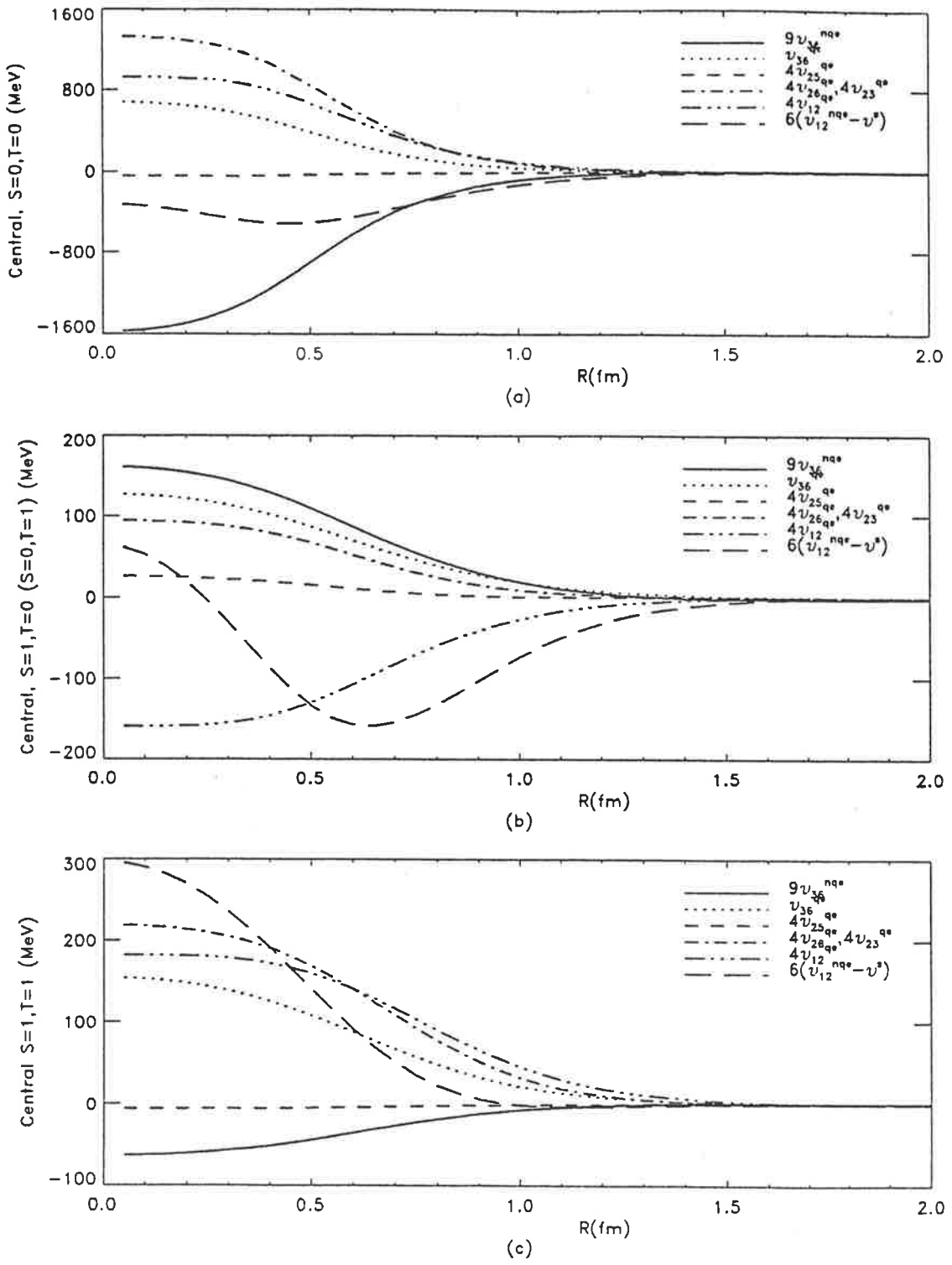


Figure 5.3: Individual contributions for all the diagrams making up the QOPEP. The S=0,T=0 and S=0,T=1 (S=1,T=0) and S=1,T=1 channels for the central potential are shown here.

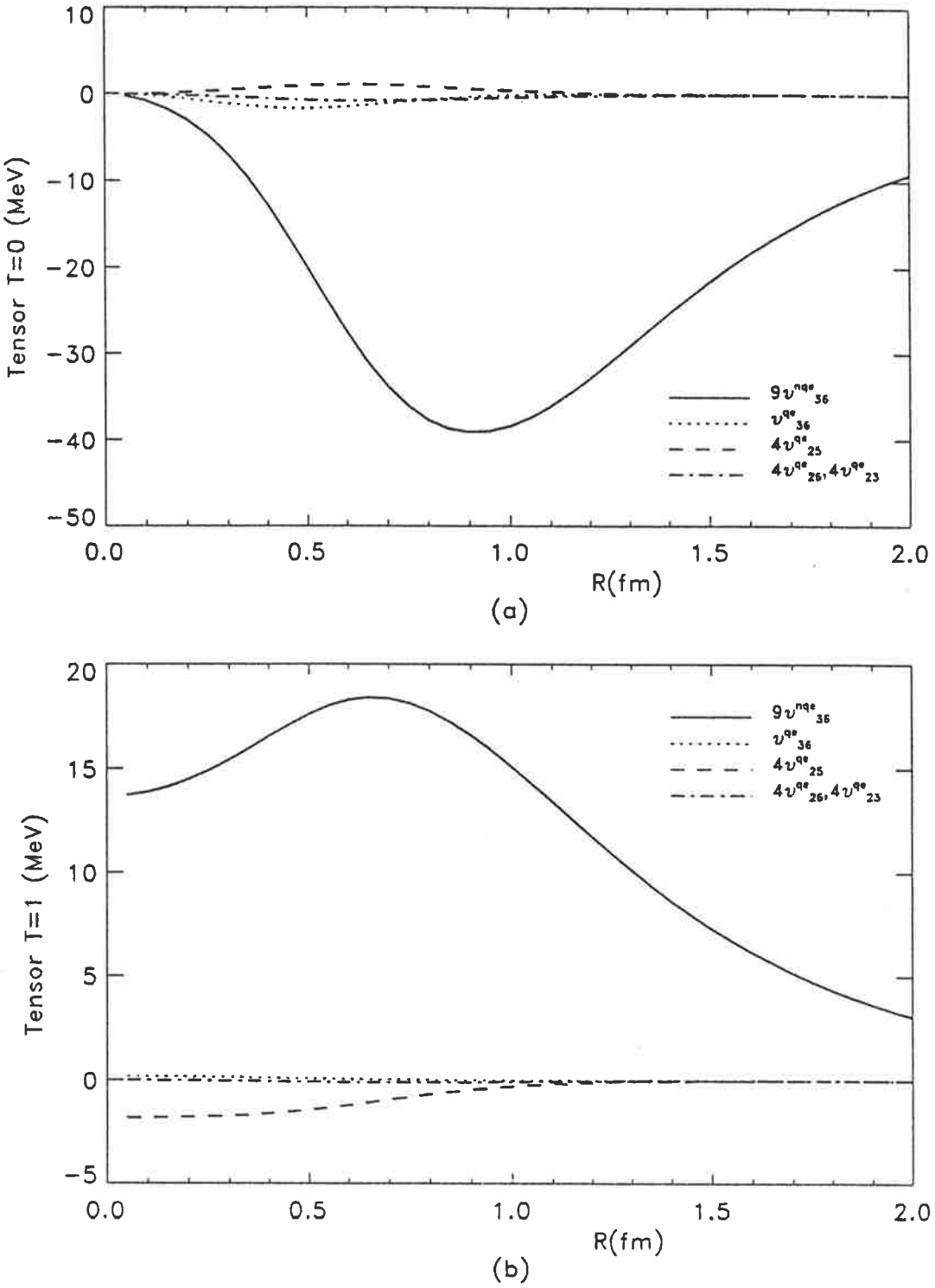


Figure 5.4: Individual contributions for all the diagrams making up the QOPEP. The S=1,T=0 and S=1,T=1 channels for the tensor potential are shown here.

factors like $e^{-\beta^2 R^2}$ drop quickly to zero at intermediate ranges making the integral small in both the short and medium ranges. The reason this doesn't occur in the central terms is because the function $I_{scal}(R)$ is finite at R=0.

The central singlet-even (triplet-even) potential gets contributions from many terms, most of which are repulsive. The medium range attraction for the singlet-even and triplet-even states comes from the intracluster term $(v_{12}^{nqe} - v^s)$. This term is neglected in some calculations [Hol84, FaFer83, Faes+83, Brä85, Brä90, Fern87], justifying this with the reasoning that it cancels out exactly because it is a nucleon self energy term. This will only be correct if the total wave function $\psi$ from (3.3) is not antisymmetrized with respect to quark pairs from different clusters. This requires A=1 in (3.5), which would leave out all the short range dynamics. With the total antisymmetrization of the six-quark wave function, there is a residue instead of cancellation. In fact, whereas this term vanishes at long distances, at short range the effects of quark exchange from different nucleons in the normalization function (4.73) makes a significant contribution to the interaction process. We also find that the term $v_{25}^{qe}$ (represented by the diagram (d) in Fig 3.1) gives only a negligible contribution in any state.

One of the reasons for the repulsion in singlet-odd and triplet-odd states is the $R^2$ divergence in the normalization function N for these states, which is due to the Pauli principle. For these states, QOPEP and OPEP with a form factor go in opposite directions at short distances. This is because the OPEP with a form factor may not reproduce the complicated structure at very short range. The main reason for QOPEP being repulsive in these states is quark exchange. From this we can see that it is the quark exchange which produces the short range repulsion.

## 5.3 Meson Exchange Potentials

In Fig 5.5 and Fig 5.6 we have plotted the total central and tensor potentials as calculated from (3.17) . Also on the same plots are three different meson exchange potentials :

(a) OPEP-FF, which is the OPEP with a monopole form factor as used in the Bonn potential [Ma+87] .

(b) OPE, which is just the pure OPEP for point nucleons

(c) the Paris potential [Cot73, Lac80]

From Fig 5.5 and Fig 5.6 we can see that although all the long range results are the same as the OPEP for point nucleons, the short range behaviour of the QOPEP exhibits different features. Firstly, the central potential is repulsive for $r < 0.5fm$ in all NN states. This is supportive of the phenomenological repulsive core used in all meson exchange potentials. Also, the singlet-even (triplet-even) central and the tensor potentials behave like an OPEP-FF with a cut-off mass of 700 MeV which agrees with the proposal by [De+91, Hol+90, AWT+89] for the use of a soft pion form factor in meson exchange potentials. Strong repulsion can be found in the singlet-odd and triplet-odd states. However, the OPEP-FF is attractive in these states because the cut-off mass is larger than the pion mass. In view of the arbitrary nature of the short-range cut-off used in meson exchange potentials we believe that the short range attraction of the OPEP-FF is not a very desirable feature. In fact, the form factor should act to slightly suppress the OPEP at intermediate distances but cannot be expected to represent the complex physics in the region where nucleons physically overlap. Neither the OPEP-PN nor the OPEP-FF gives the short range repulsion for all NN states, whereas the QOPEP can. We can also see from Fig 5.5 that the overall behaviour of QOPEP resembles that of the Paris potential [Cot73, Lac80] in the parameterised form for all NN states.

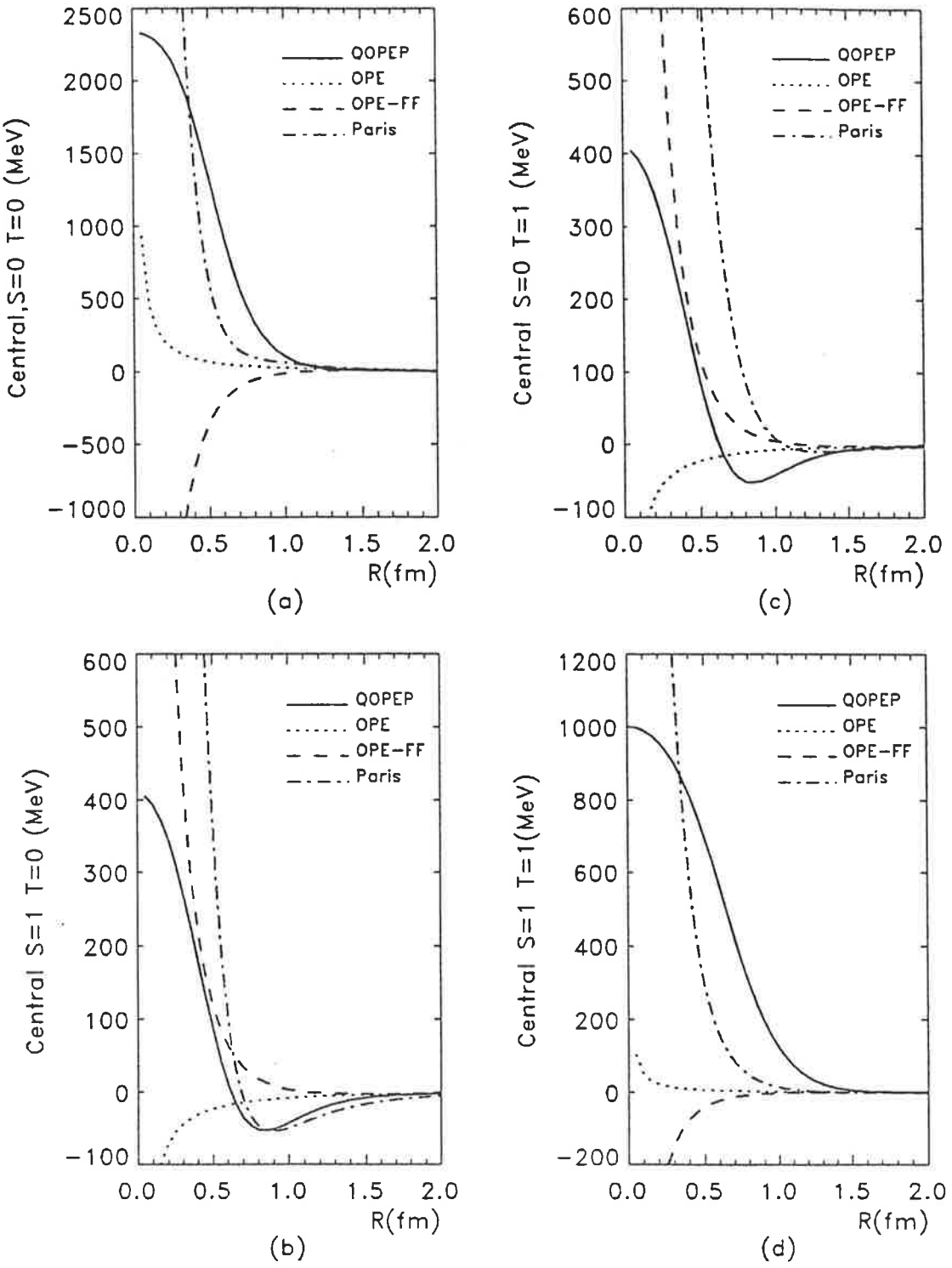


Figure 5.5: Comparison of the QOPEP with various meson OPEP. The S=0,T=0 and S=0,T=1 (S=1,T=0) and S=1,T=1 channels for the central potential are shown here. The solid line is the QOPEP, the dotted line OPE for point nucleons, dashed line OPE with Bonn form factor cutoff mass=700MeV, and dash-dot line the Paris potential.

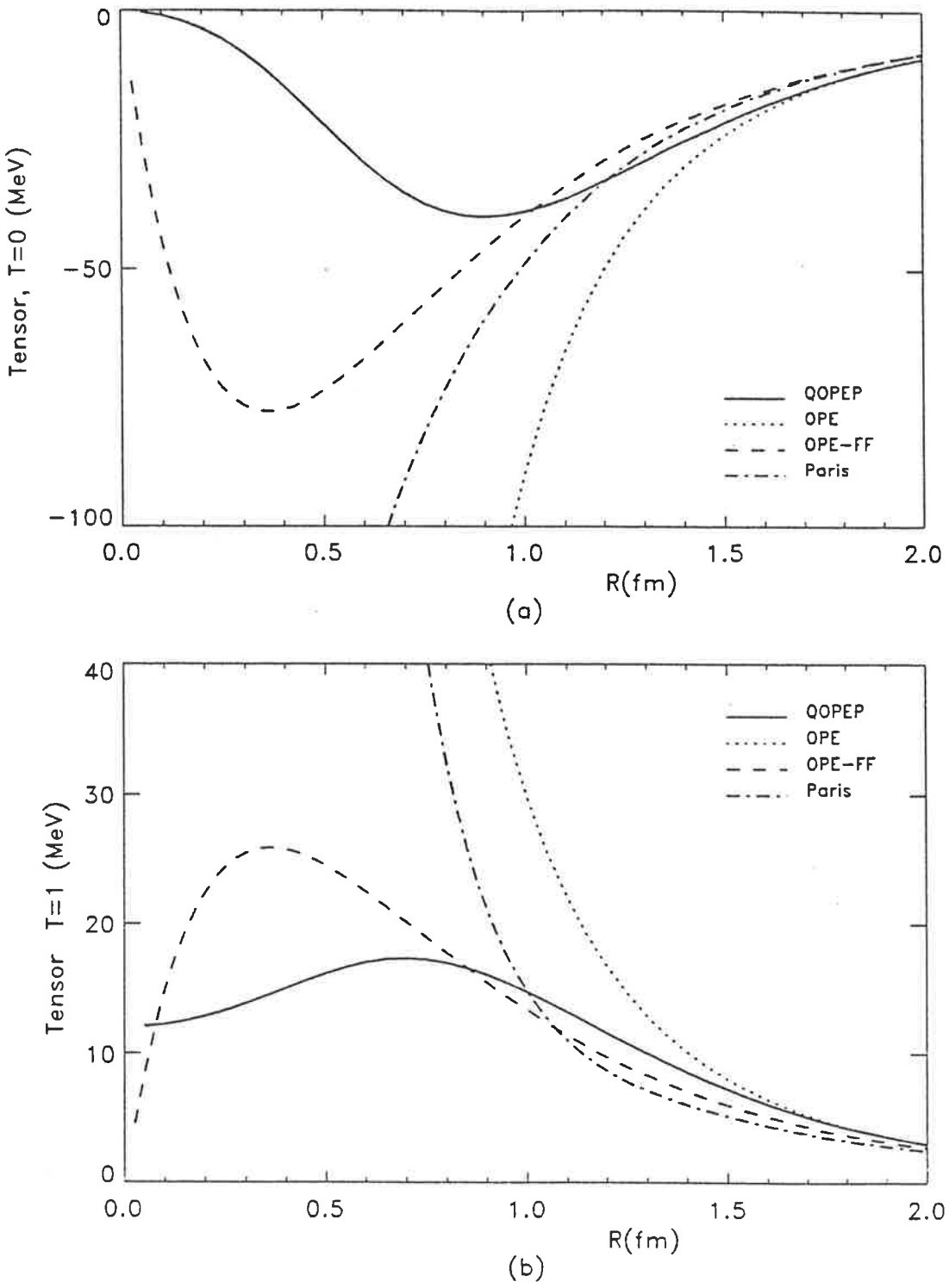


Figure 5.6: Comparison of the QOPEP with various meson OPEP. The S=1,T=0 and S=1,T=1 channels for the tensor potential are shown here.The solid line is the QOPEP, the dotted line OPE for point nucleons, dashed line OPE with Bonn form factor cutoff mass=700MeV, and dash-dot line the Paris potential.

## 5.4 Form Factors

The contact term in NN OPEP is normally removed by the Poorman's procedure. This doesn't occur in this calculation as the nucleon is considered to be a composite particle. However, we treat the pion as a point particle; which gives us a contact term in the potential of equation (3.11), so the problem of pion size needs to be considered.

We can do this in two ways. Firstly,we could ignore the contact piece in a way similar to the Poorman's procedure in NN OPEP, or we could apply a form factor at the quark-pion vertex. The results of these two procedures are given in Fig 5.7 and Fig 5.8.

Changes in the behaviour of the QOPEP are observed. Without the contact piece, the potentials become weak and attractive at short range. The contact force basically determines the central part of the QOPEP. The importance of the $\delta$ function term indicates that the short range repulsion depends heavily on the nucleon wave function overlap at short distances. The fact that finite size effects of the nucleon dominate the NN interaction at these distances tells us that many body effects are large at these ranges. This may be the reason why many mesons and even phenomenological treatments are needed in all variations of meson exchange NN potentials.

Two types of form factors used to incorporate the pion size are :

$$F(q^2) = \frac{\Lambda^2 - m_\pi^2}{q^2 + \Lambda^2} \tag{5.2}$$

for the Bonn [Ma+87] monopole form and

$$F(q^2) = \sqrt{\frac{\Lambda^2}{q^2 + \Lambda^2}} \tag{5.3}$$

for the square root form suggested by [FaFer83, Faes+83, Brä90, Brä85, Fern87, FerOs86]. From Fig 5.7 we can see that the form factors make the predominant contributions to the repulsion in the resulting NN potential. Their role is similar to the contact term in the

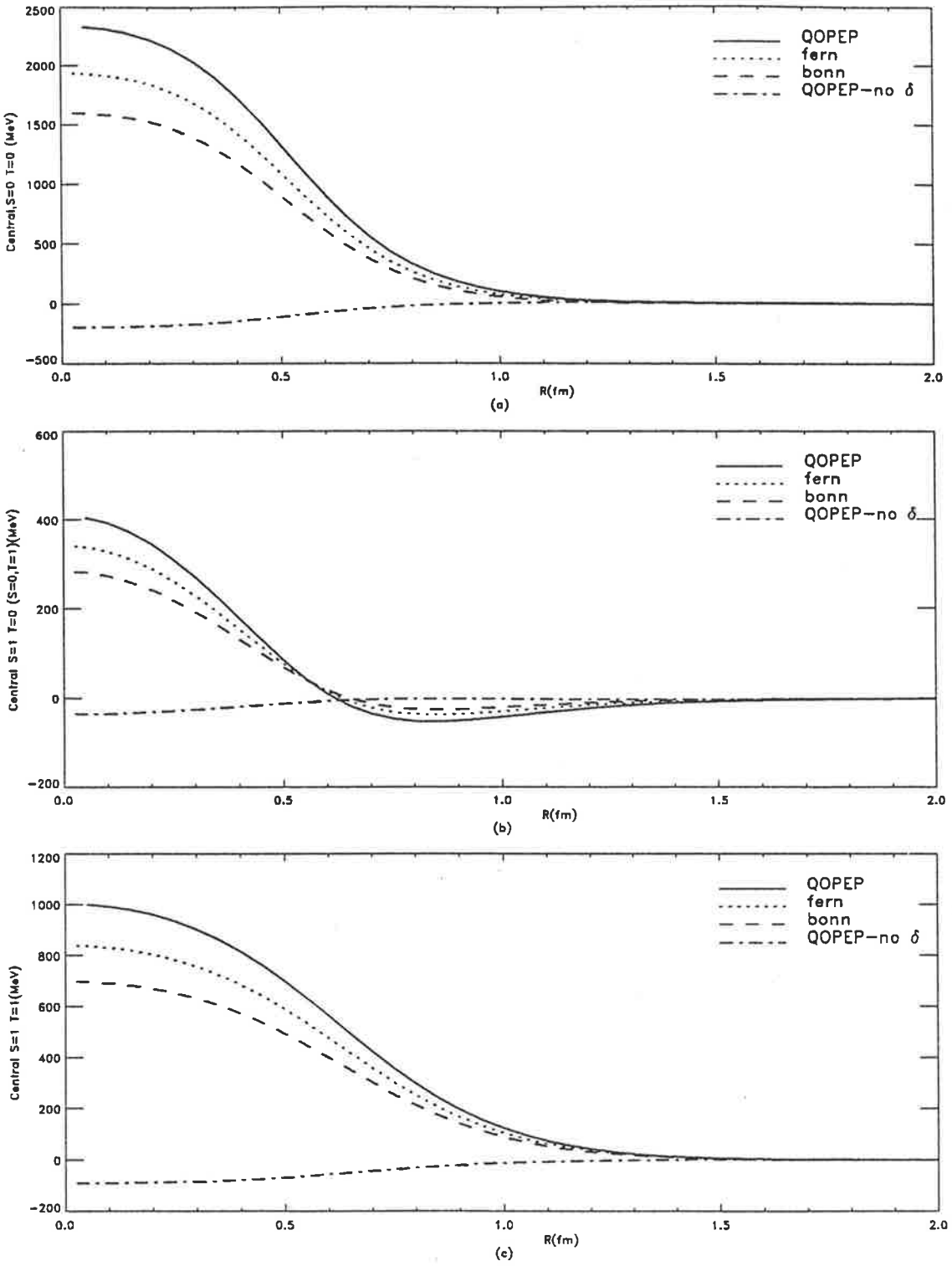


Figure 5.7: Comparison of the QOPEP with QOPEP with form factors and without the $\delta$ term added in the central channels. The solid line is the QOPEP, dotted line, labelled fern, the QOPEP with square root form factor, dashed line, labelled bonn, the QOPEP with monopole form factor, and dash-dot line QOPEP with no $\delta$ interaction.

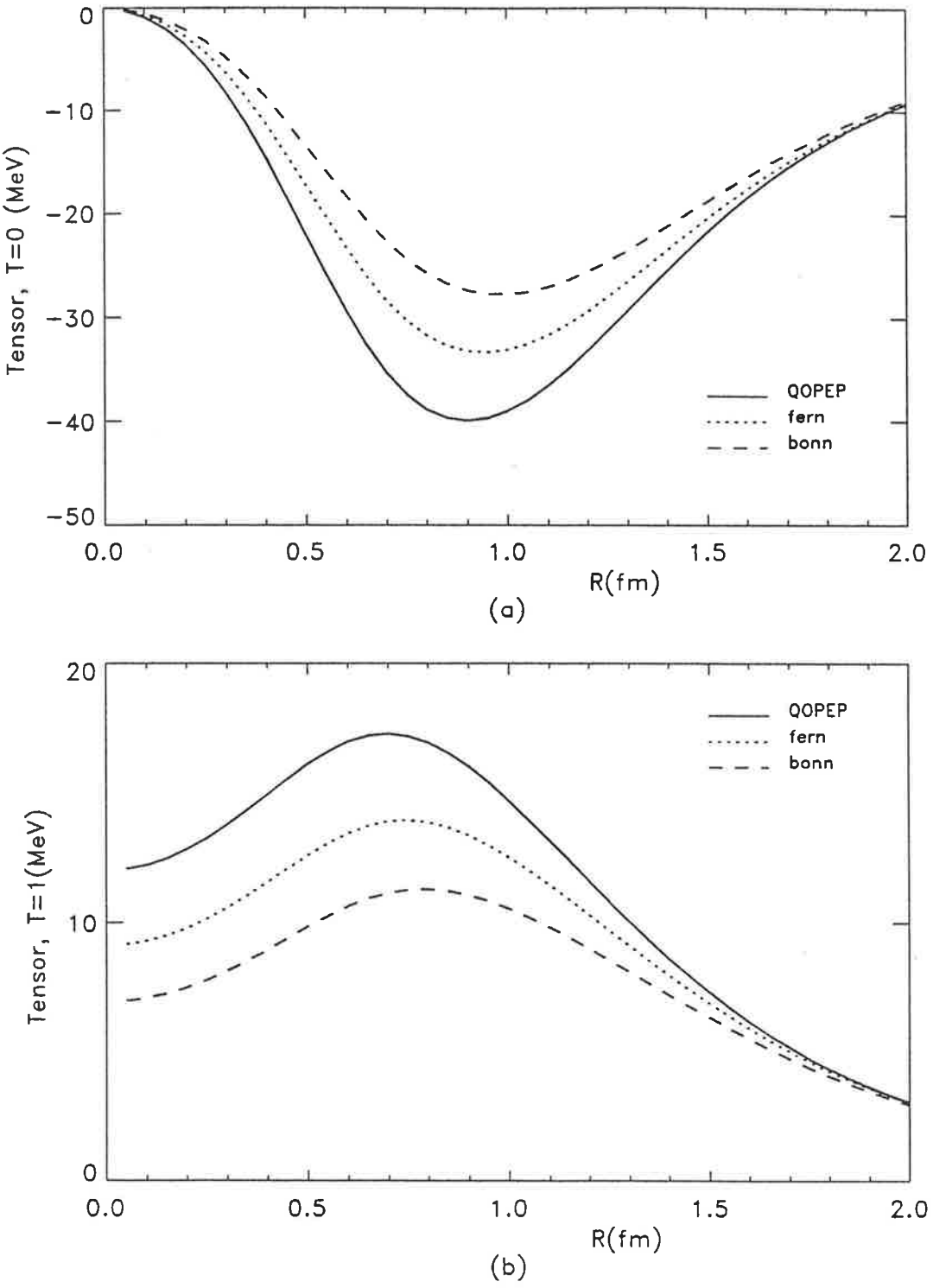


Figure 5.8: Comparison of the QOPEP with QOPEP with form factors in the tensor channels. The $\delta$ term doesn't contribute in the tensor case.The solid line is the QOPEP, dotted line, labelled fern, the QOPEP with square root form factor, dashed line, labelled bonn, the QOPEP with monopole form factor.

central QOPEP. Unlike the contact force which affects the central part only, form factors weaken both the central and tensor parts. As the cut-off mass increases, the form factor results approach the results of the contact term which is the limiting case for $\lambda \to \infty$. This is true for both the total potentials and the individual terms in equation (3.17). From this we find that the QOPEP with a point-like pion gives the maximum repulsion. On the other hand, if one takes the short range repulsion as an indication of the correct dynamics at the quark level, one can conclude from the usual phenomenology of the core that the quark-pion coupling must be almost point-like. This implies that the pion has a very small size.

## 5.5 Comparisons with One Gluon Exchange Potential

The One Gluon Exchange Potential (OGEP) as calculated at the quark level is also important at short range. We look at the OGEP as calculated by Holinde [Hol84] and explained in detail in Chapter 2. The two parameter sets used are those given by Fernandez, Faessler, Lübick and Shimizu (FFLS) [Faes+83] and Oka and Yazaki (OY) [Oka84]. The parameter sets are given below.

- FFLS :- $m = 355MeV$, $\beta^{-1} = .475fm$, $a = 34.5MeV \cdot fm$, $\alpha_s = .97$
- OY :- $m = 300MeV$, $\beta^{-1} = .6fm$, $a = 62.5MeV \cdot fm$, $\alpha_s = 1.39$

In Fig 5.9 and Fig 5.10 the comparison between the QOPEP and the OGEP are given for both parameter sets. In the tensor channels Fig 5.10 we have compared the OGE with only the exchange terms from the QOPEP. Overall the QOPEP is dominated by the direct term which is much larger. In the tensor channels we can see then that the OGE is not going to contribute very much at all to the overall tensor force of the N-N interaction. In Fig 5.9 we can see that in (a) and (d) the QOPEP has a much larger size than the OGE and in the other channels there is a comparable magnitude.

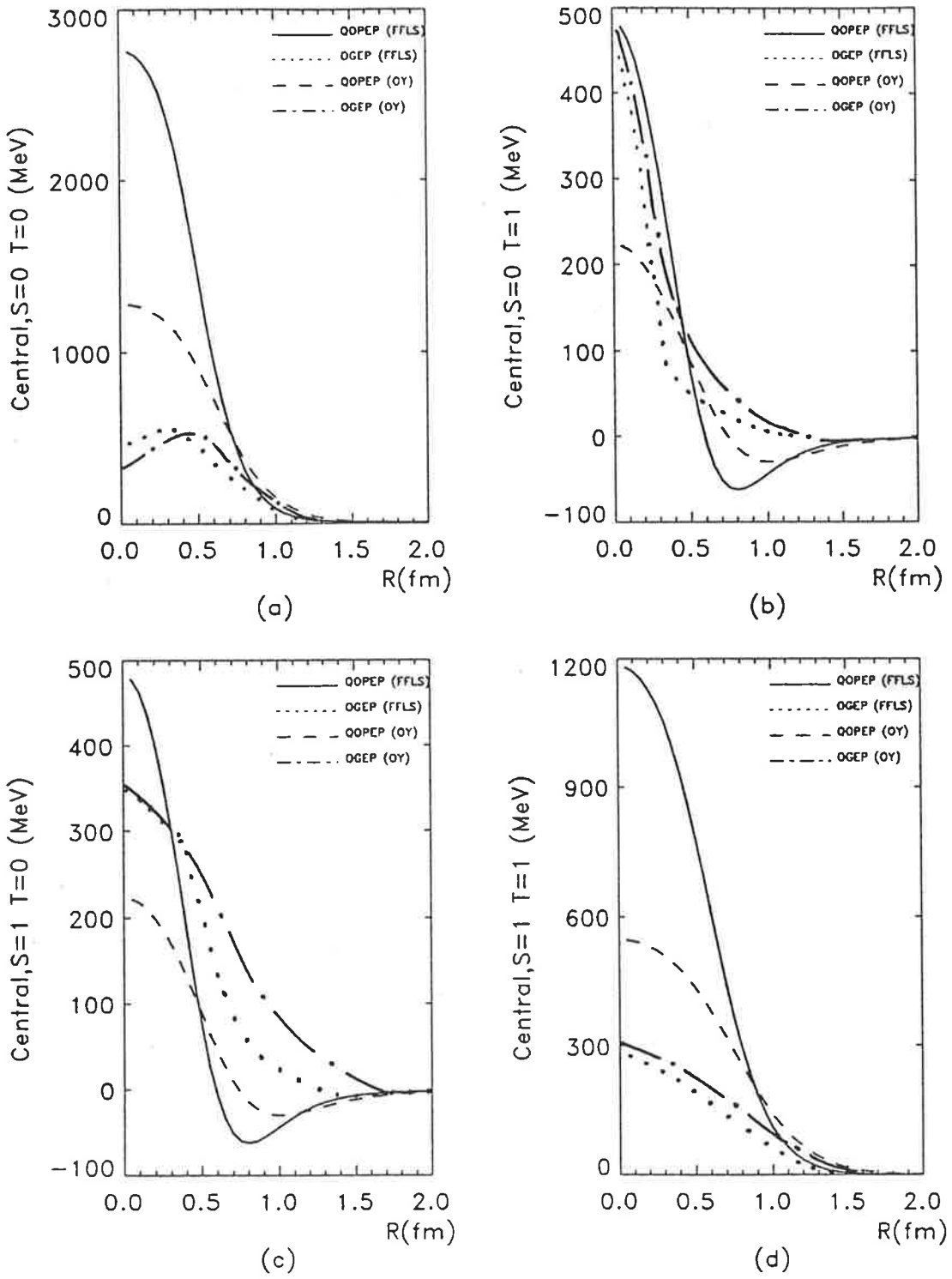


Figure 5.9: Comparison of the QOPEP and OGEP as calculated by Holinde [Hol84] in the central channels. Both parameter sets are used for each potential. The solid line is QOPEP with FFLS parameter set, dotted line is OGEP with FFLS parameter set, dashed line is QOPEP with OY parameter set and dash-dot line is OGE with OY parameter set.

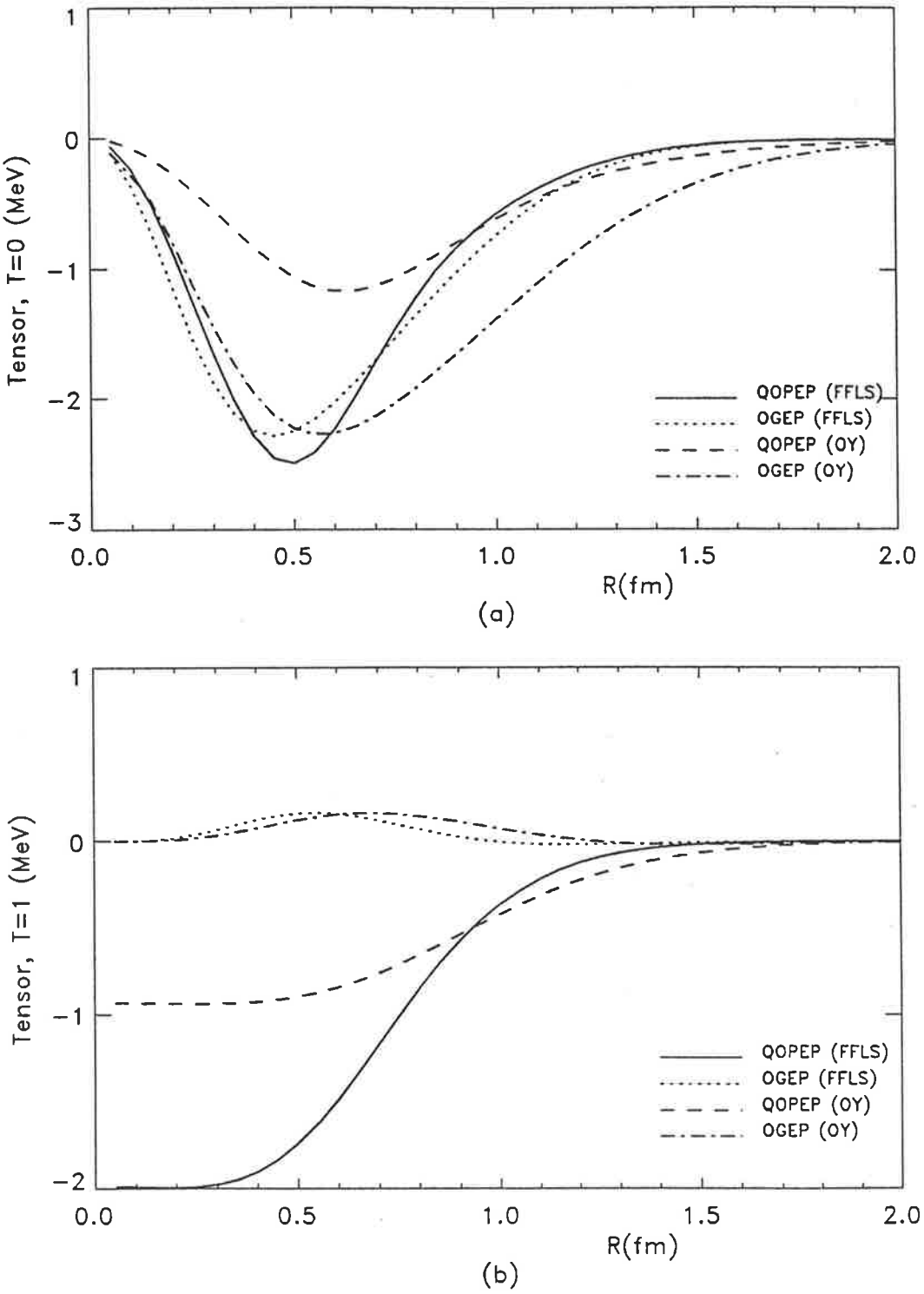


Figure 5.10: Comparison of the QOPEP calculated here with the OGEP as calculated by Holinde [Hol84], in the tensor channels. Both parameter sets are used for each potential. The QOPEP shown is only for the exchange terms. The solid line is QOPEP with FFLS parameter set, dotted line is OGEP with FFLS parameter set, dashed line is QOPEP with OY parameter set and dash-dot line is OGE with OY parameter set.

# Chapter 6

# Conclusions

There is still a great deal to be learnt before our understanding of the short range nuclear force is even close to being complete. We have found that while the structure of this force is complex, many of its features can be understood in terms of the exchange of quarks between nucleons. It is these quark exchange terms which contribute to the short range repulsion. In the central channels all the terms contribute and the medium range attraction in the singlet-even (triplet-even) states is caused by the intracluster term $(v^{12(nqe)} - v^s)$. In examining the tensor potential we find that the quark exchange terms have only a small effect. This is contrary to the suggestion of Guichon and Miller [Guich+84], namely that the short range quark exchange force would be large enough to account for the discrepancy found when comparing the experimental D/S state ratio with theoretical predictions for soft pion-nucleon form factors. In comparing the QOPEP with various meson exchange potentials we found that the qualitative features of the QOPEP agree quite well with the Paris meson exchange potential. The major result of our work is the formulation of a complete analytical expression for the Quark One Pion Exchange Potential. From this starting point a number of extensions or new lines of investigation are possible.

One area of work underway at the moment is the calculation of phase shifts in the NN interaction using the QOPEP. Supplemented by some residual meson exchange this

should permit a good fit to world N-N data. The potential could also be extended to allow for the up-down quark mass difference. This difference is one of the possible mechanisms which allows Charge Symmetry Breaking to occur. Using this potential allows for a more microscopic description of CSB. The same techniques which we have used could also be applied to the microscopic description of the hyperon-nucleon interaction.

Another line of investigation would be to improve on the Born-Oppenheimer approximation. Finally, one might like to see the effect of using more sophisticated quark models.

# Appendix A

# Properties of the Antisymmetry Operator A

## A.1 Antisymmetry Operator A

Look at the antisymmetry operator A. We have

$$A = 1 - \sum_{i=1}^{3}\sum_{j=4}^{6} P_{ij} + \sum_{\substack{k,m=1 \\ m>k}}^{3}\sum_{\substack{l,n=4 \\ n>l}}^{6} P_{kl}\, P_{mn} - P_{14}P_{25}P_{36} \tag{A.1}$$

We want to show that this is equal to

$$A = (1 - \sum_{i=1}^{3}\sum_{j=4}^{6} P_{ij})(1 - P) \tag{A.2}$$

when acting on a two nucleon state, where $P$ is the nucleon exchange operator and $P \equiv P_{14}P_{25}P_{36}$. Expanding out (A.2) gives us

$$A = 1 - P - \sum_{i=1}^{3}\sum_{j=4}^{6} P_{ij} + \sum_{i=1}^{3}\sum_{j=4}^{6} P_{ij}P \tag{A.3}$$

Comparing (A.3) with (A.1) we can see that all we have to show is that

$$\sum_{\substack{k,m=1 l,n=4 \\ m>k \quad n>l}}^{3} \sum^{6} P_{kl}\, P_{mn} = \sum_{i=1}^{3} \sum_{j=4}^{6} P_{ij} P \tag{A.4}$$

Look at the LHS first. We operate with this on two nucleons; nucleon A with quarks 1,2,3 (123) and nucleon B with quarks 4,5,6 (456). The solution to this is

$$\begin{aligned} \sum_{\substack{k,m=1 l,n=4 \\ m>k \quad n>l}}^{3} \sum^{6} P_{kl}\, P_{mn} |(123)(456)> &= |(453)(126)> + |(463)(152)> + |(425)(136)> \\ &+ |(426)(153)> + |(145)(236)> + |(146)(253)> \\ &+ |(156)(423)> + |(563)(412)> + |(526)(413)> \end{aligned} \tag{A.5}$$

For the RHS we have

$$\begin{aligned} \sum_{i=1}^{3} \sum_{j=4}^{6} P_{ij} P |(123)(456)> &= |(156)(423)> + |(416)(523)> + |(451)(623)> \\ &+ |(256)(143)> + |(426)(153)> + |(452)(163)> \\ &+ |(356)(124)> + |(436)(125)> + |(453)(126)> \end{aligned} \tag{A.6}$$

Using the property that any two quarks in the same nucleon can be exchanged producing a minus sign we have that the LHS = RHS. From this we can now say that A can be written in the form of (A.2).

## A.2 Commutation Relation

We need to show that $\sum_{i=1}^{3}\sum_{j=4}^{6} P_{ij}$ and $P$ commute, ie

$$\left[\sum_{i=1}^{3}\sum_{j=4}^{6} P_{ij}, P\right] = 0 \tag{A.7}$$

or

$$\sum_{i=1}^{3}\sum_{j=4}^{6} P_{ij}P - P\sum_{i=1}^{3}\sum_{j=4}^{6} P_{ij} = 0 \tag{A.8}$$

To show this we operate both on $|(123)(456)>$ and show that the LHS =RHS.

$$\sum_{i=1}^{3}\sum_{j=4}^{6} P_{ij}P|(123)(456)>= P\sum_{i=1}^{3}\sum_{j=4}^{6} P_{ij}|(123)(456)> \tag{A.9}$$

Do the LHS first. This gives us

$$\begin{aligned}\left(\sum_{i=1}^{3}\sum_{j=4}^{6} P_{ij}\right) P|(123)(456)> &= |(156)(423)> +|(416)(523)> +|(451)(623)> \\ &+ |(256)(143)> +|(426)(153)> +|(452)(163)> \\ &+ |(356)(124)> +|(436)(125)> +|(453)(126)>\end{aligned} \tag{A.10}$$

For the RHS we have

$$\begin{aligned}P\left(\sum_{i=1}^{3}\sum_{j=4}^{6} P_{ij}\right) |(123)(456)> &= |(156)(423)> +|(436)(125)> +|(256)(143)> \\ &+ |(451)(623)> +|(356)(124)> +|(452)(163)> \\ &+ |(416)(523)> +|(453)(126)> +|(426)(153)>\end{aligned} \tag{A.11}$$

From this we have LHS = RHS.

## A.3 Normalisation

We want to show that the normalisation can be written as

$$N = 20 < \varphi_{\mathbf{a}}\varphi_{\mathbf{b}}|(1-9P_{36})(1-P)|\varphi_{\mathbf{a}}\varphi_{\mathbf{b}} > \tag{A.12}$$

The normalisation is

$$\begin{aligned} N &= <\psi|\psi> \\ &= <\varphi_{\mathbf{a}}\varphi_{\mathbf{b}}|AA|\varphi_{\mathbf{a}}\varphi_{\mathbf{b}}> \\ &= <\varphi_{\mathbf{a}}\varphi_{\mathbf{b}}|(1-\sum_{i=1}^{3}\sum_{j=4}^{6}P_{ij})(1-P)(1-\sum_{i=1}^{3}\sum_{j=4}^{6}P_{ij})(1-P)|\varphi_{\mathbf{a}}\varphi_{\mathbf{b}}> \end{aligned} \tag{A.13}$$

We have shown in the previous section that all the terms commute. This means that we can write (A.13) as

$$\begin{aligned} N &= <\varphi_{\mathbf{a}}\varphi_{\mathbf{b}}|(1-\sum_{i=1}^{3}\sum_{j=4}^{6}P_{ij})(1-\sum_{i=1}^{3}\sum_{j=4}^{6}P_{ij})(1-P)(1-P)|\varphi_{\mathbf{a}}\varphi_{\mathbf{b}}> \\ &= 2<\varphi_{\mathbf{a}}\varphi_{\mathbf{b}}|(1-\sum_{i=1}^{3}\sum_{j=4}^{6}P_{ij})(1-\sum_{i=1}^{3}\sum_{j=4}^{6}P_{ij})(1-P)|\varphi_{\mathbf{a}}\varphi_{\mathbf{b}}> \end{aligned} \tag{A.14}$$

Expanding out the first two terms gives

$$(1-\sum_{i=1}^{3}\sum_{j=4}^{6}P_{ij})(1-\sum_{i=1}^{3}\sum_{j=4}^{6}P_{ij}) = 1-2\sum_{i=1}^{3}\sum_{j=4}^{6}P_{ij}+\sum_{i=1}^{3}\sum_{j=4}^{6}\sum_{k=1}^{3}\sum_{l=4}^{6}P_{ij}P_{kl} \tag{A.15}$$

We operate to the right of

$$\left(1-2\sum_{i=1}^{3}\sum_{j=4}^{6}P_{ij}+\sum_{i=1}^{3}\sum_{j=4}^{6}\sum_{k=1}^{3}\sum_{l=4}^{6}P_{ij}P_{kl}\right)(1-P)|(123)(456)> \tag{A.16}$$

To simplify things we do each term individually.

$$1(1-P)|(123)(456)>=(1-P)|(123)(456)> \tag{A.17}$$

$$-2\sum_{i=1}^{3}\sum_{j=4}^{6}P_{ij}(1-P)|(123)(456)>=-18P_{36}(1-P)|(123)(456)> \tag{A.18}$$

The final term has four possibilities :

if $i=k$ and $j=l$

$$\begin{aligned}\sum_{i=1}^{3}\sum_{j=4}^{6}\sum_{k=1}^{3}\sum_{l=4}^{6}P_{ij}P_{kl}(1-P)|(123)(456)> &= \sum_{i=1}^{3}\sum_{j=4}^{6}P_{ij}P_{ij}(1-P)|(123)(456)> \\ &= 9(1-P)|(123)(456)> \end{aligned} \tag{A.19}$$

if $i=k$ and $j\neq l$

$$\begin{aligned}\sum_{i=1}^{3}\sum_{j=4}^{6}\sum_{k=1}^{3}\sum_{l=4}^{6}P_{ij}P_{kl}(1-P)|(123)(456)> &= \sum_{i=1}^{3}\sum_{j=4}^{6}\sum_{l=4}^{6}P_{ij}P_{il}(1-P)|(123)(456)> \\ &= -2\sum_{i=1}^{3}\sum_{l=4}^{6}P_{il}(1-P)|(123)(456)> \\ &= -18P_{36}(1-P)|(123)(456)> \end{aligned} \tag{A.20}$$

if $i\neq k$ and $j=l$

$$\begin{aligned}\sum_{i=1}^{3}\sum_{j=4}^{6}\sum_{k=1}^{3}\sum_{l=4}^{6}P_{ij}P_{kl}(1-P)|(123)(456)> &= \sum_{i=1}^{3}\sum_{j=4}^{6}\sum_{k=1}^{3}P_{ij}P_{kj}(1-P)|(123)(456)> \\ &= -2\sum_{k=1}^{3}\sum_{j=4}^{6}P_{kj}(1-P)|(123)(456)> \\ &= -18P_{36}(1-P)|(123)(456)> \end{aligned} \tag{A.21}$$

if $i\neq k$ and $j\neq l$

$$\sum_{i=1}^{3}\sum_{j=4}^{6}\sum_{k=1}^{3}\sum_{l=4}^{6}P_{ij}P_{kl}(1-P)|(123)(456)> = -36P_{36}(1-P)|(123)(456)> \tag{A.22}$$

Substituting these results back into (A.14) gives finally for the normalisation

$$2 < \phi_{\mathbf{a}}\phi_{\mathbf{b}}|[1+9-18P_{36}-18P_{36}-18P_{36}-36P_{36}](1-P)|\phi_{\mathbf{a}}\phi_{\mathbf{b}} >=$$

$$20 < \phi_{\mathbf{a}}\phi_{\mathbf{b}}|(1-9P_{36})(1-P)|\phi_{\mathbf{a}}\phi_{\mathbf{b}} > \qquad \text{(A.23)}$$

and the normalisation can be written as

$$N = 20 < \varphi_{\mathbf{a}}\varphi_{\mathbf{b}}|(1-9P_{36})(1-P)|\varphi_{\mathbf{a}}\varphi_{\mathbf{b}} > \qquad \text{(A.24)}$$

# Appendix B

# Rules for Converting quark operators to Nucleon operators

The isospin dependence for the One Gluon Exchange process is fixed by the following general principles.

(i) The elementary quark-quark amplitude is flavour independent.

(ii) There are no first order processes like diagram (a) from Fig 2.2.

The matrix elements of the quark operators on the left side between the spin-isospin states are identical to the matrix elements on the right side between the usual Pauli spinors describing the nucleon spin-isospin state. The sum goes over the quarks in the nucleon cluster. The rules used are given below and taken from Holinde [Hol84]

$$\sum_i 1_i \rightarrow 3 \times 1^N \tag{B.1}$$

$$\sum_i \sigma_i \rightarrow \sigma^N \tag{B.2}$$

$$\sum_i \tau_i \rightarrow \tau^N \tag{B.3}$$

$$\sum_i \sigma_i \tau_i \rightarrow \frac{5}{3} \sigma^N \tau^N \tag{B.4}$$

$$\sum_{i\neq j} \sigma_i^m \sigma_j^n \to -2\delta_{mn} 1_N \tag{B.5}$$

$$\sum_{i\neq j} \sigma_i^m \tau_j^n \to -\frac{2}{3}\sigma_N^m \tau_N^n \tag{B.6}$$

$$\sum_{i\neq j} \sigma_i^m \sigma_j^n \tau_i^l \to \frac{2}{3}\delta_{mn}\tau_N^l \tag{B.7}$$

$$\sum_{i\neq j\neq k} \sigma_i^m \sigma_j^n \sigma_k^l \to -2(\delta_{mn}\sigma_N^l + \delta_{ml}\sigma_N^n + \delta_{nl}\sigma_N^m) \tag{B.8}$$

$$\sum_{i\neq j\neq k} \sigma_i^m \sigma_j^n \tau_k^l \to -\frac{10}{3}\delta_{mn}\tau_N^l \tag{B.9}$$

$$\sum_{i\neq j\neq k} \sigma_i^m \sigma_j^n \sigma_k^l \tau_k^s \to -\frac{10}{3}\delta_{mn}\sigma_N^l \tau_N^s + \frac{2}{3}\delta_{ml}\sigma_N^n \tau_N^s + \frac{2}{3}\delta_{nl}\sigma_N^m \tau_N^s \tag{B.10}$$

When using these substitution rules for the case of One Pion Exchange we need extra rules to allow for the additional isospin dependence. These are taken from [Liu+92]

$$\sum_{n\neq m} \sigma_n^i \sigma_m^j \tau_n^a \tau_m^b \to \frac{10}{3}\delta_{ij}\delta_{ab} - 2\varepsilon_{ijq}\varepsilon_{abr}\sigma_N^q \tau_N^r \tag{B.11}$$

$$\sum_{n\neq m\neq l} \sigma_n^i \sigma_m^j \sigma_l^k \tau_n^a \tau_m^b \to \frac{2}{3}\delta_{ab}(5\delta_{ij}\sigma_N^k - \delta_{jk}\sigma_N^i - \delta_{ki}\sigma_N^j) - \varepsilon_{ijk}\varepsilon_{abr}\tau_N^r \tag{B.12}$$

$$\begin{aligned}\sum_{n\neq m\neq l} \sigma_n^i \sigma_m^j \sigma_l^k \tau_n^a \tau_m^b \tau_l^c \to{}& \frac{10}{3}(\delta_{ij}\delta_{ab}\sigma_N^k \tau_N^c + \delta_{jk}\delta_{bc}\sigma_N^i \tau_N^a + \delta_{ki}\delta_{ca}\sigma_N^j \tau_N^b) - 2\varepsilon_{ijk}\varepsilon_{abc} \\ &- \frac{2}{3}\Big[\delta_{ab}\tau_N^c(\delta_{ik}\sigma_N^j + \delta_{kj}\sigma_N^i) + \delta_{ca}\tau_N^b(\delta_{ij}\sigma_N^k + \delta_{jk}\sigma_N^i) \\ &+ \delta_{bc}\tau_N^a(\delta_{ij}\sigma_N^k + \delta_{ik}\sigma_N^j)\Big]\end{aligned} \tag{B.13}$$

# Appendix C

# Detailed Calculation for Obtaining the Spin-Isospin Matrix Elements

In this Appendix we will go through the steps in detail to get from the formula given in (4.31) to the nucleon operator form given in the Tables 4.1,4.2 and 4.3. To make it a more thorough description we will start from the matrix element and include the steps not given in the chapter.

## C.1 Scalar Matrix Element

We have for the matrix element

$$M_{scal}^{36(qe)}(\hat{O}(\sigma),\hat{O}(\tau)) = \frac{1}{4}\sum_{l,l'}\eta_S^{36(qe)}\eta_T^{36(qe)} \tag{C.1}$$

with

$$\eta_S^{36(qe)} = \sum_{l_{1245},l_{36}} 4(2l_{1245}+1)(2l_{36}+1)(-)^{l_{36}+1}(2(-)^{l_{36}+1}-1) \left\{ \begin{array}{ccc} l & l' & l_{1245} \\ \frac{1}{2} & \frac{1}{2} & l_{36} \\ \frac{1}{2} & \frac{1}{2} & S \end{array} \right\}^2$$

$$\eta_T^{36(qe)} = \sum_{\mu_{1245},\mu_{36}} 4(2\mu_{1245}+1)(2\mu_{36}+1)(-)^{\mu_{36}+1}(2(-)^{\mu_{36}+1}-1) \left\{ \begin{array}{ccc} l & l' & \mu_{1245} \\ \frac{1}{2} & \frac{1}{2} & \mu_{36} \\ \frac{1}{2} & \frac{1}{2} & T \end{array} \right\}^2 \tag{C.2}$$

These are solved for each value of $l$ and $l'$ to give

$$\begin{aligned} \eta_S^{36(qe)}(0,0) &= (3-2S) \\ \eta_S^{36(qe)}(0,1) &= \frac{1}{3}(2S+3) \\ \eta_S^{36(qe)}(1,0) &= \frac{1}{3}(2S+3) \\ \eta_S^{36(qe)}(1,1) &= \frac{1}{9}(15-2S) \end{aligned} \tag{C.3}$$

and similarly for $\eta_T^{36(qe)}$ by replacing the S with T. This gives us

$$M_{scal}^{36(qe)}(S,T) = \frac{1}{4}\left[(3-2S)(3-2T) + \frac{2}{9}(2S+3)(2T+3) + \frac{1}{81}(15-2S)(15-2T)\right] \tag{C.4}$$

which gives a solution for each S and T. These are :

$$\begin{aligned} M_{scal}^{36(qe)}(S=0,T=0) &= \frac{31}{9} \\ M_{scal}^{36(qe)}(S=0,T=1) &= \frac{59}{27} \\ M_{scal}^{36(qe)}(S=1,T=0) &= \frac{59}{27} \\ M_{scal}^{36(qe)}(S=1,T=1) &= \frac{175}{81} \end{aligned} \tag{C.5}$$

We wish to put this into nucleon operator form

$$M_{scal}^{36(qe)}(S,T) = A\vec{1}_{\mathbf{a}}\vec{1}_{\mathbf{b}} + B\vec{\sigma}_{\mathbf{a}}\cdot\vec{\sigma}_{\mathbf{b}} + C\vec{\tau}_{\mathbf{a}}\cdot\vec{\tau}_{\mathbf{b}} + D\vec{\sigma}_{\mathbf{a}}\cdot\vec{\sigma}_{\mathbf{b}}\vec{\tau}_{\mathbf{a}}\cdot\vec{\tau}_{\mathbf{b}} \tag{C.6}$$

This will give a set of simultaneous equations which can be solved for A,B,C,D. The equations to be solved are:

$$M(0,0) = A - 3B - 3C + 9D = \frac{31}{9} \tag{C.7}$$

$$M(1,0) = A + B - 3C - 3D = \frac{59}{27} \tag{C.8}$$

$$M(0,1) = A - 3B + C - 3D = \frac{59}{27} \tag{C.9}$$

$$M(1,1) = A + B + C + D = \frac{175}{81} \tag{C.10}$$

from (C.7) we get

$$A = 3B + 3C - 9D + \frac{31}{9} \tag{C.11}$$

Substituting (C.11) into (C.8) gives

$$\begin{aligned} B &= \frac{59}{27} - \frac{31}{9} - 3B - 3C + 9D + 3C + 3D \\ 4B &= -\frac{34}{27} + 12D \\ B &= -\frac{17}{54} + 3D \end{aligned} \tag{C.12}$$

Similarly from substituting (C.7) into (C.9) we get

$$C = -\frac{17}{54} + 3D \tag{C.13}$$

Using (C.10) and the appropriate subtitutions we get

$$\begin{aligned} D &= \frac{175}{81} - \frac{31}{9} - 3(-\frac{17}{54} + 3D) - 3(-\frac{17}{54} + 3D) + 9D + \frac{17}{54} - 3D + \frac{17}{54} - 3D \\ 16D &= \frac{100}{81} \\ D &= \frac{25}{324} \end{aligned} \tag{C.14}$$

Substituting (C.14) into (C.12) and (C.13) gives

$$B = C = -\frac{1}{12} \tag{C.15}$$

and

$$A = \frac{9}{4} \tag{C.16}$$

We have for our solution now

$$\begin{aligned} M^{36(qe)}_{scal}(S,T) &= \frac{9}{4}\vec{1}_{\mathbf{a}}\vec{1}_{\mathbf{b}} - \frac{1}{12}\vec{\sigma}_{\mathbf{a}}\cdot\vec{\sigma}_{\mathbf{b}} - \frac{1}{12}\vec{\tau}_{\mathbf{a}}\cdot\vec{\tau}_{\mathbf{b}} + \frac{25}{324}\vec{\sigma}_{\mathbf{a}}\cdot\vec{\sigma}_{\mathbf{b}}\vec{\tau}_{\mathbf{a}}\cdot\vec{\tau}_{\mathbf{b}} \\ &= \frac{9}{4}\left[(1 - \frac{1}{27}\vec{\tau}_{\mathbf{a}}\cdot\vec{\tau}_{\mathbf{b}})\vec{1}_{\mathbf{a}}\vec{1}_{\mathbf{b}} - \frac{1}{27}(1 - \frac{25}{27}\vec{\tau}_{\mathbf{a}}\cdot\vec{\tau}_{\mathbf{b}})\vec{\sigma}_{\mathbf{a}}\cdot\vec{\sigma}_{\mathbf{b}}\right] \end{aligned} \tag{C.17}$$

which is the form given in the tables for the scalar spin-isospin matrix elements.

## C.2 Tensor Spin-Isospin Matrix Elements

For the tensor spin-isospin matrix elements the method is the same except that the form we wish to present the results in is written as:

$$M^{ij}_{tens} = \left[A\vec{1}_{\mathbf{a}}\vec{1}_{\mathbf{b}} + B\vec{\tau}_{\mathbf{a}}\cdot\vec{\tau}_{\mathbf{b}}\right] S_{12}(\hat{R}) \tag{C.18}$$

This is solved in the same way as the scalar term. The simultaneous equations are

$$\begin{aligned} M(1,0) &= A - 3B \\ M(1,1) &= A + B \end{aligned} \tag{C.19}$$

To obtain the tensor matrix element for the example we are looking at the isospin matrix element is the same and for the spin matrix element we use (4.51).

Evaluating the full matrix element gives us for each isospin channel

$$\begin{aligned} M_{tens}^{36(qe)}(1,0) &= \frac{17}{27} \\ M_{tens}^{36(qe)}(1,1) &= \frac{1}{81} \end{aligned} \tag{C.20}$$

Uisng the simulatneous equations (C.19) we arrive at

$$\begin{aligned} \frac{17}{27} &= A - 3B \\ \frac{1}{81} &= A + B \end{aligned} \tag{C.21}$$

Solving this our final solution is

$$M_{tens}^{36(qe)}(S,T) = \frac{1}{6}\left(1 - \frac{25}{162}\vec{\tau}_N^{\mathbf{a}} \cdot \vec{\tau}_N^{\mathbf{b}}\right) S_{\mathbf{ab}}(\hat{R}) \tag{C.22}$$

# Appendix D

# Quark Potential Calculation in Detail

In this appendix we will take one of the more complicated quark potentials and go through the calculation in detail. It will involve both the central and tensor spin-isospin matrix elements as well as the radial terms to combine together to give the final form. The potential we will look at is $v_{25}^{qe}$.

## D.1 The Potential

We start with the potential in the form given in (3.20).

$$v_{25}^{qe} = -9\frac{<\phi_a\phi_b|V^{OPE}(25)P_{36}^{\sigma\tau xc}(1-P^{\sigma\tau xc})|\phi_a\phi_b>}{<\phi_a\phi_b|(1-9P_{36}^{\sigma\tau xc})(1-P^{\sigma\tau xc})|\phi_a\phi_b>} \tag{D.1}$$

with

$$V^{OPE}(25) = \frac{f_{\pi qq}^2}{m_\pi^2}4\pi\int\frac{d^3q}{(2\pi)^3}\frac{\vec{\sigma}_2\cdot q\vec{\sigma}_5\cdot q}{q^2+m_\pi^2}\vec{\tau}_2\cdot\vec{\tau}_5 e^{iq\cdot(r_2-r_5)} \tag{D.2}$$

Following the formalism used in (3.23) we can separate the potential into the individual matrix elements to make the evaluation easier. This gives us

$$\begin{aligned} v_{25}^{qe} &= -\frac{9}{N}\frac{f_{\pi qq}^2}{m_\pi^2}4\pi\int\frac{d^3q}{(2\pi)^3}\frac{1}{q^2+m_\pi^2} < \varphi_{\mathbf{a}}^x\varphi_{\mathbf{b}}^x|e^{iq\cdot(r_2-r_5)}P_{36}^x(1-(-)^{(S+T)}P^x)|\varphi_{\mathbf{a}}^x\varphi_{\mathbf{b}}^x > \\ &\times < \varphi_{\mathbf{a}}^c\varphi_{\mathbf{b}}^c|P_{36}^c|\varphi_{\mathbf{a}}^c\varphi_{\mathbf{b}}^c >< \varphi_{\mathbf{a}}^{\sigma\tau}\varphi_{\mathbf{b}}^{\sigma\tau}|\vec{\tau}_2\cdot\vec{\tau}_5\vec{\sigma}_2\cdot q\vec{\sigma}_5\cdot qP_{36}^{\sigma\tau}|\varphi_{\mathbf{a}}^{\sigma\tau}\varphi_{\mathbf{b}}^{\sigma\tau} > \\ &= -\frac{3}{N}\frac{f_{\pi qq}^2}{m_\pi^2}4\pi\int\frac{d^3q}{(2\pi)^3}\frac{1}{q^2+m_\pi^2} < \varphi_{\mathbf{a}}^x\varphi_{\mathbf{b}}^x|e^{iq\cdot(r_2-r_5)}P_{36}^x(1-(-)^{(S+T)}P^x)|\varphi_{\mathbf{a}}^x\varphi_{\mathbf{b}}^x > \\ &\times < \varphi_{\mathbf{a}}^{\sigma\tau}\varphi_{\mathbf{b}}^{\sigma\tau}|\vec{\tau}_2\cdot\vec{\tau}_5\vec{\sigma}_2\cdot q\vec{\sigma}_5\cdot qP_{36}^{\sigma\tau}|\varphi_{\mathbf{a}}^{\sigma\tau}\varphi_{\mathbf{b}}^{\sigma\tau} > \end{aligned} \tag{D.3}$$

We can now evaluate the matrix elements individually and arrive at a total solution. The spin-isospin matrix elements need to be calculated in both the scalar and tensor case.

## D.2 Spin-Isospin Matrix Element

We start first with the spin-isospin matrix element. This can be written in the form given by (4.5)

$$\begin{aligned} M^{25}(\hat{O}(\sigma)\hat{O}(\tau)) = \frac{1}{4}\sum_{ll'l_1l_1'} &< (l\tfrac{1}{2})\tfrac{1}{2}(l'\tfrac{1}{2})\tfrac{1}{2} : SM|\vec{\sigma}_2\cdot q\vec{\sigma}_5\cdot qP_{36}^{\sigma}|(l_1\tfrac{1}{2})\tfrac{1}{2}(l_1'\tfrac{1}{2})\tfrac{1}{2};SM > \\ &\times < (l\tfrac{1}{2})\tfrac{1}{2}(l'\tfrac{1}{2})\tfrac{1}{2} : TM_T|\vec{\tau}_2\cdot\vec{\tau}_5P_{36}^{\tau}|(l_1\tfrac{1}{2})\tfrac{1}{2}(l_1'\tfrac{1}{2})\tfrac{1}{2};TM_T > \end{aligned} \tag{D.4}$$

We will look at just the spin term for the moment. From (4.23) we know that it can be expanded out into two terms; the scalar and tensor. We will do the scalar term first.

### D.2.1 scalar spin-isospin matrix element

We have for $\lambda = 0$

$$(\vec{\sigma}_2\cdot q\vec{\sigma}_5\cdot q)_{\lambda=0} = \frac{1}{3}q^2\vec{\sigma}_2\cdot\vec{\sigma}_5 \tag{D.5}$$

We will concentrate on only the spin dependent terms to calculate the matrix element adding in the constants in the final phase. The matrix element is

$$\eta_S^{25}(ll'l_1l_1') =< (l\tfrac{1}{2})\tfrac{1}{2}(l'\tfrac{1}{2})\tfrac{1}{2}; SM|\vec{\sigma}_2 \cdot \vec{\sigma}_5 P_{36}^{\sigma}|(l_1\tfrac{1}{2})\tfrac{1}{2}(l_1'\tfrac{1}{2})\tfrac{1}{2}; SM > \tag{D.6}$$

To be able to operate the operators we need to recouple the left and right hand sides to have the quarks required on their own. First recouple the right hand side to get quarks 3 and 6 together. Doing this and showing only the right hand side for simplicity, gives

$$\eta_S^{25}(ll'l_1l_1')_{RHS} = \sum_{l_{1245},l_{36}} 2[(2l_{1245}+1)(2l_{36}+1)]^{\frac{1}{2}} \begin{Bmatrix} l_1 & l_1' & l_{1245} \\ \frac{1}{2} & \frac{1}{2} & l_{36} \\ \frac{1}{2} & \frac{1}{2} & S \end{Bmatrix} \times P_{36}^{\sigma}|(l_1l_1')l_{1245}(\tfrac{1}{2}\tfrac{1}{2})l_{36}; SM > \tag{D.7}$$

We operate the $P_{36}$ to the right and get

$$\eta_S^{25}(ll'l_1l_1')_{RHS} = \sum_{l_{1245},l_{36}} 2[(2l_{1245}+1)(2l_{36}+1)]^{\frac{1}{2}}(-)^{l_{36}+1} \times \begin{Bmatrix} l_1 & l_1' & l_{1245} \\ \frac{1}{2} & \frac{1}{2} & l_{36} \\ \frac{1}{2} & \frac{1}{2} & S \end{Bmatrix} |(l_1l_1')l_{1245}(\tfrac{1}{2}\tfrac{1}{2})l_{36}; SM > \tag{D.8}$$

Now recouple the RHS back.

$$\eta_S^{25}(ll'l_1l_1')_{RHS} = \sum_{l_{1245},l_{36},\lambda,\kappa} 2(2l_{1245}+1)(2l_{36}+1)[(2\lambda+1)(2\kappa+1)]^{\frac{1}{2}}(-)^{l_{36}+1} \times \begin{Bmatrix} l_1 & l_1' & l_{1245} \\ \frac{1}{2} & \frac{1}{2} & l_{36} \\ \frac{1}{2} & \frac{1}{2} & S \end{Bmatrix} \begin{Bmatrix} l_1 & l_1' & l_{1245} \\ \frac{1}{2} & \frac{1}{2} & l_{36} \\ \lambda & \kappa & S \end{Bmatrix} |(l_1\tfrac{1}{2})\lambda(l_1'\tfrac{1}{2})\kappa; SM > \tag{D.9}$$

We now look at the left hand side (LHS)

$$\eta_S^{25}(ll'l_1l_1')_{LHS} =< (l\tfrac{1}{2})\tfrac{1}{2}(l'\tfrac{1}{2})\tfrac{1}{2}; SM|\vec{\sigma}_2 \cdot \vec{\sigma}_5 \tag{D.10}$$

We need to first recouple nucleons 1 and 2 separately. Do nucleon 1 first

$$< (\tfrac{1}{2}\tfrac{1}{2})l; \tfrac{1}{2}| = \sum_{l_{13}} (-)^{l+l_{13}+1}[(2l+1)(2l_{13}+1)]^{\frac{1}{2}} \left\{ \begin{matrix} \frac{1}{2} & \frac{1}{2} & l \\ \frac{1}{2} & \frac{1}{2} & l_{13} \end{matrix} \right\} < (\tfrac{1}{2}\tfrac{1}{2})l_{13}q_2; \tfrac{1}{2}| \tag{D.11}$$

with $q_i = \frac{1}{2}$ the spin for quark $i$. Similarly for nucleon 2 we get

$$< (\tfrac{1}{2}\tfrac{1}{2})l'; \tfrac{1}{2}| = \sum_{l_{46}} (-)^{l'+l_{46}+1}[(2l'+1)(2l_{46}+1)]^{\frac{1}{2}} \left\{ \begin{matrix} \frac{1}{2} & \frac{1}{2} & l \\ \frac{1}{2} & \frac{1}{2} & l_{46} \end{matrix} \right\} < (\tfrac{1}{2}\tfrac{1}{2})l_{46}q_5; \tfrac{1}{2}| \tag{D.12}$$

This gives for the LHS:

$$\begin{aligned} \eta_S^{25}(ll'l_1l_1')_{LHS} &= \sum_{l_{13},l_{46}} (-)^{2+l+l'+l_{13}+l_{46}}[(2l+1)(2l'+1)(2l_{13}+1)(2l_{46}+1)]^{\frac{1}{2}} \\ &\times \left\{ \begin{matrix} \frac{1}{2} & \frac{1}{2} & l \\ \frac{1}{2} & \frac{1}{2} & l_{13} \end{matrix} \right\} \left\{ \begin{matrix} \frac{1}{2} & \frac{1}{2} & l \\ \frac{1}{2} & \frac{1}{2} & l_{46} \end{matrix} \right\} < (l_{13}q_2)\tfrac{1}{2}(l_{46}q_5)\tfrac{1}{2}; SM|\vec{\sigma}_2 \cdot \vec{\sigma}_5 \end{aligned} \tag{D.13}$$

We now recouple to get quarks 2 and 5 together.

$$\begin{aligned} \eta_S^{25}(ll'l_1l_1')_{LHS} &= \sum_{l_{13},l_{46}} (-)^{2+l+l'+l_{13}+l_{46}}[(2l+1)(2l'+1)(2l_{13}+1)(2l_{46}+1)]^{\frac{1}{2}} \\ &\times \left\{ \begin{matrix} \frac{1}{2} & \frac{1}{2} & l \\ \frac{1}{2} & \frac{1}{2} & l_{13} \end{matrix} \right\} \left\{ \begin{matrix} \frac{1}{2} & \frac{1}{2} & l \\ \frac{1}{2} & \frac{1}{2} & l_{46} \end{matrix} \right\} 2[(2l_{1346}+1)(2l_{25}+1)]^{\frac{1}{2}} \left\{ \begin{matrix} l_{13} & l_{46} & l_{1346} \\ \frac{1}{2} & \frac{1}{2} & l_{25} \\ \frac{1}{2} & \frac{1}{2} & S \end{matrix} \right\} \\ &\times < (l_{13}l_{46})l_{1346}(\tfrac{1}{2}\tfrac{1}{2})l_{25}; SM|\vec{\sigma}_2 \cdot \vec{\sigma}_5 \end{aligned} \tag{D.14}$$

Operating $\vec{\sigma}_2 \cdot \vec{\sigma}_5$ to the left:

$$\begin{aligned}
\eta_S^{25}(ll'l_1l_1')_{LHS} &= \sum_{l_{13},l_{46}} (-)^{2+l+l'+l_{13}+l_{46}} 2[(2l+1)(2l'+1)(2l_{13}+1) \\
&\times (2l_{46}+1)(2l_{1346}+1)(2l_{25}+1)]^{\frac{1}{2}} (-2(-)^{l_{25}}-1) \left\{ \begin{matrix} \frac{1}{2} & \frac{1}{2} & l \\ \frac{1}{2} & \frac{1}{2} & l_{13} \end{matrix} \right\} \left\{ \begin{matrix} \frac{1}{2} & \frac{1}{2} & l \\ \frac{1}{2} & \frac{1}{2} & l_{46} \end{matrix} \right\} \\
&\times \left\{ \begin{matrix} l_{13} & l_{46} & l_{1346} \\ \frac{1}{2} & \frac{1}{2} & l_{25} \\ \frac{1}{2} & \frac{1}{2} & S \end{matrix} \right\} < (l_{13}l_{46})l_{1346}(\tfrac{1}{2}\tfrac{1}{2})l_{25}; SM| \qquad \text{(D.15)}
\end{aligned}$$

We now need to recouple it back to its original configuration.

$$\begin{aligned}
\eta_S^{25}(ll'l_1l_1')_{LHS} &= \sum_{l_{13},l_{46},\lambda'} \sum_{l_{1346},l_{25},\kappa'} 2(-)^{l+l'+l_{13}+l_{46}} [(2l+1)(2l'+1)(2\lambda'+1) \\
&\times (2\kappa'+1)(2l_{13}+1)(2l_{46}+1)]^{\frac{1}{2}} (2l_{25}+1)(2l_{1346}+1)(-2(-)^{l_{25}}-1) \\
&\times \left\{ \begin{matrix} \frac{1}{2} & \frac{1}{2} & l \\ \frac{1}{2} & \frac{1}{2} & l_{13} \end{matrix} \right\} \left\{ \begin{matrix} \frac{1}{2} & \frac{1}{2} & l \\ \frac{1}{2} & \frac{1}{2} & l_{46} \end{matrix} \right\} \left\{ \begin{matrix} l_{13} & l_{46} & l_{1346} \\ \frac{1}{2} & \frac{1}{2} & l_{25} \\ \frac{1}{2} & \frac{1}{2} & S \end{matrix} \right\} \left\{ \begin{matrix} l_{13} & l_{46} & l_{1346} \\ \frac{1}{2} & \frac{1}{2} & l_{25} \\ \lambda' & \kappa' & S \end{matrix} \right\} \\
&\times < (l_{13}\tfrac{1}{2})\lambda'(l_{46}\tfrac{1}{2})\kappa'; SM| \qquad \text{(D.16)}
\end{aligned}$$

Now recouple the nucleons separately back using

$$\begin{aligned}
< (q_1q_3)l_{13}q_2; \lambda'| &= \sum_{l_{12}} (-)^{1+l_{12}+l_{13}} [(2l_{12}+1)(2l_{13}+1)]^{\frac{1}{2}} \left\{ \begin{matrix} \lambda' & \frac{1}{2} & l_{13} \\ \frac{1}{2} & \frac{1}{2} & l_{12} \end{matrix} \right\} < (\tfrac{1}{2}\tfrac{1}{2})l_{12}\tfrac{1}{2}; \lambda'| \\
< (q_4q_6)l_{46}q_5; \kappa'| &= \sum_{l_{45}} (-)^{1+l_{45}+l_{46}} [(2l_{45}+1)(2l_{46}+1)]^{\frac{1}{2}} \left\{ \begin{matrix} \kappa' & \frac{1}{2} & l_{46} \\ \frac{1}{2} & \frac{1}{2} & l_{45} \end{matrix} \right\} < (\tfrac{1}{2}\tfrac{1}{2})l_{45}\tfrac{1}{2}; \kappa'| \qquad \text{(D.17)}
\end{aligned}$$

Substituting (D.17) into (D.16) gives:

$$\begin{aligned}
\eta_S^{25}(ll'l_1l_1')_{LHS} &= \sum_{l_{13},l_{46},\lambda'} \sum_{l_{1346},l_{25},\kappa'} \sum_{l_{12},l_{45}} 2(-)^{l+l'+l_{12}+l_{45}} [(2l+1)(2l'+1)(2\lambda'+1) \\
&\times (2\kappa'+1)(2l_{12}+1)(2l_{45}+1)]^{\frac{1}{2}} (2l_{25}+1)(2l_{1346}+1)(2l_{13}+1)
\end{aligned}$$

$$\times \quad (2l_{46}+1)(-2(-)^{l_{25}}-1)\left\{\begin{matrix}\frac{1}{2} & \frac{1}{2} & l\\ \frac{1}{2} & \frac{1}{2} & l_{13}\end{matrix}\right\}\left\{\begin{matrix}\frac{1}{2} & \frac{1}{2} & l\\ \frac{1}{2} & \frac{1}{2} & l_{46}\end{matrix}\right\}\left\{\begin{matrix}\lambda' & \frac{1}{2} & l_{13}\\ \frac{1}{2} & \frac{1}{2} & l_{12}\end{matrix}\right\}\left\{\begin{matrix}\kappa' & \frac{1}{2} & l_{46}\\ \frac{1}{2} & \frac{1}{2} & l_{45}\end{matrix}\right\}$$

$$\times \left\{\begin{matrix} l_{13} & l_{46} & l_{1346}\\ \frac{1}{2} & \frac{1}{2} & l_{25}\\ \frac{1}{2} & \frac{1}{2} & S\end{matrix}\right\}\left\{\begin{matrix} l_{13} & l_{46} & l_{1346}\\ \frac{1}{2} & \frac{1}{2} & l_{25}\\ \lambda' & \kappa' & S\end{matrix}\right\} < (l_{12}\tfrac{1}{2})\lambda'(l_{45}\tfrac{1}{2})\kappa'; SM| \qquad \text{(D.18)}$$

We can now combine the RHS and LHS to give :

$$\begin{aligned}\eta_S^{25}(ll'l_1l_1') = & \sum_{l_{12},l_{13},l_{45}}\sum_{l_{46},l_{1245},l_{1346}}\sum_{l_{25},l_{36},\lambda}\sum_{\lambda',\kappa,\kappa'} 4(-)^{l+l'+l_{36}+1+l_{12}+l_{45}}(-2(-)^{l_{25}}-1)\\
& \times (2l_{1245}+1)(2l_{36}+1)(2l_{1346}+1)(2l_{25}+1)(l_{13}+1)(2l_{46}+1)[(2l_{12}+1)\\
& \times (2l_{45}+1)(2\lambda+1)(2\lambda'+1)(2\kappa+1)(2\kappa'+1)(2l+1)(2l'+1)]^{\frac{1}{2}}\\
& \times \left\{\begin{matrix}\frac{1}{2} & \frac{1}{2} & l\\ \frac{1}{2} & \frac{1}{2} & l_{13}\end{matrix}\right\}\left\{\begin{matrix}\frac{1}{2} & \frac{1}{2} & l\\ \frac{1}{2} & \frac{1}{2} & l_{46}\end{matrix}\right\}\left\{\begin{matrix}\lambda' & \frac{1}{2} & l_{13}\\ \frac{1}{2} & \frac{1}{2} & l_{12}\end{matrix}\right\}\left\{\begin{matrix}\kappa' & \frac{1}{2} & l_{46}\\ \frac{1}{2} & \frac{1}{2} & l_{45}\end{matrix}\right\}\\
& \times \left\{\begin{matrix} l_{13} & l_{46} & l_{1346}\\ \frac{1}{2} & \frac{1}{2} & l_{25}\\ \frac{1}{2} & \frac{1}{2} & S\end{matrix}\right\}\left\{\begin{matrix} l_{13} & l_{46} & l_{1346}\\ \frac{1}{2} & \frac{1}{2} & l_{25}\\ \lambda' & \kappa' & S\end{matrix}\right\}\left\{\begin{matrix} l_1 & l_1' & l_{1245}\\ \frac{1}{2} & \frac{1}{2} & l_{36}\\ \frac{1}{2} & \frac{1}{2} & S\end{matrix}\right\}\left\{\begin{matrix} l_1 & l_1' & l_{1245}\\ \frac{1}{2} & \frac{1}{2} & l_{36}\\ \lambda & \kappa & S\end{matrix}\right\}\\
& \times < (l_{12}\tfrac{1}{2})\lambda'(l_{45}\tfrac{1}{2})\kappa'; SM|(l_1\tfrac{1}{2})\lambda(l_1'\tfrac{1}{2})\kappa; SM > \qquad \text{(D.19)}\end{aligned}$$

and finally

$$\begin{aligned}\eta_S^{25}(ll'l_1l_1') = & \sum_{l_{46},l_{1245},l_{1346}}\sum_{l_{25},l_{36},l_{13}}\sum_{\lambda,\kappa} 4(-)^{l+l'+l_{36}+1+l_{12}+l_{45}}(-2(-)^{l_{25}}-1)\\
& \times (2l_{1245}+1)(2l_{36}+1)(2l_{1346}+1)(2l_{25}+1)(l_{13}+1)(2l_{46}+1)\\
& \times (2\lambda+1)(2\kappa+1)[(2l_1'+1)(l_1+1)(2l+1)(2l'+1)]^{\frac{1}{2}}\\
& \times \left\{\begin{matrix}\frac{1}{2} & \frac{1}{2} & l\\ \frac{1}{2} & \frac{1}{2} & l_{13}\end{matrix}\right\}\left\{\begin{matrix}\frac{1}{2} & \frac{1}{2} & l\\ \frac{1}{2} & \frac{1}{2} & l_{46}\end{matrix}\right\}\left\{\begin{matrix}\lambda' & \frac{1}{2} & l_{13}\\ \frac{1}{2} & \frac{1}{2} & l_{12}\end{matrix}\right\}\left\{\begin{matrix}\kappa' & \frac{1}{2} & l_{46}\\ \frac{1}{2} & \frac{1}{2} & l_{45}\end{matrix}\right\}\end{aligned}$$

$$\times \left\{ \begin{matrix} l_{13} & l_{46} & l_{1346} \\ \frac{1}{2} & \frac{1}{2} & l_{25} \\ \frac{1}{2} & \frac{1}{2} & S \end{matrix} \right\} \left\{ \begin{matrix} l_{13} & l_{46} & l_{1346} \\ \frac{1}{2} & \frac{1}{2} & l_{25} \\ \lambda' & \kappa' & S \end{matrix} \right\} \left\{ \begin{matrix} l_1 & l_1' & l_{1245} \\ \frac{1}{2} & \frac{1}{2} & l_{36} \\ \frac{1}{2} & \frac{1}{2} & S \end{matrix} \right\} \left\{ \begin{matrix} l_1 & l_1' & l_{1245} \\ \frac{1}{2} & \frac{1}{2} & l_{36} \\ \lambda & \kappa & S \end{matrix} \right\}$$
$$\times \quad \delta(\lambda\lambda')\delta(\kappa\kappa')\delta(l_{12}l_1)\delta(l_{45}l_1'). \tag{D.20}$$

Similarly for the isospin matrix element we obtain

$$\begin{aligned}
\eta_T^{25}(ll'l_1l_1') = & \sum_{\mu_{46},\mu_{1245},\mu_{1346}} \sum_{\mu_{25},\mu_{36},\mu_{13}} \sum_{\lambda,\kappa} 4(-)^{l+l'+\mu_{36}+1+\mu_{12}+\mu_{45}}(-2(-)^{\mu_{25}}-1) \\
& \times \quad (2\mu_{1245}+1)(2\mu_{36}+1)(2\mu_{1346}+1)(2\mu_{25}+1)(\mu_{13}+1)(2\mu_{46}+1) \\
& \times \quad (2\lambda+1)(2\kappa+1)[(2l_1'+1)(l_1+1)(2l+1)(2l'+1)]^{\frac{1}{2}} \\
& \times \quad \left\{ \begin{matrix} \frac{1}{2} & \frac{1}{2} & l \\ \frac{1}{2} & \frac{1}{2} & \mu_{13} \end{matrix} \right\} \left\{ \begin{matrix} \frac{1}{2} & \frac{1}{2} & l \\ \frac{1}{2} & \frac{1}{2} & \mu_{46} \end{matrix} \right\} \left\{ \begin{matrix} \lambda' & \frac{1}{2} & \mu_{13} \\ \frac{1}{2} & \frac{1}{2} & \mu_{12} \end{matrix} \right\} \left\{ \begin{matrix} \kappa' & \frac{1}{2} & \mu_{46} \\ \frac{1}{2} & \frac{1}{2} & \mu_{45} \end{matrix} \right\} \\
& \times \left\{ \begin{matrix} \mu_{13} & \mu_{46} & \mu_{1346} \\ \frac{1}{2} & \frac{1}{2} & \mu_{25} \\ \frac{1}{2} & \frac{1}{2} & T \end{matrix} \right\} \left\{ \begin{matrix} \mu_{13} & \mu_{46} & \mu_{1346} \\ \frac{1}{2} & \frac{1}{2} & \mu_{25} \\ \lambda' & \kappa' & T \end{matrix} \right\} \left\{ \begin{matrix} l_1 & l_1' & \mu_{1245} \\ \frac{1}{2} & \frac{1}{2} & \mu_{36} \\ \frac{1}{2} & \frac{1}{2} & T \end{matrix} \right\} \left\{ \begin{matrix} l_1 & l_1' & \mu_{1245} \\ \frac{1}{2} & \frac{1}{2} & \mu_{36} \\ \lambda & \kappa & T \end{matrix} \right\} \\
& \times \quad \delta(\lambda\lambda')\delta(\kappa\kappa')\delta(\mu_{12}l_1)\delta(\mu_{45}l_1')
\end{aligned} \tag{D.21}$$

(D.20) and (D.21) can be substituted into (D.4) to obtain our final spin-isospin matrix element. From this we can get a numerical solution for each S and T.

$$\begin{aligned}
M_{scal}^{25(qe)}(0,0) &= \frac{7}{3} \\
M_{scal}^{25(qe)}(1,0) &= \frac{1}{9} \\
M_{scal}^{25(qe)}(0,1) &= \frac{1}{9} \\
M_{scal}^{25(qe)}(1,1) &= \frac{73}{81}
\end{aligned} \tag{D.22}$$

Using the method outlined in the previous appendix we obtain the set of simultaneous

equations:

$$A - 3B - 3C + 9D = \frac{7}{3} \tag{D.23}$$

$$A + B - 3C - 3D = \frac{1}{9} \tag{D.24}$$

$$A - 3B + C - 3D = \frac{1}{9} \tag{D.25}$$

$$A + B + C + D = \frac{73}{81} \tag{D.26}$$

Solving these gives us

$$\begin{aligned} A &= \frac{25}{36} \\ B = \frac{1}{108} &= C \\ D &= \frac{61}{324} \end{aligned} \tag{D.27}$$

and our matrix element can be written as

$$M^{25(qe)}_{scal}(S,T) = \frac{25}{36}\left[(1 + \frac{1}{75}\vec{\tau}_{\mathbf{a}} \cdot \vec{\tau}_{\mathbf{b}})\vec{\mathrm{l}}_{\mathbf{a}}\vec{\mathrm{l}}_{\mathbf{b}} + \frac{1}{75}(1 + \frac{61}{3}\vec{\tau}_{\mathbf{a}} \cdot \vec{\tau}_{\mathbf{b}})\vec{\sigma}_{\mathbf{a}} \cdot \vec{\sigma}_{\mathbf{b}}\right] \tag{D.28}$$

### D.2.2 Tensor spin-isospin matrix element

For the spin operator we have for $\lambda = 2$

$$(\vec{\sigma}_2 \cdot q\vec{\sigma}_5 \cdot q)_{\lambda=2} = \frac{q^2}{3} S_{ij}(\hat{q}) \tag{D.29}$$

Using as our starting point the results obtained in (4.38) we have

$$M^{25(qe)}_{tens}(S,T) = \frac{1}{4} \sum_{l,l',l_1,l'_1} \eta^{25(qe)}_S(l,l',l_1,l'_1)\eta^{25(qe)}_T(l,l',l_1,l'_1) \tag{D.30}$$

where the isospin term is the same as before

$$\begin{aligned}\eta_T^{25}(ll'l_1l_1') = & \sum_{\mu_{46},\mu_{1245},\mu_{1346}} \sum_{\mu_{25},\mu_{36},\mu_{13}} \sum_{\lambda,\kappa} 4(-)^{l+l'+\mu_{36}+1+\mu_{12}+\mu_{45}}(-2(-)^{\mu_{25}}-1) \\ & \times (2\mu_{1245}+1)(2\mu_{36}+1)(2\mu_{1346}+1)(2\mu_{25}+1)(\mu_{13}+1)(2\mu_{46}+1) \\ & \times (2\lambda+1)(2\kappa+1)[(2l_1'+1)(l_1+1)(2l+1)(2l'+1)]^{\frac{1}{2}} \\ & \times \begin{Bmatrix} \frac{1}{2} & \frac{1}{2} & l \\ \frac{1}{2} & \frac{1}{2} & \mu_{13} \end{Bmatrix} \begin{Bmatrix} \frac{1}{2} & \frac{1}{2} & l \\ \frac{1}{2} & \frac{1}{2} & \mu_{46} \end{Bmatrix} \begin{Bmatrix} \lambda' & \frac{1}{2} & \mu_{13} \\ \frac{1}{2} & \frac{1}{2} & \mu_{12} \end{Bmatrix} \begin{Bmatrix} \kappa' & \frac{1}{2} & \mu_{46} \\ \frac{1}{2} & \frac{1}{2} & \mu_{45} \end{Bmatrix} \\ & \times \begin{Bmatrix} \mu_{13} & \mu_{46} & \mu_{1346} \\ \frac{1}{2} & \frac{1}{2} & \mu_{25} \\ \frac{1}{2} & \frac{1}{2} & T \end{Bmatrix} \begin{Bmatrix} \mu_{13} & \mu_{46} & \mu_{1346} \\ \frac{1}{2} & \frac{1}{2} & \mu_{25} \\ \lambda' & \kappa' & T \end{Bmatrix} \begin{Bmatrix} l_1 & l_1' & \mu_{1245} \\ \frac{1}{2} & \frac{1}{2} & \mu_{36} \\ \frac{1}{2} & \frac{1}{2} & T \end{Bmatrix} \begin{Bmatrix} l_1 & l_1' & \mu_{1245} \\ \frac{1}{2} & \frac{1}{2} & \mu_{36} \\ \lambda & \kappa & T \end{Bmatrix} \\ & \times \delta(\lambda\lambda')\delta(\kappa\kappa')\delta(\mu_{12}l_1)\delta(\mu_{45}l_1') \end{aligned} \tag{D.31}$$

and the spin term is that given in (4.51)

$$\begin{aligned}\eta_S^{25(qe)} = & \sum_{l_{1245},l_{36},\lambda,\kappa} 2(2l_{1245}+1)(2l_{36}+1)[(2\lambda+1)(2\kappa+1)]^{\frac{1}{2}}(-)^{l_{36}+1} \\ & \times \begin{Bmatrix} l_1 & l_1' & l_{1245} \\ \frac{1}{2} & \frac{1}{2} & l_{36} \\ \frac{1}{2} & \frac{1}{2} & 1 \end{Bmatrix} \begin{Bmatrix} l_1 & l_1' & l_{1245} \\ \frac{1}{2} & \frac{1}{2} & l_{36} \\ \lambda & \kappa & 1 \end{Bmatrix} \begin{Bmatrix} \frac{1}{2} & \frac{1}{2} & S \\ \lambda & \kappa & S \\ 1 & 1 & 2 \end{Bmatrix} \begin{Bmatrix} \frac{1}{2} & \frac{1}{2} & S \\ \frac{1}{2} & \frac{1}{2} & S \\ 1 & 1 & 2 \end{Bmatrix}^{-1} \\ & \times \frac{1}{6} < (l\tfrac{1}{2})\tfrac{1}{2}||\vec{\sigma}_2||(l_1\tfrac{1}{2})\tfrac{1}{2} >< (l'\tfrac{1}{2})\tfrac{1}{2}||\vec{\sigma}_5||(l_1'\tfrac{1}{2})\tfrac{1}{2} > S_{\mathbf{ab}}(\hat{q}) \end{aligned} \tag{D.32}$$

We now need to evaluate the reduced matrix elements

$$< (l\tfrac{1}{2})\tfrac{1}{2}||\vec{\sigma}_2||(l_1\tfrac{1}{2})\tfrac{1}{2} > \tag{D.33}$$

$$< (l'\tfrac{1}{2})\tfrac{1}{2}||\vec{\sigma}_5||(l_1'\tfrac{1}{2})\tfrac{1}{2} > \tag{D.34}$$

As they have the same stucture we will show the results for (D.33). From deShalit and Talmi [DeshTal] we have the rules for evaluating reduced matrix elements. For $\sigma_i(i =$

$1,2,4,5)$ we have

$$< (l_{\frac{1}{2}})_{\frac{1}{2}} || \vec{\sigma}_i || (l_1 \tfrac{1}{2})_{\frac{1}{2}} >= (-)^{\lambda+\frac{3}{2}} \sqrt{2} [(2\lambda+1)(2l+1)(2l_1+1)]^{\frac{1}{2}} \sqrt{6} \left\{ \begin{matrix} l & \frac{1}{2} & \frac{1}{2} \\ \lambda & l_1 & 1 \end{matrix} \right\} \left\{ \begin{matrix} \frac{1}{2} & l & \frac{1}{2} \\ l_1 & \frac{1}{2} & 1 \end{matrix} \right\} \quad \text{(D.35)}$$

This will then give us for the spin matrix element

$$\begin{aligned} \eta_S^{25(qe)} &= \sum_{l_{1245}, l_{36}, \lambda, \kappa} 6(2l_{1245}+1)(2l_{36}+1)(2\lambda+1)(2\kappa+1) \\ &\times [(2l+1)(2l'+1)(2l_1+1)(2l_1'+1)]^{\frac{1}{2}} (-)^{l_{36}+\lambda+\kappa} \\ &\times \left\{ \begin{matrix} l_1 & l_1' & l_{1245} \\ \frac{1}{2} & \frac{1}{2} & l_{36} \\ \frac{1}{2} & \frac{1}{2} & 1 \end{matrix} \right\} \left\{ \begin{matrix} l_1 & l_1' & l_{1245} \\ \frac{1}{2} & \frac{1}{2} & l_{36} \\ \lambda & \kappa & 1 \end{matrix} \right\} \left\{ \begin{matrix} \frac{1}{2} & \frac{1}{2} & S \\ \lambda & \kappa & S \\ 1 & 1 & 2 \end{matrix} \right\} \\ &\times \left\{ \begin{matrix} l & \frac{1}{2} & \frac{1}{2} \\ \lambda & l_1 & 1 \end{matrix} \right\} \left\{ \begin{matrix} \frac{1}{2} & l & \frac{1}{2} \\ l_1 & \frac{1}{2} & 1 \end{matrix} \right\} \left\{ \begin{matrix} l' & \frac{1}{2} & \frac{1}{2} \\ \kappa & l_1' & 1 \end{matrix} \right\} \left\{ \begin{matrix} \frac{1}{2} & l' & \frac{1}{2} \\ l_1' & \frac{1}{2} & 1 \end{matrix} \right\} 6 S_{\mathbf{ab}}(\hat{q}) \end{aligned} \quad \text{(D.36)}$$

This now enables us to numerically solve the spin-isospin matrix element. The solutions are :

$$\begin{aligned} M_{tens}^{25(qe)}(1,0) &= -\frac{1}{18} \\ M_{tens}^{25(qe)}(1,1) &= \frac{5}{162} \end{aligned} \quad \text{(D.37)}$$

Using the method given in Appendix C we get :

$$\begin{aligned} -\frac{1}{18} &= A - 3B \\ \frac{5}{162} &= A + B \end{aligned} \quad \text{(D.38)}$$

Solving this gives us

$$A = \frac{1}{108}$$

$$B = -\frac{7}{324} \tag{D.39}$$

and we obtain for our matrix element

$$M_{tens}^{25(qe)}(S,T) = \frac{1}{108}\left(1 - \frac{7}{3}\vec{\tau}_{\mathbf{a}} \cdot \vec{\tau}_{\mathbf{b}}\right) S_{\mathbf{ab}}(\hat{q}) \tag{D.40}$$

## D.3 Radial Matrix Element

We now need to evaluate the radial matrix element. This was given in (D.3). This is

$$\eta_R^{25(qe)} = < \varphi_{\mathbf{a}}^x \varphi_{\mathbf{b}}^x || e^{iq\cdot(r_2 - r_5)} P_{36}^x (1 - (-)^{(S+T)} P^x) || \varphi_{\mathbf{a}}^x \varphi_{\mathbf{b}}^x > \tag{D.41}$$

where $\varphi_{\mathbf{a}}^x$ and $\varphi_{\mathbf{b}}^x$ are the spatial wave functions given in (3.18). Expanding and separating the matrix element into two terms and ignoring the spin-isospin phase factor for the moment gives

$$\begin{aligned}
\eta_R^{25(qe)} &= < \varphi_{\mathbf{a}}^x(123)\varphi_{\mathbf{b}}^x(456) || e^{iq\cdot(r_2 - r_5)} P_{36}^x || \varphi_{\mathbf{a}}^x(123)\varphi_{\mathbf{b}}^x(456) > - \\
&\quad < \varphi_{\mathbf{a}}^x(123)\varphi_{\mathbf{b}}^x(456) || e^{iq\cdot(r_2 - r_5)} P_{36}^x P^x || \varphi_{\mathbf{a}}^x(123)\varphi_{\mathbf{b}}^x(456) > \\
&= < \varphi_{\mathbf{a}}^x(123)\varphi_{\mathbf{b}}^x(456) || e^{iq\cdot(r_2 - r_5)} || \varphi_{\mathbf{a}}^x(126)\varphi_{\mathbf{b}}^x(453) > - \\
&\quad < \varphi_{\mathbf{a}}^x(123)\varphi_{\mathbf{b}}^x(456) || e^{iq\cdot(r_2 - r_5)} || \varphi_{\mathbf{a}}^x(453)\varphi_{\mathbf{b}}^x(126) > \\
&= A - B
\end{aligned} \tag{D.42}$$

We now calculate the terms separately

$$A = < \varphi_{\mathbf{a}}^x(123)\varphi_{\mathbf{b}}^x(456) || e^{iq\cdot(r_2 - r_5)} || \varphi_{\mathbf{a}}^x(126)\varphi_{\mathbf{b}}^x(453) >$$

$$= \left[\left(\frac{\beta^2}{\pi}\right)^{\frac{9}{4}}\right]^4 \int d^3r_1 \int d^3r_2 \int d^3r_3 \int d^3r_4 \int d^3r_5 \int d^3r_6 e^{-\frac{\beta^2}{2}(r_1-\frac{R}{2})^2} e^{-\frac{\beta^2}{2}(r_2-\frac{R}{2})^2}$$
$$\times e^{-\frac{\beta^2}{2}(r_3-\frac{R}{2})^2} e^{-\frac{\beta^2}{2}(r_4+\frac{R}{2})^2} e^{-\frac{\beta^2}{2}(r_5+\frac{R}{2})^2} e^{-\frac{\beta^2}{2}(r_6+\frac{R}{2})^2} e^{iq\cdot(r_2-r_5)} e^{-\frac{\beta^2}{2}(r_1-\frac{R}{2})^2}$$
$$\times e^{-\frac{\beta^2}{2}(r_2-\frac{R}{2})^2} e^{-\frac{\beta^2}{2}(r_6-\frac{R}{2})^2} e^{-\frac{\beta^2}{2}(r_4+\frac{R}{2})^2} e^{-\frac{\beta^2}{2}(r_5+\frac{R}{2})^2} e^{-\frac{\beta^2}{2}(r_3+\frac{R}{2})^2}$$

$$= \left(\frac{\beta^2}{\pi}\right)^9 \int d^3r_1 e^{-\beta^2(r_1-\frac{R}{2})^2} \int d^3r_2 e^{-\beta^2(r_2-\frac{R}{2})^2+iq\cdot r_2} \int d^3r_3 e^{-\frac{\beta^2}{2}(2r_3^2+\frac{R^2}{2})}$$
$$\times \int d^3r_4 e^{-\beta^2(r_4+\frac{R}{2})^2} \int d^3r_5 e^{-\beta^2(r_5+\frac{R}{2})^2-iq\cdot r_5} \int d^3r_6 e^{-\frac{\beta^2}{2}(2r_6^2+\frac{R^2}{2})} \tag{D.43}$$

Using the integral function

$$\int_0^\infty d^3x e^{-a^2x^2} = \frac{\pi^{\frac{3}{2}}}{a^3} \tag{D.44}$$

We get

$$A = \left(\frac{\beta^2}{\pi}\right)^9 \left(\frac{\pi^{\frac{3}{2}}}{\beta^3}\right)^4 e^{-\frac{\beta^2R^2}{2}} \int d^3r_2 e^{-\beta^2(r_2^2-r_2R+\frac{R^2}{4}-\frac{iq\cdot r_2}{\beta^2})} \int d^3r_5 e^{-\beta^2(r_5^2+r_5R+\frac{R^2}{4}+\frac{iq\cdot r_2}{\beta^2})} \tag{D.45}$$

Using the method of completing the squares we arrive at:

$$A = \left(\frac{\beta^2}{\pi}\right)^9 \left(\frac{\pi^{\frac{3}{2}}}{\beta^3}\right)^4 e^{-\frac{\beta^2R^2}{2}} e^{-\frac{\beta^2R^2}{2}} \int d^3r_2 e^{-\beta^2[r_2-\frac{1}{2}(\frac{iq}{\beta^2}+R)]^2} e^{\frac{\beta^2}{4}[\frac{iq}{\beta^2}+R]^2}$$
$$\times \int d^3r_5 e^{-\beta^2[r_5+\frac{1}{2}(\frac{iq}{\beta^2}+R)]^2} e^{\frac{\beta^2}{4}[\frac{iq}{\beta^2}+R]^2}$$

$$= \left(\frac{\beta^2}{\pi}\right)^9 \left(\frac{\pi^{\frac{3}{2}}}{\beta^3}\right)^4 e^{-\beta^2R^2} \left(\frac{\pi^{\frac{3}{2}}}{\beta^3}\right)^2 e^{-\frac{q^2}{2\beta^2}} e^{iq\cdot R} e^{\frac{\beta^2R^2}{2}}$$

$$= e^{-\frac{\beta^2R^2}{2}} e^{-\frac{q^2}{2\beta^2}} e^{iq\cdot R} \tag{D.46}$$

Now evaluate B

$$
\begin{aligned}
B &= < \varphi^x_{\mathbf{a}}(123)\varphi^x_{\mathbf{b}}(456)||e^{iq\cdot(r_2-r_5)}||\varphi^x_{\mathbf{a}}(453)\varphi^x_{\mathbf{b}}(126) > \\
&= \left(\frac{\beta^2}{\pi}\right)^9 \int d^3r_1 e^{-\beta^2 r_1^2 - \frac{\beta^2 R^2}{4}} \int d^3r_2 e^{-\beta^2 r_2^2 - \frac{\beta^2 R^2}{4} + iq\cdot r_2} \int d^3r_3 e^{-\beta^2(r_3-\frac{R}{2})^2} \\
&\quad \times \int d^3r_4 e^{-\beta^2 r_4^2 - \frac{\beta^2 R^2}{4}} \int d^3r_5 e^{-\beta^2 r_5^2 - \frac{\beta^2 R^2}{4} - iq\cdot r_5} \int d^3r_6 e^{-\beta^2(r_6+\frac{R}{2})^2} \\
&= \left(\frac{\beta^2}{\pi}\right)^9 \left(\frac{\pi^{\frac{3}{2}}}{\beta^3}\right)^4 e^{-\beta^2 R^2} \int d^3r_2 e^{-\beta^2(r_2-\frac{iq}{2\beta^2})^2} e^{-\frac{q^2}{4\beta^2}} \int d^3r_5 e^{-\beta^2(r_5+\frac{iq}{2\beta^2})^2} e^{-\frac{q^2}{4\beta^2}} \\
&= e^{-\beta^2 R^2} e^{-\frac{q^2}{2\beta^2}} \qquad \text{(D.47)}
\end{aligned}
$$

This will give for the radial matrix element

$$
\begin{aligned}
\eta_R^{25(qe)} &= A - B \\
&= e^{-\frac{\beta^2 R^2}{2}} e^{-\frac{q^2}{2\beta^2}} e^{iq\cdot R} - e^{-\beta^2 R^2} e^{-\frac{q^2}{2\beta^2}} \\
&= e^{-\frac{\beta^2 R^2}{2}} e^{-\frac{q^2}{2\beta^2}} \left(e^{iq\cdot R} - e^{-\frac{\beta^2 R^2}{2}}\right) \qquad \text{(D.48)}
\end{aligned}
$$

Together with the factor from the spin-isospin matrix element for the nucleon exchange term we get as our final answer

$$
\eta_R^{25(qe)} = e^{-\frac{\beta^2 R^2}{2}} e^{-\frac{q^2}{2\beta^2}} \left(e^{iq\cdot R} - (-)^{(S+T)} e^{-\frac{\beta^2 R^2}{2}}\right) \qquad \text{(D.49)}
$$

From the above we can now evaluate the potential using (D.3) as a starting point and substitute in the solutions for the matrix elements, remembering the constants as well.

$$
v^{25(qe)} = -\frac{f^2_{\pi qq}}{m^2_\pi} 4\pi \frac{3}{N} \int \frac{d^3q}{(2\pi)^3} \frac{1}{(q^2+m^2_\pi)} \eta_R^{25(qe)} \left[M^{25(qe)}_{scal} + M^{25(qe)}_{tens}\right] \qquad \text{(D.50)}
$$

The integrals have been evaluated in chapter, so using the method outlined in there we arrive at our potential.

$$v^{25(qe)} = -\frac{f_{\pi qq}^2}{3m_\pi^2}\frac{4\pi}{N}e^{-\frac{\beta^2 R^2}{2}}\left[M_{scal}^{25(qe)}\left(I_s(R) - (-)^{(S+T)}e^{-\frac{\beta^2 R^2}{2}}F\right) + M_{tens}^{25(qe)}I_t(R)\right] \tag{D.51}$$

# Appendix E

# Quark-Pion Coupling Constant

The quark pion coupling constant can be related to the nucleon pion coupling constant. In order to do this let two clusters interact through pion exchange between the quarks. At an arbitrarily large distance the central part of the interaction between the clusters can be given by

$$V_c(R) = \frac{1}{3}\frac{f_{\pi qq}^2}{4\pi}\frac{e^{-m_\pi R}}{R}\tilde{\rho}(im_\pi)^2\left(\frac{5}{3}\right)^2(\vec{\sigma}_N\cdot\vec{\sigma}_N)(\vec{\tau}_N\cdot\vec{\tau}_N) \tag{E.1}$$

where R is the relative distance between the centers of the two clusters; $\sigma_N$ and $\tau_N$ are the spin and isospin operators which act in nucleon space ; $\tilde{\rho}(q)$ is the fourier transform of the quark density in the cluster with normalisation $\tilde{\rho}(q=0)=1$. The finite size effect of the clusters can be factorised at large distances by means of the factor $\tilde{\rho}(im_\pi)^2$. Equation (E.1) can be viewed as a generalisation of the Gauss theorem for two spherical distributions for the case of a Yukawa interaction. The Coulomb interaction for two spherical distributions can be obtained by setting $m_\pi \to 0$ , and omitting spin-isospin factors, with the result that the interaction is equivalent to the case where the charges are concentrated at the centre of the spherical distributions. By comparing (E.1) with the standard Yukawa potential

$$V_c(R) = \frac{1}{3}\frac{f_{\pi NN}^2}{4\pi}\frac{e^{-m_\pi R}}{R}(\vec{\sigma}_N\cdot\vec{\sigma}_N)(\vec{\tau}_N\cdot\vec{\tau}_N) \tag{E.2}$$

we get

$$f_{\pi qq} = \frac{3}{5} f_{\pi NN} \ \tilde{\rho}(im_\pi)^{-1} \tag{E.3}$$

For the gaussian distribution of the radial function , including center of mass corrections we have

$$\tilde{\rho}(q) = e^{-\frac{q^2}{6\beta^2}} \tag{E.4}$$

where $\beta$ is related to the harmonic oscillator length by its inverse. Substituting this in equation (E.1) gives us

$$f_{\pi qq} = \frac{3}{5} f_{\pi NN} e^{-\frac{q^2}{6\beta^2}}. \tag{E.5}$$

For the nucleon pion coupling constant we use the value

$$\frac{f^2_{\pi NN}}{4\pi} = 0.082. \tag{E.6}$$

# Bibliography


[AbLe73] Abers ; Lee *Phys Rep* **9C** (1973)1-141

[Ba77] G. W. Barry; *Phys Rev* **D16** (1977) 2886

[Ber+87] J. R. Bergervoet et al.; *Phys Rev Lett* **59**(1987)2255

[Bh+80] R. K. Bhaduri et al; *Phys Rev Lett* **44** (1980) 1369

[BoOp27] M. Born, J. R. Oppenheimer; *Ann Physik* **84** (1927) 457

[Boz+83] M. Bozoian, H. J. Weber; *Phys Rev C* **28**(1983)811

[Brä85] K. Bräuer; *Zeit. Phys.* **A320**(1985)609

[Brä90] K. Bräuer et al; *Nucl. Phys.* **A507**(1990)599

[Bro+76] G. E. Brown, A. D. Jackson; *The Nucleon-Nucleon Interaction* ( North-Holland, Amsterdam 1976)

[Bro79] G. E. Brown, M. Rho; *Phys. Lett.* **B82**(1979)383

[Bugg84] D. V. Bugg; *Nucl Phys* **A416** (1984)227c-242c

[Ca+83] J. Carlson et al.; *Phys Rev* **D 27**(1983) 233

[Cel77] W. Celmaster; *Phys Rev* **D 15**(1977) 1391

[Clo79] F. E. Close; *An Introduction to Quarks and Partons* (Academic Press 1979)

[Cot73] W. N. Cottingham et al; *Phys Rev* **D8**(1973)800

[CvGo83] M. Cvetic, B. Golli et al; *Nucl Phys* **A 395**(1983) 349

[De+91] S. Deister et al; *Few-Body Systems* **10**(1991)1

[DeG+75] T. DeGrand et al; *Phys Rev* **D12** (1975)2060

[DeR+75] A. DeRújula, H. Georgi, S. L. Glashow; *Phys. Rev.* **D12**(1975)147

[DeshTal] A. deShalit, I. Talmi; *Nuclear Shell Theory*(New York Academic Press 1963)

[DeT78] C. DeTar; *Phys Rev* **D17** (1978) 323

[DoJo80] J. F. Donoglove, K. Johnson; *Phys Rev* **D21** (1980) 1975

[Ed57] A. R. Edmonds; *Angular Momentum in Quantum Mechanics* ( 1957)

[ElHol84] G. Elster, K. Holinde; *Phys Lett* **B136**(1984)135

[ElHol84a] G. Elster, K. Holinde; *Phys Lett* **B149**(1984)293

[Faes+82] A. Faessler et al; *Phys Lett* 112 12(1982)201

[FaFer83] A. Faessler, F. Fernandez; *Phys. Lett.* **B124**(1983)145

[Faes+83] A. Faessler et al; *Nucl. Phys.* **A402**(1983)555

[FaSq75] G. T. Fariley, E. J. Squires; *Nucl Phys* **B93** (1975) 56

[FaSq75a] G. T. Fariley, E. J. Squires; *Acta Phys Pol* **B6** (1975) 893

[FerOs86] F. Fernandez, E. Oset; *Nucl Phys* **A455**(1986)720

[Fern87] F. Fernandez; *Phys Lett* **B188** (1987)314

[Fey71] R. P. Feynman, M. Kislinger, F Ravndal; *Phys. Rev.* **D3**(1971)2706

[Fla82] D. Flamm, F. Schoberl; *Introduction to the Quark Model of Elementary Particles* (Gordon and Breach 1982)

[GaLe] J. Gasser, H. Leutwyler; *Phys Rep* **87** (1982)77

[Gel64] M. Gell-Mann; *Phys Lett* **8** (1964)214

[Ge81] A. Gersten; *Recent Progress in Many Body Theories* (ed. J. Zabolitzky et al. Springer Verlag, Berlin 1981 p51)

[Gros79] F. Gross; *preprint* W M PP 79/4

[Guich+84] P. A. M. Guichon, G. A. Miller; *Phys Lett* **B134**(1984)15

[HaKu78] P. Hasenfratz, J. Kuti; *Phys Rep.* **40C**(1978)

[He26] W. Heisenberg; *Zeit. Phys.* **38**(1926) 411

[He26] W. Heisenberg; *Zeit. Phys.* **39**(1926) 499

[He26] W. Heisenberg; *Zeit. Phys.* **41**(1927) 239

[HeLo26] W. Heitler, F. London; *Zeit. Phys.* **44**(1926) 455

[Hel67] L. Heller; *Rev Mod Phys* **39**(1967)584

[He+90] E. M. Henley, T. Oka, J. D. Vergados; *Few Body Systems* **9** (1990)75

[Hol82] K. Holinde; *Phys Lett* **B118**(1982)266

[Hol84] K. Holinde; *Nucl Phys* **A415**(1984)477

[HolJoh84] K. Holinde M. Johnson; *Phys Lett* **B144**(1984)13

[Hol+90] K. Holinde, A. W. Thomas; *Phys Rev* **C42**(1990)R1195

[IsKa78] N. Isgur, G. Karl; *Phys Rev* **D 18**(1978) 4187

[IsKa79] N. Isgur, G. Karl; *Phys Rev* **D 19**(1979) 2653

[IsKa79a] N. Isgur, G. Karl; *Phys Rev* **D 20**(1979) 1191

[Is80] N. Isgur; *Proceedings of Baryon 80* (1980) (Univ. of Toronto Press)

[Jo75] K. Johnson; *Acta Phys Pol* **B6** (1975) 865

[Jo+77] M. Jones, R. H. Dalitz, P. R. Hogan; *Nucl Phys* **B 129**(1977) 45

[Kan77] M. Kanimura; *Prog. Theor. Phys.* **62**(1977) 236

[Lac80] M. Lacome et al; *Phys Rev* **C21**(1980)861

[Liu82] K. F. Liu ;*Phys Lett* **114B** (1982) 222

[LiWo82] K. F. Liu, C. W. Wong; *Phys Lett* **113B** (1982)1

[Liu+92] G. Liu, M. Swift, A.W. Thomas; *Preprint* ADP-92-175/T109

[Lib77] D. Liberman; *Phys. Rev.* **D16**(1977)1542

[Ma+87] R. Machleidt, K. Holinde, C. Elster; *Phys. Rep.* **149**(1987)p84

[MaPa78] W. Marciano, H. Pagels; *Phys Rep* **36C**(1978)138-276

[Mill84] G. A. Miller; *Int Rev Nucl Phys* **1**(1984)189

[Mor90] P. D. Morley, D. L. Pursey, S. A. Williams; *Phys. Rev.* **C42**(1990)2698

[Obu90] I. T. Obukhovsky, A. M. Kusainov; *Phys. Lett.* **B238**(1990)142

[OkYa83] M. Oka, K. Yazaki; *Nucl Phys* **A402** (1983) 477

[Oka84] M. Oka, K. Yazaki; *Int. Rev. Nucl. Phys* **1**(1984)489 (ed. W. Weise)

[OnSch82] G. Ono, F. Schöberl; *Phys Lett* **B 118** (1982) 419

[PaLo70] M. H. Partovi, E. L. Lomon ; *Phys Rev* **D2**(1970)1999

[Pa75] H. Pagels; *Phys Rep* **16C**(1975)220-311

[Reid68] R. V. Reid; *Ann Phys* **50**(1968)411

[Rob81] D. Robson; *Prog in Part and Nucl Phys* **8** (1981) 257

[Schn75] H. J. Schnitzer; *Phys Rev Lett* **35** (1975)1540

[Shim84] K. Shimizu; *Phys Lett* **B148** (1984)418

[Shi+62] I. Shimodaya et al.; *Prog. Theor Phys* **27**(1962)793

[Slat63] J. C. Slater; *Quantum Theory of Molecules and Solids* (Vol 1 McGraw-Hill 1963)

[Tak89] S. Takeuchi et al; *Nucl. Phys.* **A405**(1989)777

[Theb+80] S. Theberge, A. W. Thomas, G. A. Miller; *Phys Rev* **D22**(1980) 2838

[Theb+81] S. Theberge, A. W. Thomas, G. A. Miller; *Phys Rev* **D23**(1981) 2106(E)

[AWT83] A. W. Thomas; *Adv in Nucl Phys* **13**(1983)1

[AWT+89] A. W. Thomas, K. Holinde; *Phys Rev Lett* **63**(1989)2025

[Vin+91] R. Vinh Mau, et al; *Phys. Rev. Lett.* **67**(1991)1392

[WaSh80] C.S. Warke, R Shanker; *Phys Rev* **C21**(1980)2643

[Whe37] J. A. Wheeler; *Phys Rev* **52**(1937) 1083,1107

[Wil+58] K. Wildermuth et al.; *Nucl. Phys.* **7**(1958) 150

[Wil78] R. S. Willey; *Phys. Rev.* **D18**(1978)270

[Wo82] C. W. Wong *Phys Rev* **D24** (1982)1416

[Zwe64] G. Zweig; *Cern Preprint* TH-412 (1964)

# Publications

" Charge Symmetry Breaking in the Reaction $np \rightarrow d\pi^o$ "

J. A. Niskanen, M. Sebestyen, A. W. Thomas

*Phys. Rev.* **C 38** (1988) 838

" Pion Absorption on Polarised $^3He$ "

J. A. Niskanen, L. Swift, A. W. Thomas

*Phys. Rev.* **C 40** (1989) 2420

" The Role of Nucleon Structure in the $NN$ Interaction - Effects of Pion Exchange Between Quarks"

G. Q. Liu, M. Swift, A. W. Thomas

Preprint ADP-92-175/T109

# Charge symmetry breaking in the reaction $np \to d\pi^0$

J. A. Niskanen,* M. Sebestyen, and A. W. Thomas
*Physics Department, The University of Adelaide, Adelaide, South Australia 5001, Australia*
(Received 22 June 1987)

By extending a coupled channels model which has proven successful in describing the reaction $pp \to \pi^+ d$, we make predictions for charge symmetry breaking effects in the reaction $np \to d\pi^0$. We find that nucleon and delta mass differences at vertices where pions are emitted or absorbed are important (as for $np$ elastic scattering). However, $\eta$-$\pi^0$ mixing is also important in pion production. We predict forward-backward asymmetries in the pion production differential cross section as large as 1% (for laboratory energies below 800 MeV). The asymmetries induced in polarization observables are small.

## I. INTRODUCTION

If we understood the strong interaction completely, a knowledge of its symmetry properties would be little more than a convenience. However, at the present time we are still struggling to develop a consistent, microscopic understanding of the nucleon-nucleon ($NN$) system, with models ranging from pure phenomenology, through one-boson exchange, to explicit quark models. All of these models have free parameters which are adjusted to fit elastic $NN$ data, and, in some cases, data on pion production. The lure, which has prompted a number of groups to make the very difficult measurements necessary to reveal small symmetry breaking effects, is that these may test different combinations of the parameters from those already fitted. It may even be that some models can be rejected on the basis of these further tests.

A recent experiment on elastic $np$ scattering[1] revealed a new (class IV) piece of the $NN$ force.[2] Further experiments along that line should help to clarify the relationship between a quark-level description of the short-distance force and the long-distance, one-pion-exchange (OPE) force. In this work, our interest is in the pion production reaction $np \to d\pi^0$. Of course, in a charge-independent world this is directly related to the reaction $pp \to \pi^+ d$, which has been exhaustively studied theoretically and experimentally. As this is the prototype meson production reaction, it is crucial to push the various models for it to their limits in order to redefine our understanding of short-distance (high-momentum transfer) physics.[3]

Much of the pioneering work on charge symmetry breaking (CSB) in this reaction has been carried out by Henley, Miller, and collaborators,[4,5] They were the first to observe the dominance of $\eta$-$\pi^0$ mixing [see Fig. 5(a)] as a reaction mechanism. Since the role of the $\eta$ in the $NN$ system has never been very clear, this opportunity to sharpen our understanding is quite important. Our work has confirmed the importance of the $\eta$-$\pi^0$ mechanism for CSB in the $np \to d\pi^0$ reaction.

The $\Delta$ resonance plays an important role in pion production. The earlier work of Cheung, Henley, and Miller (CHM) used a modification of the Chew-Wick model of the delta.[6] This description is now out of date,[7] and we include an explicit $\Delta$ baryon instead–along the lines of Green and Niskanen.[8] One final new feature of our work which deserves note is that we compute not only the effects on $d\sigma/d\Omega$, but also on various polarization observables. [In the $n$-$p$ elastic case it proved advantageous to measure $\Delta A$ ( $A_n - A_p$ ) at the zero in $A_n(\theta)$].[1,2]

The details of the calculation are given in Sec. II. In Sec. III we discuss the results, with particular consideration of possible experimental tests. Finally, in Sec. IV we make some concluding remarks.

## II. THEORETICAL FRAMEWORK

Our model for the isospin conserving amplitudes for $np \to d\pi^0$ is that of Green and Niskanen.[8] It is based on the nonrelativistic, one-body pion production operator

$$H = -\frac{f}{\mu} \sum_{i=1,2} \vec{\sigma}_i \cdot [\vec{\nabla} \tau_i \cdot \boldsymbol{\phi}(\vec{x}_i) + (2M)^{-1} \{ \vec{p}_i, \tau_i \cdot \boldsymbol{\pi}(\vec{x}) \}] \ . \tag{2.1}$$

Here, $f^2/4\pi = 0.081$, $\vec{p}_i$ is the momentum of nucleon $i$ [mass $M = (m_n + m_p)/2$], and $\boldsymbol{\phi}$ and $\boldsymbol{\pi}$ are the pion field and its conjugate momentum. The latter have the matrix elements

$$\begin{aligned} \langle \pi_j \vec{q} \mid \phi_i(\vec{x}) \mid 0 \rangle &= \delta_{ij} (2\omega_q)^{-1/2} e^{-i\vec{q}\cdot\vec{x}} , \\ \langle \pi_j \vec{q} \mid \pi_j(\vec{x}) \mid 0 \rangle &= i \delta_{ij} (\omega_q/2)^{1/2} e^{-i\vec{q}\cdot\vec{x}} . \end{aligned} \tag{2.2}$$

While $\mu$ should be the $\pi^+$ mass, we shall use the average pion mass (138.1 MeV), with negligible error.

There is a well-known ambiguity concerning the form of the nonrelativistic $\pi N$ coupling. In particular, the second Galilean-invariant term is quite model dependent. Omitting it would lead to a 20% scaling of the reaction cross section which could be compensated by a slight readjustment of the OPE cutoff parameter.

As we have already remarked, the $\Delta$ resonance plays a

 

crucial role in this reaction, being primarily responsible for the large bump in the cross section near 600 MeV ($E_{\rm lab}$). In order to describe the meson $-N\rightleftarrows\Delta$ vertices, we introduce the transition spins and isospins ($\vec{S}_i$ and $\mathbf{T}_i$) of Sugawara and von Hippel.[9] The dominant mesons are, of course, $\rho$ and $\pi$. Their exchange, illustrated in Fig. 1, introduces $\Delta N \pm N\Delta$ components into the wave function. This leads to a set of coupled Schrödinger equations[8]

$$\left[-\frac{d^2}{dr^2}+\frac{L(L+1)}{r^2}-k^2+MV_1\right]u(r)=-M\sum_i V_2(i)w_i(r)\ ,$$
$$\left\{-\frac{d^2}{dr^2}+\frac{L_i(L_i+1)}{r^2}+M_\Delta\left[\Delta-M-i\frac{\Gamma_i}{2}-E+V_3(i)\right]\right\}w_i(r)=-M_\Delta V_2(i)u(r)\ . \tag{2.3}$$

Here $u(r)$ and $w_i(r)$ are the relative $NN$ and $\Delta N \pm N\Delta$ wave functions, $k^2=ME_{\rm lab}/2$ and $E$ is the c.m. energy. The mass parameters appearing in Eq. (2.3) are $\Delta$, the mass of the delta; $M_\Delta$, the $\Delta-N$ reduced mass; and $\Gamma_i$, the width of the delta. (The latter is energy and state dependent, as described in Ref. 8.)

For the diagonal $NN$ potential ($V_1$) we use the Reid soft-core potential,[10] suitably adjusted[8] to avoid double counting the iterated, $N$-$\Delta$ box diagrams (see Fig. 2). The diagonal $\Delta$-$N$ potential ($V_3$) is set to zero in this work, while the charge-independent transition potential is

$$V_2=\frac{\mu}{3}\frac{ff^*}{4\pi}\mathbf{T}_1\cdot\boldsymbol{\tau}_2\left\{S_{12}^{\rm II}\left[V_T(\mu r)-\frac{f_{NN\rho}^2}{f^2}\frac{\rho}{\mu}V_T(\rho r)\right]+\vec{S}_1\cdot\vec{\sigma}_2\left[V_c(\mu r)+\frac{2f_{NN\rho}^2}{f^2}\frac{\rho}{\mu}V_c(\rho r)\right]\right\}+(1\rightleftarrows2)\ . \tag{2.4}$$

The $\Delta N\pi$ coupling constant is $f^{*2}/4\pi=0.35$ (in order to fit the width of the delta), and

$$f_{\Delta N\rho}=f_{\Delta N\pi}\frac{f_{NN\rho}}{f_{NN\pi}}=f_{NN\rho}\frac{f^*}{f}\ , \tag{2.5}$$

with $f_{NN\rho}=(m_\rho/2M)g_\rho(1+\kappa_\rho)$, $g_\rho^2/4\pi=0.55$, and $\kappa_\rho=6.0$.[11] The transition tensor operator is

$$S_{12}^{\rm II}=3\vec{S}_1\cdot\hat{\mathbf{r}}\vec{\sigma}_2\cdot\hat{\mathbf{r}}-\vec{S}_1\cdot\vec{\sigma}_2\ , \tag{2.6}$$

and

$$V_i(\mu r)=Y_i(\mu r)-(\Lambda/\mu)^3Y_i(\Lambda r)\ ,$$
$$Y_c(x)=\frac{e^{-x}}{x}\ , \tag{2.7}$$
$$Y_T(x)=(1+3/x+3/x^2)Y_c(x)\ .$$

The monopole cutoff masses used in the potential are $\Lambda=700$ MeV for the pion and 950 MeV for the $\rho$.

Once the $N\Delta\pm\Delta N$ component is included in the wave function, the delta can participate in the pion production process as shown in Fig. 3. The transition potential first generates an intermediate $\Delta$ which subsequently decays. Although $s$-wave $\pi\dot{N}$ rescattering is necessary (particularly for polarization observables), and has been included as in Ref. 8, it is important to note that the contribution of the $\Delta$ isobar is dominant above 400 MeV ($E_{\rm lab}$). The present model has been very successful in reproducing and predicting both cross sections and polarization observables in the $pp\to d\pi^+$ reaction. It should therefore provide a suitable starting point for calculating charge-symmetry breaking in $np\to d\pi^0$.

The differential cross section in $np\to d\pi^0$ (including an extra factor of $\frac{1}{2}$ compared with $pp\to d\pi^+$) can be written

$$\frac{d\sigma}{d\Omega}=\frac{1}{8}\frac{1}{(2\pi)^2}\frac{\omega_q qM}{2k}\sum_{\mu SM}|\langle\psi_d^\mu|H_{\rm prod}|\phi^{SM}\rangle|^2\ . \tag{2.8}$$

Notice that different spin states ($SM$) of the $NN$ system do not interfere with each other. Because of the Pauli exclusion principle, singlet ($S=0$) initial states with isospin one ($T=1$) give rise to pion final states of odd angular

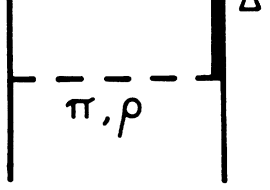


FIG. 1. The meson exchange mechanism responsible for the $NN$ and $N\Delta$ channel coupling.

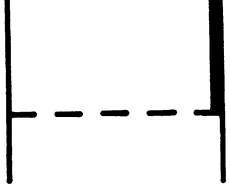

FIG. 2. A contribution to $NN$ scattering which arises from coupling to the $N\Delta$ channel and must not be double counted.

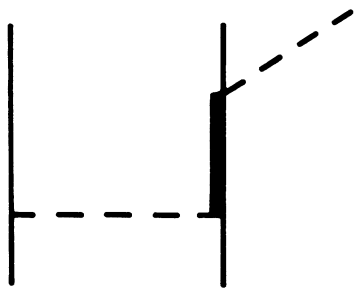

FIG. 3. The lowest-order process whereby coupling to the $N\Delta$ channel leads to pion production.

momentum ($l_\pi$) only. Triplet $T=1$ states give rise to $l_\pi$ even. Thus, each term in Eq. (2.8) contains either a sum of terms even in $l_\pi$ squared, or a sum of odd-$l_\pi$ squared. Consequently, the differential cross section is symmetric about 90°. This is an example of the theorem of Barshay and Temmer.[12]

On the other hand, if isospin is broken at some stage of the reaction, an initial singlet state with $T=0$ may give rise to an $l_\pi$-even final state. The interference of this amplitude with the charge-symmetric amplitude will produce a forward-backward asymmetry. It is easily seen that such an asymmetry also breaks charge symmetry. Similar considerations apply to other observables which are either symmetric or antisymmetric in the charge-symmetric case (e.g., $A_{xx}$, $A_{yy}$, $A_{zz}$, $it_{11}$).

We now turn to consider the possible mechanisms for charge-symmetry breaking. In the case of *n-p* elastic scattering, Miller, Williams, and Thomas found that the largest single source was the *n-p* mass difference at the $NN\pi$ vertex.[2] This introduces charge asymmetric couplings $H_1$ and $H_2$, where the nonrelativistic reduction of $H_{\pi NN}$ is

$$H_{\pi NN}=H_0+H_1+H_2 \ . \tag{2.9}$$

$H_0$ was given in Eq(.2.1) and

$$H_1=-\delta\frac{f}{\mu}\vec{\sigma}\cdot\vec{\nabla}\phi_3 \ , \tag{2.10}$$

$$H_2=-\delta\frac{f}{\mu}\vec{\sigma}\cdot(\vec{p}+\vec{p}\,')(\tau\times\boldsymbol{\phi})_3 \ , \tag{2.11}$$

where $\delta$ is given by

$$\delta=(M_n-M_p)/(M_n+M_p)=(M_n-M_p)/2M \ . \tag{2.12}$$

Taking $H_1$ and $H_2$ into account leads to a CSB *NN* potential of the form

$$V_\delta=\delta\frac{f^2}{4\pi}\frac{\mu}{3}\{(\tau_1+\tau_2)_z[S_{12}V_T(\mu r)+\vec{\sigma}_1\cdot\vec{\sigma}_2V_c(\mu r)] -6(\tau_1\times\tau_2)_z(\vec{\sigma}_1\times\vec{\sigma}_2)\cdot\vec{L}V_{LS}(\mu r)\} \ , \tag{2.13}$$

with

$$S_{12}=3\vec{\sigma}_1\cdot\hat{\mathbf{r}}\vec{\sigma}_2\cdot\hat{\mathbf{r}}-\vec{\sigma}_1\cdot\vec{\sigma}_2\cdot \ , \tag{2.14}$$

$$V_{LS}(x)=\frac{1}{x}\frac{d}{dx}V_c(x) \ . \tag{2.15}$$

[We include the same form factor as in Eq. (2.7).]

Using the classification of Henley and Miller,[4] the first term in Eq. (2.13) is of class III, and the second, class IV. The former is zero for the *n-p* system, whereas the latter can give rise to transitions from $T=0$ to $T=1$, and hence, contribute to the forward-backward asymmetry. (It can only act in NN states with $L=J$.) In practice, because pion production is so dominated by the $\Delta$ isobar, this effect is actually very small for the $np\rightarrow d\pi^0$ reaction.

One might also expect to find a coupling at the $\Delta N\pi$ vertex, analogous to (2.10) or (2.11), which would break charge symmetry. Ultimately, the source of such terms is the underlying *u-d* quark mass difference. For example, if one postulates a pseudoscalar coupling to constituent *u* and *d* quarks, and allows for $m_u\neq m_d$, one arrives at precisely Eqs. (2.9), (2.1), (2.10), and (2.11) in the limit of nonrelativistic nucleons (with $\delta=(m_d-m_u)/[3(m_d+m_u)]$). Applying exactly the same procedure to the $\Delta N\pi$ vertex with SU(6) wave functions one finds

$$H_{\Delta N\pi}=H_0'+H_2' \ , \tag{2.16}$$

with

$$H_0'=-\frac{f^*}{\mu}\vec{S}\cdot\vec{\nabla}\mathbf{T}\cdot\boldsymbol{\phi} \ , \tag{2.17}$$

$$H_2'=-\delta\frac{f^*}{\mu}\vec{S}\cdot(\vec{p}+\vec{p}\,')(\mathbf{T}\times\boldsymbol{\phi})_3 \ . \tag{2.18}$$

(There is no contribution analogous to $H_1$ because the $\Delta\rightleftarrows N$ transition requires a transition isospin operator.) Having justified the presence of $H_2'$ in this way, we shall nevertheless use Eq. (2.12) for $\delta$ at the $\Delta N\pi$ vertex too.

Using the charge-symmetry breaking couplings at both the $NN\pi$ and $\Delta N\pi$ vertices, one readily finds the following CSB transition potential:

$$V_\delta^{tr}(\mathrm{OPE})=\frac{\delta ff^*}{4\pi}\frac{\mu}{3}\{T_{1z}[S_{12}^{II}V_T(\mu r)+\vec{S}_1\cdot\vec{\sigma}_2V_c(\mu r)] -6(\mathbf{T}_1\times\tau_2)_z(\vec{S}_1\times\vec{\sigma}_2)\cdot\vec{L}V_{LS}(\mu r)\} +(1\leftrightarrow 2) \ . \tag{2.19}$$

(Note that this does have a class III piece because of the $H_1$ term at the $\pi NN$ vertex.) It is important to note that, contrary to the *NN* case, this term, which is like a class III term, also induces an isospin change from $T=0$ *NN* states into $T=1$ $\Delta N\pm N\Delta$ states. Furthermore, since the *N* and $\Delta$ are distinguishable particles, the isospin 1 state can have either spin 1 or 2, and these can couple to the tensor coupled $L=J\pm 1$ *NN* states as well as to the uncoupled ones. This feature can contribute in two ways: as an isospin one admixture in the $T=0$ states in the *initial* or the *final* states (i.e., in the deuteron[13]). In the present work we do not consider the effect of the very small isospin breaking in the deuteron. Once the isospin 1 components—either *NN* or $\Delta N\pm N\Delta$—have been generated, they naturally lead to pion production through the action of $H_0'$ [Eq. (2.17)]. The mixing is computed by extending the coupled equations (2.3).

In addition to having isospin breaking occur *prior* to

the pion production, it is possible to have a pion production vertex of type (2.10), as shown in Fig. 4. This allows production directly from isospin 0 states, since the vertex does not involve any operator to change the isospin. We expect that this should not be a large effect in the $\Delta$ region, since the initial state is an $NN$ state.

The $\eta$ and $\pi^0$ meson mixing contributes both to the transition potential from $T=0$ to $T=1$ states [Fig. 5(a)] and to the final pion production vertex [Fig. 5(b)]. However, the $\eta\pi$ mixing potential is of type III and does not directly contribute to $np$ scattering. For the process $np \to \Delta N \pm N\Delta$, it has the form

$$V^{tr}_{\eta\pi} = -\frac{f_\pi^* f_\eta}{4\pi}\frac{\mu}{3}\frac{\langle \eta \mid H \mid \pi\rangle}{2(\eta^2-\mu^2)} T_{13}\left\{S^{II}_{12}\left[V_T(\mu r) - \left[\frac{\eta}{\mu}\right]^3 V_T(\eta r)\right] + \vec{S}_1\cdot\vec{\sigma}_2\left[V_c(\mu r) - \left[\frac{\eta}{\mu}\right]^3 V_c(\eta r)\right]\right\} + (1\leftrightarrow 2)\ . \tag{2.20}$$

Except for a factor of $\frac{1}{2}$, this is completely analogous to the corresponding interaction in the pure $NN$ case. This factor comes because for each particle becoming a $\Delta$, there are only two possible time orderings versus four for nucleons. If the same monopole form factors are used for both $\pi^0$ and $\eta$, the form factors cancel and the potential is like a OPE with a very long-ranged ($\eta^{-1}$) cutoff. Its action is like that of the first term of Eq. (2.19), only (depending on $f_\eta$) larger, since the coefficient in front is larger. For $\langle \eta \mid H \mid \pi\rangle$ we shall use the value $-4000$ MeV$^2$, extracted from electromagnetic mass splittings.[14] The $\eta NN$ coupling constant $f_\eta = g_\eta \mu/2M$ is difficult to extract from $NN$ scattering, and is very badly determined, with the values ranging from $g_\eta^2/4\pi \approx 0.5$ on the basis of SU(6) symmetry, to $\approx 4$ from OBE fits for $NN$ scattering.[11] The CSB in this particular reaction could be one way to get a handle on this coupling constant. For $g_\eta^2/4\pi = 3.68$ from Ref. 11 the coefficient in Eq. (2.20) is 5 times larger than in Eq. (2.19). However, the first term in Eq. (2.19) is not the main contribution to the mass difference effect. In fact, the second class IV term contributes about as much to the asymmetry of the cross section as the $\eta\pi$ mixing just considered.

The $\eta\pi$ mixing effect in the pion production vertex [Fig. 5(b)] is not negligible, even though it acts only in the $np$ states. The reason is that the effective isospin violating pion production coupling

$$H^{\text{prod}}_{\eta\pi} = -\frac{f_\eta}{\mu}\frac{\langle \eta \mid H \mid \pi\rangle}{2(\eta^2+\vec{q}^2)^{1/2}[(\mu^2+\vec{q}^2)-(\eta^2+\vec{q}^2)]^{1/2}}\vec{\sigma}\cdot\vec{\nabla}\phi_3\ , \tag{2.21}$$

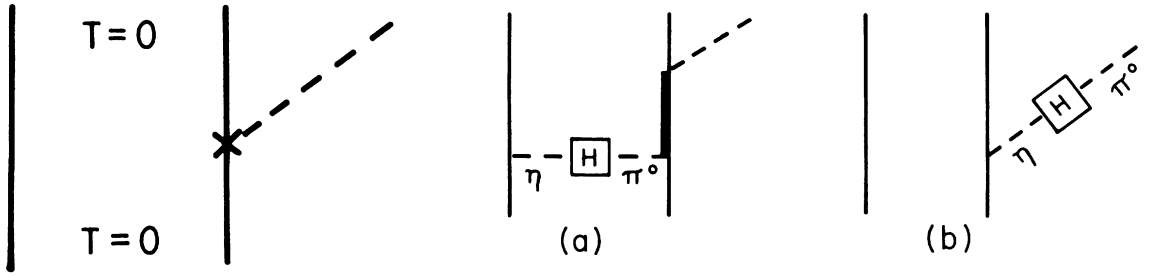


FIG. 4. A direct, charge-symmetry breaking contribution to the $np \to d\pi^0$ amplitude—corresponding to $H_1$ of Eq. (2.10).

FIG. 5. The two lowest-order mechanisms by which $\eta$-$\pi^0$ mixing can contribute to CSB.

is about 5 times larger than in Eq. (2.10), for the parameter values given earlier.

## III. RESULTS

In Fig. 6 the contributions to the forward-backward asymmetry from the various mechanisms presented in Sec. II are shown for the neutron energies 580 MeV (right on top of the Δ resonance) and 477 MeV (the energy of the recent CSB measurement in *np* scattering). The largest contributions are from the class IV interaction arising from the baryon mass splitting (δ, dotted curves), and the class III $np \to N\Delta$ transition due to $\eta\pi$ mixing [Fig. 5(a), long dashes]. However, including $\eta\pi$ mixing at the production vertex, as depicted in Fig. 5(b), decreases the $\eta\pi$-mixing effect by more than one-half.

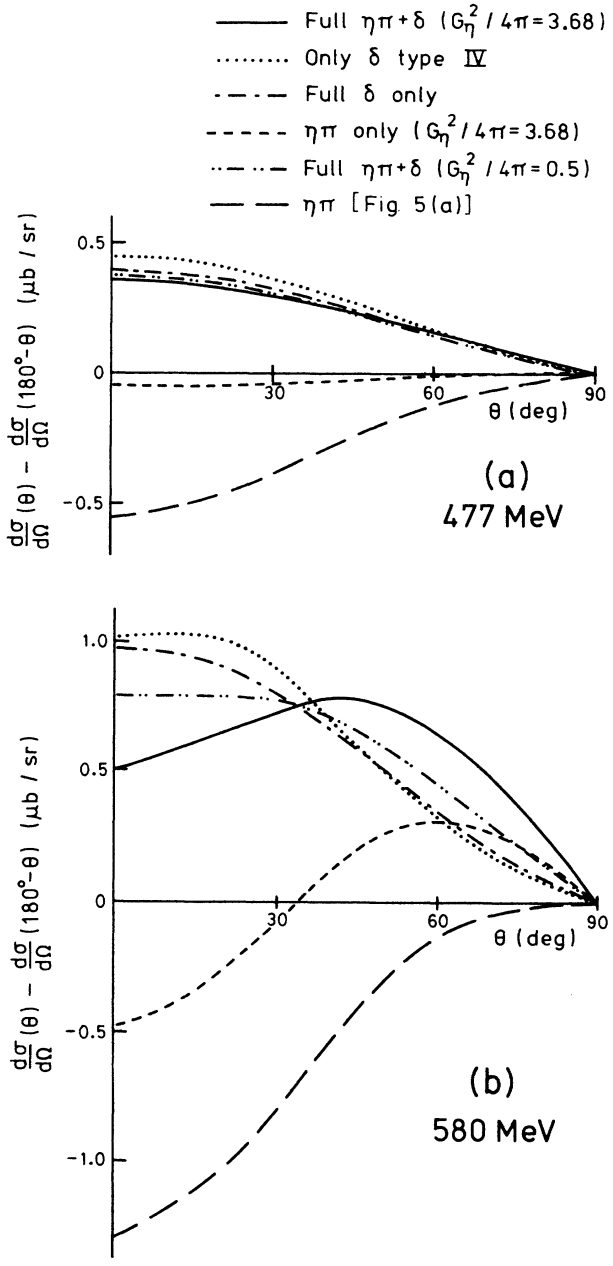


FIG. 6. (a) The forward-backward asymmetry for the $np \to d\pi^0$ cross section (in the c.m. system) at a neutron laboratory energy ($T_n$) of 477 MeV. The solid curve is the full effect of δ (*n-p* mass difference in pion exchange) and $\eta$-$\pi^0$ mixing (with $g_{\eta NN}^2/4\pi=3.68$); the dotted curve includes only δ (type IV); dot-dash is full δ only; short dash is full $\eta$-$\pi^0$; long dash is $\eta$-$\pi$, but only Fig. 5(a); dot-dot-dash is full δ plus $\eta$-$\pi$, but with $g_{\eta NN}^2/4\pi=0.5$. (b) As for (a) but at $T_n=580$ MeV. (N.B. $\theta$ is the angle between the initial neutron and the outgoing deuteron.)

A comparison of our results with those of Cheung *et al.*[5] reveals agreement on the sign of the $\eta$-$\pi$ mixing effect [note, however, that they omit Fig. 5(b)]. On the other hand, the class IV pionic contribution appears to have the opposite sign. This difference may be caused by a difference in the sign of the mass splitting used for the Δ resonances, which in their case were calculated using the Chew-Low model,[6] rather than the quark model (which agrees with experiment).

The large size of the $\eta\pi$-mixing effects follows because the numerical factors in Eqs. (2.20) and (2.21) are relatively large. This result obviously depends directly on the value of the $\eta NN$ coupling constant, which is probably poorly known ($g_\eta^2/4\pi=3.68$ is used in these curves[11]). Anyhow, this is a large cancellation of the two types of $\eta\pi$ contributions. The full *np* mass difference effect is shown by the dot-dashed curve. By comparison with the dotted curve it can be seen that the "type III'" $N\Delta$ transition potential has a relatively minor effect. The solid curve gives the total sum of all contributions. Finally, in order to show the effect of the $\eta NN$ coupling, the result with $g_\eta^2/4\pi=0.5$ [which is more consistent with the SU(6) quark model] is shown by the dot-dot-dashed curve.

Studies of charge-symmetry breaking in the low-energy N-N system have shown that the $\eta'$ meson can be important. In particular, it has been suggested that one should consider $\eta'$-$\pi^0$ and $\eta$-$\pi^0$ mixing together. Since studies of N-N scattering determine the $\eta' NN$ coupling even less precisely than that for $\eta NN$, any calculation of this effect should at best be considered an indication of its possible size. For simplicity we have chosen $g_{\eta' NN}$ equal to $g_{\eta NN}$. For the mixing amplitudes we take $\langle \eta \mid H \mid \pi^0 \rangle = -5900$ MeV$^2$ and $\langle \eta' \mid H \mid \pi^0 \rangle = -5500$ MeV$^2$, which are more recent[15,16] than the conservative value for $\langle \eta \mid H \mid \pi^0 \rangle$ used elsewhere in this paper. In Fig. 7 we show the forward backward asymmetry in $np \to d\pi^0$ at 477 and 580 MeV resulting from $\eta$-$\pi^0$ mixing with the newer mixing matrix element, the $\eta'$-$\pi^0$ mixing contribution and the total result (including baryon mass differences). For the $\eta'$-$\pi^0$ contribution, as for $\eta$-$\pi^0$, there is some cancellation between the term involving rescattering through the Δ [Fig. 5(a)] and purely external emission [Fig. 5(b)]. Unlike the low-energy situation, there does not appear to be any tendency for cancellation between the $\eta$-$\pi^0$ and $\eta'$-$\pi^0$ contributions.

To illustrate the energy dependence, the total results for several energies are shown in Fig. 8. The trend roughly follows the size of the isospin conserving cross sections which are shown in Fig. 9. There is a maximum asymmetry in the Δ region ($\approx$600 MeV laboratory energy), just as there is a maximum in the cross section. The

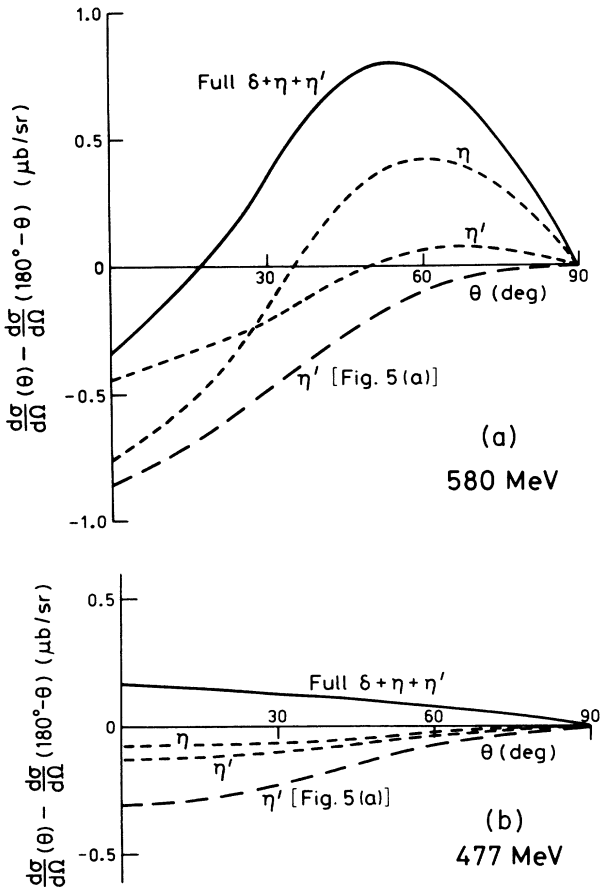


FIG. 7. The forward-backward asymmetry for $np \to d\pi^0$ at 477 and 580 MeV. Here we include the possibility of $\eta'$-$\pi^0$ mixing as well. In these curves $g^2_{\eta NN}/4\pi$ was taken equal to $g^2_{\eta' NN}/4\pi$ (i.e., 3.68), and the mixing matrix elements were $\langle \eta \mid H \mid \pi^0 \rangle = -5900\ \mathrm{MeV}^2$ and $\langle \eta' \mid H \mid \pi^0 \rangle = -5500\ \mathrm{MeV}^2$.

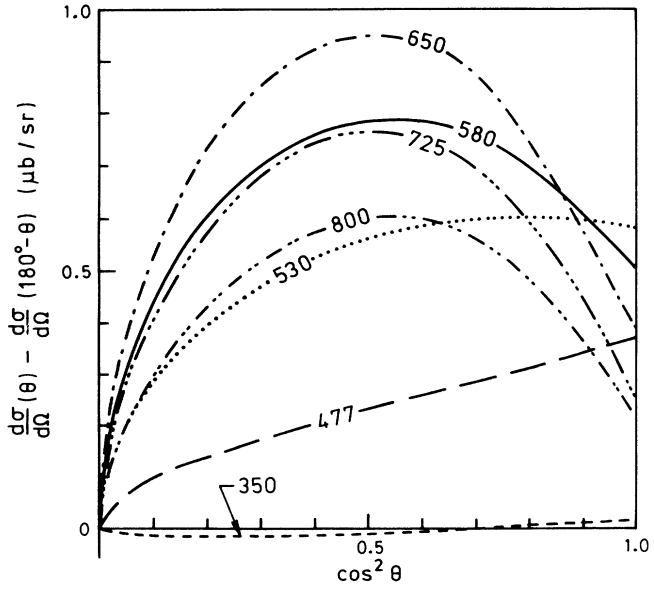


FIG. 8. The full prediction of the forward-backward asymmetry for several neutron laboratory energies.

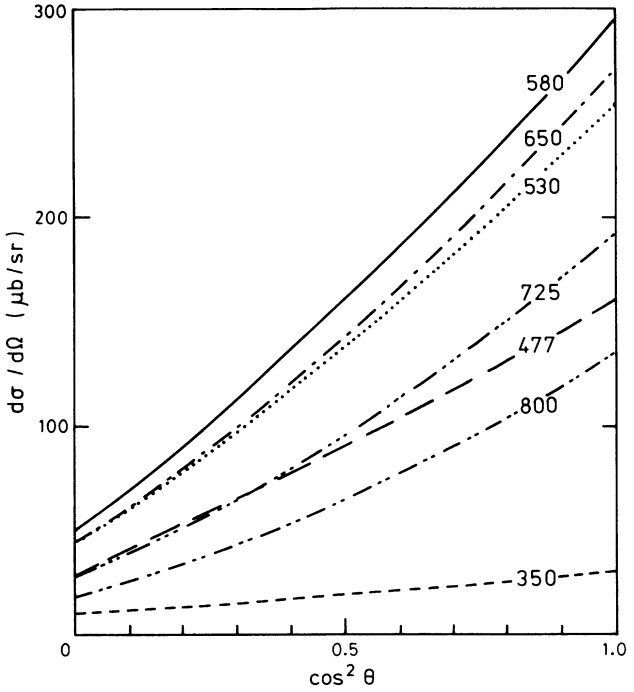


FIG. 9. Our prediction for the full differential cross section for $np \to d\pi^0$ at the same energies as Fig. 8.

angular structure is, however, very different from the isospin conserving cross sections. With the exception of the energies below 500 MeV, the asymmetry is maximized at a common angle of about 45°. For the lowest energies, the asymmetry is very small. A better indication of the relative size of the effect is given in Fig. 10. There the energy dependence of the asymmetry between the forward and backward direction is shown as a fraction of the production cross section at the angles 0°, 45°, and 60°. Obviously, $\theta \approx 45°$ is the best for observing the asymmetry for all energies above 500 MeV, since for this angle it is absolutely maximized and is also large proportionally.

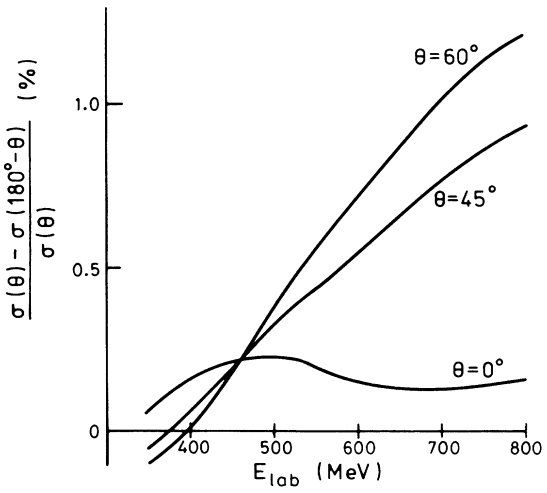


FIG. 10. The foward-backward asymmetry in $d\sigma/d\Omega$ for $np \to d\pi^0$ as a percentage of $d\sigma/d\Omega$, at three c.m. angles (0°, 45°, and 60°) as a function of neutron laboratory energy.

With the presently conceivable experiments, the effects of the CSB in the reaction $np \to d\pi^0$ should be clearest in the cross section. However, because of the neatness of null experiments, we examined this more speculative possibility. The deuteron polarization $iT_{11}$ goes through zero at 90°, if charge symmetry is unbroken. Since this is a very small observable (as compared with its possible maximum values), it is apparently a result of very delicate cancellation of relatively large amplitudes, and as such, could be sensitive to small effects like charge-symmetry breaking.

Unfortunately, this very sensitivity can make it difficult to compute this quantity from a model. In our model, the agreement with experiment[17] at $E_{pp}=650$ MeV ($T_\pi \approx 180$ MeV) is reasonable (Fig. 11), and we calculated the effect of charge-symmetry breaking on $iT_{11}$. The result was $iT_{11}(90°)=-0.006$, and the zero point was shifted by $\Delta\theta=+0.75°$. Allowing for the fact that the slope may be overestimated by a factor of 2 (Fig. 11), this shift could perhaps be as large as 1.5°. It would be very interesting to know whether it is beyond present experimental capabilities to see such an effect.

As a final illustration of the usefulness of measuring $\Delta\theta$ as well as $\Delta\sigma$, we briefly mention the results of a phenomenological study of the variation of these observables. For the result quoted earlier we used the CSB amplitudes from our model. Suppose we now allow the signs of the real and imaginary parts of the three dominant CSB amplitudes ($NN \to \pi D$: $^3S_1 \to p$, $^3D_2 \to f$, and $^1P_1 \to d$) to vary arbitrarily. Then we find that $\Delta\sigma$ may vary by a factor of 10, while $\Delta\theta$ varies by a factor of 2. There is little relationship between the size of the effect on $\Delta\theta$ or $\Delta\sigma$. While this exercise is little more than a game, it does illustrate that if we really wish to pin down the CSB amplitudes, and hence test the model as thoroughly as possible, measurements of the forward-backward asymmetry ($\Delta\sigma$) and $\Delta\theta$ (for $iT_{11}$) are complementary.[18]

## IV. CONCLUDING REMARKS

We have presented a systematic study of charge-symmetry breaking in the Helsinki and model[8] for pion production. As suggested earlier by Cheung, Henley, and Miller,[5] the two dominant mechanisms for breaking charge symmetry involve the $n$-$p$ mass difference in pion exchange and $\eta$-$\pi^0$ mixing. The latter is particularly interesting because of the uncertainty surrounding the role of the $\eta$ in the N-N force. While there are a number of theoretical questions which need to be pursued, it is clear that further progress will be severely held back until we get some accurate experimental data with which to compare these calculations.

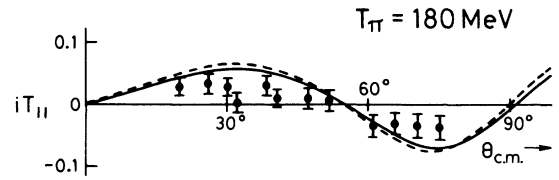


FIG. 11. The polarization parameter $iT_{11}$ for the reaction $np \to d\pi^0$, at a neutron laboratory energy of 650 MeV ($T_\pi^{c.m.} \approx 180$ MeV). The data is from Ref. 17. The solid curve (dashed curve) is our prediction with (without) CSB effects. (Note that if charge symmetry is good, $iT_{11}$ is symmetric about $\theta_{c.m.}=90°$.) In this case alone, $\theta$ is the angle between the initial proton and outgoing deuteron in the c.m. system. We use the Madison convention.

On the theoretical side, further work should be done on $\rho^0$-$\omega$ mixing, which Cheung *et al.* claimed was negligible. One would also like to see other models, especially three-body models, applied to this problem. The mixing amplitudes $\langle \eta \mid H \mid \pi^0 \rangle$ and $\langle \omega \mid H \mid \rho^0 \rangle$ have been extracted from rather old experiments. It would be very worthwhile to have a realistic estimate of the errors on these matrix elements and to know whether they could now be improved. One would also like to know the size of the photon exchange contribution to CSB.

Finally, we mention that fundamental work on the $NN\pi$ vertex, using the cloudy bag model,[19] has suggested another mechanism for CSB. The mass differences of the $u$ and $d$ quarks imply[20] that the $\pi^0 nn$ coupling should be larger than the $\pi^0 pp$ coupling by about 0.4%. This is the opposite sign from the effect of $\eta$-$\pi^0$ mixing at the vertex. Indeed, with $g^2_{\eta NN}/4\pi = 3.68(0.5)$, Eq. (2.21) implies that the $pp\pi^0$ coupling constant is about 0.7% (0.2%) larger than that for $nn\pi^0$. Thus, if taken at face value, the effect of quark mass differences would tend to cancel the effect of $\eta$-$\pi^0$ mixing. For the present, we would prefer to study this question further, particularly considering bag recoil corrections before drawing such a strong conclusion. In any case, there is some very interesting and fundamental physics to be learned.

## ACKNOWLEDGMENTS

This work was supported by the Academy of Finland, the Australian Research Grant Scheme, and the University of Adelaide. J.A.N. thanks the University of Adelaide for the warm hospitality during the academic year 1986-87. We are also grateful to G. Greeniaus for some informative discussions.

*On leave from the Department of Theoretical Physics, University of Helsinki, Helsinki, Finland.

[1]R. Abegg, *et al.*, Phys. Rev. Lett. **56**, 2571 (1986).
[2]G. A. Miller, *et al.*, Phys. Rev. Lett. **56**, 2567 (1986).
[3]D. Ashery and J. P. Schiffer, Ann. Rev. Nucl. Part. Sci. **36**, 207 (1986).
[4]E. M. Henley and G. A. Miller, in *Mesons in Nuclei*, edited by M. Rho and D. H. Wilkinson (North-Holland, Amsterdam, 1979), p. 405.
[5]C. Y. Cheung, *et al.*, Nucl. Phys. **A305**, 342 (1978); **A348**, 365

(1980).
[6]G. A. Miller, Proceedings of the 2nd International Topical Conference on Meson-Nuclear Physics, Houston, 1979, AIP Conf. Proc. No. 54, edited by E. V. Hungerford III (AIP, New York, 1979), Vol. 54, p. 561.
[7]S. Théberge, *et al.*, Phys. Rev. D **22**, 2838 (1980); **23**, 2106(E) (1981).
[8]J. A. Niskanen, Nucl. Phys. **A298**, 413 (1978); Phys. Lett. **141B**, 301 (1984); A. M. Green and J. A. Niskanen, Nucl. Phys. **A271**, 503 (1976).
[9]H. Sugawara and F. von Hippel, Phys. Rev. **172**, 1764 (1968).
[10]R. V. Reid, Ann. Phys. **50**, 411 (1968).
[11]O. Dumbrajs, *et al.*, Nucl. Phys. **B216**, 277 (1983).
[12]S. Barshay and G. M. Temmer, Phys. Rev. Lett. **12**, 728 (1964).
[13]J. A. Niskanen and A. W. Thomas, Phys. Rev. C **37**, 1755 (1988).
[14]P. C. McNamee, *et al.*, Nucl. Phys. **A249**, 483 (1975); S. A. Coon, *et al.*, *ibid.* **A287**, 381 (1977).
[15]A. Coon, *et al.*, Phys. Rev. D **34**, 2784 (1986).
[16]D. Alde *et al.*, Sov. J. Nucl. Phys. **40**, 918 (1984); F. Binon *et al.*, *ibid* **39**, 903 (1984).
[17]G. R. Smith, *et al.*, Phys. Rev. C **30**, 980 (1984).
[18]M. Sebestyen, Honours thesis, University of Adelaide, 1986.
[19]A. W. Thomas, Adv. Nucl. Phys. **13**, 1 (1984); G. A. Miller, Int. Rev. Nucl. Phys. **1**, 190 (1984).
[20]A. W. Thomas, R. P. Bickerstaff and A. Gersten, Phys. Rev. D **24**, 2539 (1981).

# Pion absorption on polarized $^3$He

J. A. Niskanen*
*TRIUMF, Vancouver, British Columbia, Canada V6T 2A3*

L. Swift and A. W. Thomas
*Department of Physics and Mathematical Physics, University of Adelaide, Adelaide, South Australia, 5001 Australia*
(Received 5 June 1989)

We show that the quasi-two-body absorption process in polarized $^3$He is sensitive to the short-distance behavior of the $T=0$ correlation function. The difference between $A_y$ calculated for a free deuteron and a "deuteron-like" pair in $^3$He exhibits characteristic, energy-dependent signature which should be accessible experimentally.

The study of high-momentum-transfer reactions, like pion absorption, is a major challenge for present-day nuclear theory.[1] Historically a great deal of effort has been devoted to the two-nucleon system and particularly the $\pi d \leftrightarrow NN$ reaction. A wide variety of theoretical approaches have been tried, including the coupled-channels method,[2,3] three-body methods,[4,5] and multiple-scattering theory.[6] This work is now being complemented by sophisticated polarization measurements.[7–9] So far each of the models can reproduce these data at a fair level of precision within a reasonable range of its unknown parameters.

In an attempt to place somewhat stronger constraints on these theories, Ashery *et al.* and Backenstoss *et al.* recently began a series of studies of quasi-two-body (Q2B) absorption on light nuclei.[10–12] In response to this, we used the coupled-channels methods of Green, Niskanen, and others[2,3] to study the sensitivity of the polarization of the outgoing proton ($P_y$) in Q2B absorption on $^3$He [$\pi^+ {}^3\mathrm{He} \rightarrow \vec{p} + p(+p)$] to the short-distance physics.[13] In particular we viewed the process as the quasifree absorption of the $\pi^+$ on a "quasideuteron" within $^3$He.

A key difference between the free deuteron and a quasideuteron within $^3$He is that the latter is much more compact. That is, the pion is absorbed on a higher-density pair. We replaced the $S$-wave part of the deuteron wave function in our calculation of pion absorption by the square root of the $T=0$ correlation function of

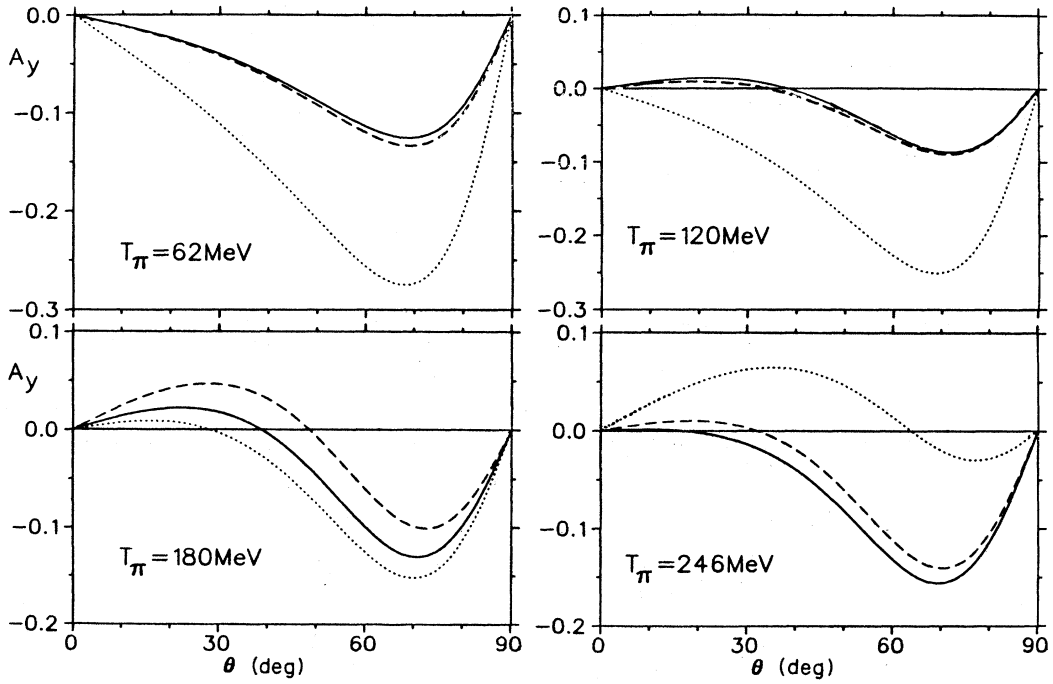


FIG. 1. The analyzing power $A_y$ for various energies. Solid curves: free $\pi^+ d \rightarrow pp$; dashed: with $^3$He reaction kinematics; dotted: with the correlation function of Friar *et al.*[14]

 

Friar *et al.*,[14] as well as a simpler parametrization suggested by the early work of Hadjimichael *et al.*[15] This wave function is expressed in terms of a scaling function times the Reid[16] deuteron wave function. The same scaling function is used to obtain the $D$-state part from the $D$ state of the Reid wave function. It turned out that the outgoing proton's polarization $P_y$ was quite sensitive to this change in the deuteron density. In particular there was a characteristic energy dependence predicted by the model which should be amenable to experimental test.

More recently, with the availability of a polarized $^3$He target in the near future,[17] it has been suggested by Gill *et al.*[18] that one might obtain some insight into the pion absorption process from Q2B of $\pi^+$ on polarized $^3$He. Here we examine this suggestion within the same model. The kinematics of the $\pi^+$ "$d$" reaction were adjusted for the different $Q$ value in the three-nucleon system. The main effect of the initial-state pion distortion was assumed to be a lowering of the overall cross section, which is unimportant for the vector analyzing power $A_y$. As in the Madison convention the positive $y$ axis is taken along $\mathbf{k}_{\text{in}}\times\mathbf{k}_{\text{out}}$. The relation to the spherical tensors is $A_y=\sqrt{2}it_{11}$ for $\pi^+$ absorption on $^3$He and $A_y=2/\sqrt{3}it_{11}$ for $\pi^+d\to pp$. It is worth noting that in terms of *two* nucleon amplitudes the expressions for $A_y$ are the same, so that in a quasifree process this observable can be directly compared between the two reactions without any proportionality constants. This is why, in the present context, we have preferred to employ the Cartesian tensors instead of the more commonly used spherical tensors even for the spin-one deuteron.

In Fig. 1 we show the predicted analyzing power for the Q2B absorption of $\pi^+$ on polarized $^3$He at a number of pion laboratory energies. The dotted curve is our full result using the wave function of Friar *et al.* For comparison we also show the results for a free deuteron (solid curve) and a free deuteron wave function with kinematics appropriate to the $^3$He reaction (dashed curve). Quite obviously the change is not due to merely different reaction kinematics.

Before discussing these curves in detail we make one cautionary remark. The quantity $A_y$ is numerically small, and therefore difficult to calculate precisely. For our model the agreement with $A_y$ data for the free deuteron is not as good as for other observables away from the region of $\Delta$ dominance (say, 140–200 MeV). Nevertheless, we do believe that the difference between the solid and dotted curves should be fairly accurately determined.

It is clear from Fig. 1 that the change in the $n-p$ correlation function has a dramatic, energy-dependent effect on $A_y$. Below the resonance, at both 62 and 120 MeV, the effect is to make $A_y$ more negative by between 0.1 and 0.2—especially at large angles. Near resonance there is little effect, while at 246 MeV $A_y$ is increased by as much as 0.15. These changes should be readily measurable with a modern, polarized target.

By experimenting with simpler changes to the quasideuteron wave function it is clear that the main reason for the changes seen in Fig. 1 is the compression of the short-distance $n-p$ wave function in $^3$He compared with the free case. Much of this sensitivity is associated with the $s$-wave pion rescattering which plays an important role in the coupled-channel calculation of pion absorption—at least off resonance. It would be a worthwhile test of our understanding of pion production to check these predictions for $A_y$, as well as our earlier ones for $P_y$.

This work was supported by the Australian Research Council.

*On leave from Department of Theoretical Physics, University of Helsinki, Finland.

[1]D. Ashery and J. P. Schiffer, Annu. Rev. Nucl. Part. Sci. **36**, 207 (1986).

[2]A. M. Green and J. A. Niskanen, Nucl. Phys. **A271**, 503 (1976).

[3]J. A. Niskanen, Nucl. Phys. **A298**, 413 (1978); Phys. Lett. **79B**, 190 (1978); **82B**, 187 (1979); **141B**, 301 (1984).

[4]I. R. Afnan and R. H. McLeod, Phys. Rev. C **31**, 1821 (1989); I. R. Afnan and B. Blankleider, *ibid.* **32**, 2006 (1985).

[5]C. Fayard, G. H. Lamot, and T. Mizutani, Phys. Rev. Lett. **45**, 524 (1980); T. Mizutani, G. Fayard, G. H. Lamot, and R. S. Nahabetian, Phys. Lett. **107B**, 177 (1981); R. S. Rinat, Y. Starkand, and E. Hammel, Nucl. Phys. **A364**, 486 (1981).

[6]W. M. Kloet and R. R. Silbar, Nucl. Phys. **A398**, 281 (1980); **A398**, 317 (1980); M. P. Locher and M. E. Sainio, Phys. Lett. **121B**, 227 (1983).

[7]D. Hutcheon *et al.* (submitted to Nucl. Phys. A); R. Abegg *et al.*, Few-Body XII, edited by B. K. Jennings (TRIUMF Report TRI-89-2, 1989), p. E8; A. Feltman *et al.*, *ibid.*, p. E11.

[8]E. Aprile *et al.*, Nucl. Phys. **A415**, 365 (1984); **A415**, 391 (1984); J. Hoftierer, *ibid.* **A412**, 273 (1984); G. Cantale *et al.*, Helv. Phys. Acta **60**, 398 (1987).

[9]W. B. Tippens *et al.*, Phys. Rev. C **36**, 1413 (1987); D. B. Barlow *et al.*, *ibid.* **37**, 1977 (1988).

[10]D. Ashery, M. A. Moinester, P. Trelle *et al.*, TRIUMF proposal 445, 1986.

[11]M. A. Moinester *et al.*, Phys. Rev. Lett. **52**, 1203 (1984); K. Aniol *et al.*, Phys. Rev. C **33**, 1714 (1986); D. Ashery *et al.*, Phys. Rev. Lett. **47**, 895 (1981).

[12]D. Gotta *et al.*, Phys. Lett. **112B**, 129 (1982); G. Backenstoss *et al.*, *ibid.* **137B**, 329 (1984); P. Weber *et al.*, Univ. of Basel report, Two-Nucleon Absorption of $\pi^+$ and $\pi^-$ on $^3$He across the $\Delta$-Resonance Region, 1989.

[13]J. A. Niskanen and A. W. Thomas, Phys. Lett. B **196**, 299 (1987).

[14]J. L. Friar, B. F. Gibson, and G. L. Payne, Annu. Rev. Nucl. Sci. **34**, 403 (1984).

[15]E. Hadjimichael, S. N. Yang, and G. E. Brown, Phys. Lett. **39B**, 594 (1972).

[16]R. Reid, Ann. Phys. (N.Y.) **50**, 411 (1968).

[17]D. R. Gill and N. R. Stevenson *et al.*, TRIUMF proposal 558, 1988.

[18]D. R. Gill (private communication).

ADP-92-175/T109

# The Role of Nucleon Structure in the $NN$ Interaction — Effects of Pion Exchange Between Quarks

G.Q. Liu, M. Swift, A.W. Thomas
Department of Physics and Mathematical Physics
University of Adelaide, Adelaide, SA 5001, AUSTRALIA
and
K. Holinde
Institut für Kernphysik, Forschungszentrum Jülich, GmbH
D-5370 Jülich, GERMANY

**Abstract**

The $NN$ interaction is studied assuming the quarks in the nucleon couple directly to the pion. To compare with the meson exchange models for the $NN$ interaction, an $NN$ potential based on the quark one pion exchange mechanism (QOPEP) is derived and investigated. Many features of the meson exchange $NN$ potentials are present in QOPEP. Overlap of nucleon wave functions and quark exchange are found to generate a repulsive core and a medium range attraction in the nucleon-nucleon potential.

## 1 Introduction

The $NN$ interaction plays a special role in the strong interaction physics. Over five decades of intensive work on this problem greatly enriched our understanding. Presently, the meson exchange mechanism is most successful in describing the empirical situation. The best known meson exchange potentials are those of the Bonn, Paris and Nijmegen [1,2,3] groups. On the other hand, it is well known that the nucleon is a composite object consisting of quarks. There are many successful quark models that can describe single hadron properties with good precision. This gives hope for

an explanation of the $NN$ interaction from the underlying quark dynamics. It is also hoped that the quark degrees of freedom will enable us to explain some ambiguities in the meson exchange models, notably the short range repulsion which is expected to depend very much on the nucleon structure. In meson exchange potentials, the short range $NN$ interaction is usually parametrized by phenomenological repulsive cores or by use of form factors, which are yet to be explained[4].

A substantial amount of information on the substructure of the nucleon has been accumulated over last thirty years. It is very tempting to utilize this information and to relate its substructure to the interaction processes. Then we may hope to understand the phenomenological parameters in terms of more fundamental quantities. Many authors [5,6,7] have attempted to explain the $NN$ interaction in terms of the *one gluon exchange* (OGE) [8] mechanism, which is reasonably successful in describing single hadron properties. Unfortunately, the $NN$ potentials based on OGE are somewhat disappointing [5,6,9]. In particular the tensor force derived from OGE is two orders of magnitude smaller than that in the meson exchange potentials. On the other hand, OGE alone can not be expected to describe the $NN$ interaction at low energies if quarks and gluons are confined within a distance of one fermi [10]. To incorporate the substructure of the nucleon and exploit the well established long range one pion exchange mechanism for the $NN$ interaction, we assume that quarks in the nucleon couple directly to the pion.

Quark pion coupling is known to be very important to guarantee chiral symmetry in more sophisticated models [11]. In the quark model, one usually treats the pion as a quark-antiquark ($q\bar{q}$) pair, therefore this picture can be viewed as including the $q\bar{q}$ creation process in the $NN$ interaction. Unlike *one gluon exchange* , $q\bar{q}$ creation is a non-perturbative effect which may play an important role in the low energy domain. The *one pion exchange* between nucleons is a well established fact, but how the pions are formed out of quarks and gluons and exchanged by the nucleons are dynamic questions to be answered by studying QCD. Judging from the long range $NN$ interaction and the success of various chiral quark models, quark pion coupling may account for a significant portion of the underlying process.

The quark-pion coupling has been used in quark model calculations refs.[12,13, 14,15] to study various aspects of the $NN$ interaction, mainly in the framework of resonating group method. In this paper we present our study of the effects of the *quark one pion exchange* (QOPE) mechanism on the $NN$ interaction. The objective of this study is to investigate the effects of nucleon substructure, which should go beyond merely yielding a form factor, and include genuine many body correlations to the $NN$ interaction. An analytic local $NN$ potential (QOPEP) is derived using the London-Heitler method [17] and compared with the well established meson potentials such as the OPEP and the Paris[2] potential. The dynamics of the QOPEP is analyzed.

In section 2) a description of the formalism is presented. The forms of the Hamiltonian and the wave function are discussed and the definition of the potential is given. Section 3) explains the evaluation of various potential terms, all of which are expressed in closed form due to the particular choice of the harmonic confinement. In section 4), numerical results of the QOPEP for the $NN$ interaction are presented and compared with the meson exchange potentials. Its relationship with the form factors used in meson exchange potentials is discussed. The many body dynamics of QOPEP is analyzed. Finally in section 5) conclusions are drawn.

# 2 The Formalism – Definition of $NN$ Potential

In this calculation, the non-relativistic quark model with a harmonic confining force is used to describe the quarks in the nucleon. We picture the nucleon as composed of three quarks interacting via the *confining force* plus some *residual forces* such as *one gluon exchange* or *one pion exchange* . For a single nucleon with only the *confining force* the Hamiltonian $H_N^{(0)}$ can be written as

$$H_N^{(0)} = \sum_{i=1}^{3} t_i + \frac{1}{2} \sum_{i \neq j=1}^{3} v_{ij}^{conf} - T_N^{CM}. \tag{2.1}$$

where $t_i$ are kinetic energies of the quarks, $T_N^{CM}$ is the kinetic energy of the nucleon. The wave function corresponding to the above Hamiltonian is of the form [16,18]

$$\Psi_N = \phi_x \chi_{m_s m_t} \zeta_c = \Phi_N \zeta_c \tag{2.2}$$

where $\phi_x$ is the symmetric spatial part, $\chi_{m_s m_t}$ is the totally symmetric spin–isospin part given by [19,20]

$$\chi_{m_s m_t} = \frac{1}{\sqrt{2}} \left\{ \left[ \left( \tfrac{1}{2}\tfrac{1}{2} \right)^0 \tfrac{1}{2} \right]^{1/2}_{m_s} \left[ \left( \tfrac{1}{2}\tfrac{1}{2} \right)^0 \tfrac{1}{2} \right]^{1/2}_{m_t} + \left[ \left( \tfrac{1}{2}\tfrac{1}{2} \right)^1 \tfrac{1}{2} \right]^{1/2}_{m_s} \left[ \left( \tfrac{1}{2}\tfrac{1}{2} \right)^1 \tfrac{1}{2} \right]^{1/2}_{m_t} \right\}. \tag{2.3}$$

$\zeta_c$ is the totally antisymmetric color part

$$\zeta_c = \frac{1}{\sqrt{6}} \epsilon_{ijk} q_1^i q_2^j q_3^k. \tag{2.4}$$

The NR quark model Hamiltonian $H$ for the NN system is then written in the following form,

$$H = H_A^{(0)} + H_B^{(0)} + \tfrac{1}{2} \sum_{i=1}^{3} \sum_{j=4}^{6} v_{ij}^{conf} + V^{(RES)} \tag{2.5}$$

where $H_A^{(0)}$ and $H_B^{(0)}$ are the Hamiltonians for single nucleons $A$ and $B$. The residual interaction term $V^{(RES)}$ contains all forces other than the confining force,

$$V^{(RES)} = \tfrac{1}{2} \sum_{i \neq j=1}^{6} v_{ij}^{res}. \tag{2.6}$$

The Heitler–London method [17] is basically a variational approach. We construct the 6–quark wave function $\Psi$ for $H$ by taking the quark model [19,20] wave function for each nucleon and then antisymmetrize all quark pairs from the two clusters. This wave function is a linear combination of the solutions of the unperturbed (i.e. confining force only ) system,

$$\Psi = A|\Psi_A \Psi_B >, \tag{2.7}$$

where $\Phi_{A,B}$ are single nucleon wave functions of eq.(2.2), $A$ is the intercluster antisymmetrizer

$$\begin{aligned} A &= 1 - \sum_{i=1}^{3} \sum_{j=4}^{6} P_{ij} + \sum_{k>m=1,\, l>n=4}^{3} \sum^{6} P_{kl} P_{mn} - P_{14} P_{25} P_{36} \\ &= \left( 1 - \sum_{i=123, j=456} P_{ij} \right) (1 - P). \end{aligned} \tag{2.8}$$

The operator $P_{ij} = P_{ij}^x P_{ij}^{\sigma\tau} P_{ij}^c$ exchanges two quarks $i$ and $j$, and $P = P_{14} P_{25} P_{36}$ interchanges two nucleons. It is seen that the total antisymmetrized 6–quark wave function satisfies the Pauli principle in both quark and nucleon levels. As will be

discussed later, the quark exchange operators in $A$ generate rich structures in the resulting $NN$ potential.

The full $NN$ potential from this model is defined as the variational energy minus the rest masses as in ref. [5].

$$V_{NN} = \frac{<\Psi|H|\Psi>}{<\Psi|\Psi>} - 2<\Psi_A|H_A|\Psi_A>, \tag{2.9}$$

In the above definition, we assume that H and $\Psi$ depend upon the quark coordinates and the center of mass separation $\boldsymbol{R}$ between the two nucleons. The quark coordinates will be integrated out keeping $\boldsymbol{R}$ fixed. The resulting $V_{NN}$ is a function of nucleon center of mass separation $\boldsymbol{R}$. A nice feature of the Heitler-London method is that the $NN$ potential terms obtained from different quark-quark forces are additive if one is consistent in the choice of the unperturbed wave function $|\Psi>$. This property enables one to study the effects of different quark-quark interaction mechanisms separately.

Following ref.[5], we separate $V_{NN}$ into three types of interaction terms,

$$V_{NN} = V_1 + V_2 + V_3, \tag{2.10}$$

where

$$V_1 = \frac{1}{N}<\Psi_A\Psi_B|\sum_{i=1}^{3}\sum_{j=4}^{6} v_{ij}(1-9P_{36})(1-P)|\Psi_A\Psi_B>, \tag{2.11}$$

$$V_2 = \frac{1}{N}<\Psi_A\Psi_B|\frac{1}{2}\left(\sum_{i\neq j=1}^{3} v_{ij} + \sum_{k\neq l=4}^{6} v_{kl}\right)(1-9P_{36})(1-P)|\Psi_A\Psi_B> - <\Psi_A|\sum_{i\neq j=1}^{3} v_{ij}|\Psi_A>, \tag{2.12}$$

$$V_3 = \frac{1}{N}<\Psi_A\Psi_B|\left(\sum_{i=1}^{6} t_i - T_A^{CM} - T_B^{CM}\right)(1-9P_{36})(1-P)|\Psi_A\Psi_B> - 2<\Psi_A|\sum_{i=1}^{3} t_i - T_A^{CM}|\Psi_A>, \tag{2.13}$$

$v_{ij}$ is the quark-quark interaction including the confining force, and $N$ is the normalization function

$$N = <\Psi|\Psi>. \tag{2.14}$$

Of the three terms in $V_{NN}$, $V_1$ includes various intercluster interactions and $V_2$ contains intracluster interactions. The term $V_3$ comes from kinetic energy contributions

which depend on the form of the nucleon radial wave function and have nothing to do with the residual quark-quark interaction studied here.

As mentioned earlier, $V^{(RES)}$ is assumed to include the *one pion exchange* component. Our purpose here is to study the effects of this *one pion exchange* piece. In the following we confine ourselves only to the OPE part in $V^{(RES)}$,

$$V^{OPE} = \frac{1}{2}\sum_{i\neq j=1}^{6} v_{ij}^{ope}, \tag{2.15}$$

where $v_{ij}^{ope}$ is the OPEP between quarks i and j,

$$v_{ij}^{ope} = G_{ij}\tau_i\cdot\tau_j[v_s^{ope}(r_{ij})\sigma_i\cdot\sigma_j + v_t^{ope}(r_{ij})\mathrm{S}(\hat{r}_{ij})]. \tag{2.16}$$

The tensor operator between two quarks $\mathrm{S}(\hat{r}_{ij})$ and the constant $G_{ij}$ are defined by

$$\mathrm{S}(\hat{r}_{ij}) = 3(\sigma_i\cdot\hat{r}_{ij})(\sigma_j\cdot\hat{r}_{ij}) - \sigma_i\cdot\sigma_j\ , \tag{2.17}$$

and

$$G_{ij} = \frac{g_{q\pi}^2}{4\pi}\frac{1}{4m_im_j} \xrightarrow{m_i=m_j=m_q} G_0 = \frac{g_{q\pi}^2}{4\pi}\frac{1}{4m_q^2}\ . \tag{2.18}$$

The pseudoscalar coupling constant $g_{q\pi}$ is related to the pseudovector coupling constant $f_{q\pi}$ by the equivalence theorem

$$G_0 = \frac{g_{q\pi}^2}{4\pi}\frac{1}{4m_q^2} = \frac{f_{q\pi}^2}{\mu^2}. \tag{2.19}$$

The relationship between quark-pion coupling constants and nucleon-pion coupling constants will be discussed later in section 4. The radial functions in eq.(2.16) are given by

$$v_s^{ope}(r_{ij}) = \frac{\mu^3}{3}[\frac{1}{\mu r_{ij}} - 4\pi\delta(\mu r_{ij})]\, e^{-\mu r_{ij}} \tag{2.20}$$

and

$$v_t^{ope}(r_{ij}) = \frac{\mu^3}{3}[\frac{1}{\mu r_{ij}} + \frac{3}{(\mu r_{ij})^2} + \frac{3}{(\mu r_{ij})^3}]\, e^{-\mu r_{ij}} \tag{2.21}$$

where $\mu$ is the pion mass. Unlike the *one gluon exchange* force, the *one pion exchange* force has no color dependence. This implies that the contribution from the direct interaction term of fig.1a does not vanish. This property is crucial to produce the long range OPEP force of the $NN$ interaction, which is observed experimentally. On the other

hand, the *one gluon exchange* affects only the short range $NN$ interaction because all contributing terms involve quark exchange between two color singlet nucleons.

In the OPEP for point nucleons the contact term in the spin–spin force $v_s$ is usually ignored by an ad hoc procedure, which basically says that the short range meson exchange potentials obtained by treating nucleons as point particles are not reliable. This problem does not exist anymore when the substructure of the nucleon is taken into account. The role of the contact term in the quark–quark OPEP will be discussed later.

Since the OPEP is color blind, the color dependence in $V_{NN}$ comes only from the exchange operators $P_{36}$ and $P$. Therefore, the color parts of the matrix elements can be calculated before the potential terms are considered later on,

$$< \zeta_c(A)\zeta_c(B)|P^c|\zeta_c(A)\zeta_c(B) >= 1, \qquad < \zeta_c(A)\zeta_c(B)|P^c_{36}|\zeta_c(A)\zeta_c(B) >= \frac{1}{3}. \quad (2.22)$$

After the color part is done, the nucleon wave functions $|\Psi_N >$ in eqs.(2.11) and (2.12) can be replaced by its color independent part, namely

$$|\Phi_N >= |\phi_x \chi_{m_s m_t} > . \quad (2.23)$$

Eqs.(2.11) and (2.12) then become

$$V_1^{OPE} = \frac{1}{N} < \Phi_A\Phi_B| \sum_{i=1}^{3}\sum_{i=4}^{6} v_{ij}^{ope}(1 - 3P_{36}^{\sigma\tau x})(1 - P^{\sigma\tau x})|\Phi_A\Phi_B >, \quad (2.24)$$

$$V_2^{OPE} = \frac{1}{N} < \Phi_A\Phi_B|\tfrac{1}{2}\left(\sum_{i\neq j=1}^{3} v_{ij}^{ope} + \sum_{k\neq l=4}^{6} v_{kl}^{ope}\right)(1 - 3P_{36}^{\sigma\tau x})(1 - P^{\sigma\tau x})|\Phi_A\Phi_B >$$

$$- < \Phi_A| \sum_{i\neq j=1}^{3} v_{ij}^{ope}|\Phi_A > \quad (2.25)$$

The reduction of various terms in eqs.(2.24) and(2.25) into analytic $NN$ potential functions is discussed in section 3.

# 3 Structure of the QOPEP

The potential given by eqs.(2.24) and (2.25) consist of two type of terms, *non-quark-exchange* and *quark-exchange*. As will be seen later, the quark-exchange-terms are

short ranged while the non–quark–exchange terms have longer range to give the asymptotic OPEP. The non–quark–exchange terms are of the form,

$$V_{ij}^{(nqe)} = \frac{1}{N} < \Phi_A\Phi_B|v_{ij}^{ope}(1 - P^{\sigma\tau x})|\Phi_A\Phi_B >, \tag{3.1}$$

the quark–exchange terms have an extra exchange operator $-3P_{36}^{\sigma\tau x}$

$$V_{ij}^{(qe)} = \frac{1}{N} < \Phi_A\Phi_B|v_{ij}^{ope}(-3P_{36}^{\sigma\tau x})(1 - P^{\sigma\tau x})|\Phi_A\Phi_B > . \tag{3.2}$$

The term

$$V_{ij}^{(s)} =< \Phi_A|v_{ij}^{ope}|\Phi_A > \tag{3.3}$$

represents corrections from the nucleon rest mass.

With the help of eqs.(3.1), (3.2) and(3.3), and using the permutation symmetries of $\Phi_A$ and $\Phi_B$, $V_1^{OPE}$ and $V_2^{OPE}$ can be further simplified to following forms,

$$V_1^{OPE} = 9V_{36}^{(nqe)} + V_{36}^{(qe)} + 4V_{14}^{(qe)} + 4V_{34}^{(qe)}, \tag{3.4a}$$

$$V_2^{OPE} = 4V_{12}^{qe} + 4V_{23}^{qe} + 6(V_{12}^{(nqe)} - V_{12}^{(s)}). \tag{3.4b}$$

Each term in the above equations is schematically represented by a diagram in fig.1. The reader should bear in mind that the diagrams in fig.1 are for classification of different terms only and do not have the same mathematical content as for the Feynman Diagrams in the field theory. They basically represent the structure of the matrix elements in the numerators of various terms in eqs.(2.24) and (2.25). The quark exchange effect in the normalization function $N$ is not fully reflected by these diagrams. These diagrams could be misleading, for example, one may think that the term represented by fig.1g cancels out exactly. But it involves the normalization function $N$ in $V_{12}^{(nqe)}$ and hence quark exchange effects, which play an important role as will be seen later.

Now we find the spin–isospin and radial structures of the eight matrix elements in eqs.(3.4).

## 3.1 Spin–Isospin Substitution Rules

The spin–isospin matrix elements of $V_1^{OPE}$ and $V_2^{OPE}$ can be obtained by the well known techniques of angular momentum recoupling as done in ref.[21]. But the particular symmetry of the quark model wave function for the nucleon allows some elegant and simple *substitution rules* [5] to be applied to this problem. The results given here are confirmed by both methods.

The essence of the *substitution rules* is to project the quark spin–isospin degrees of freedom onto nucleon spin–isospin degrees of freedom. With these rules one can use the expansion

$$P_{36}^{\sigma\tau} = \frac{1}{4}(1 + \tau_3 \cdot \tau_6)(1 + \sigma_3 \cdot \sigma_6) \tag{3.5}$$

and manipulate the quark spin isospin operators algebraically to find the corresponding nucleon operators. These rules are derived by requiring that the spin–isospin matrix elements are the same when these operators act on quark or nucleon spaces. Their validity depends upon the spin–isospin wave function of the nucleon being the totally symmetric quark model wave function of eq.(2.3). Table 1 lists all the rules needed for the present calculation. Proofs for these rules are given in the Appendix.

To illustrate the application of the rules in table 1, we give two examples. First consider the single nucleon quark spin–isospin operator

$$\sigma_1 \cdot \sigma_2 = \sum_{i=1}^{3} \sigma_1^i \sigma_2^i. \tag{3.6}$$

Using rule 5 one finds that it gives

$$\frac{1}{6}\sum_{i=1}^{3}(-2) = -1. \tag{3.7}$$

For operators involving quarks from two nucleons, one has to use the *substitution rules* for each nucleon separately. Suppose nucleon A contains quarks (123) and B (456), the operator

$$(\tau_1 \cdot \tau_4)(\sigma_1 \cdot \sigma_4)(\tau_3 \cdot \tau_6)(\sigma_3 \cdot \sigma_6) = \sum_{i,j,a,b} \sigma_1^i \sigma_3^j \tau_1^a \tau_3^b \sigma_4^i \sigma_6^j \tau_4^a \tau_6^b \tag{3.8}$$

should be replaced by

$$\sum_{i,j,a,b,q,r,s,t} \frac{1}{6}\left(\frac{10}{3}\delta_{ij}\delta_{ab} - 2\epsilon_{ijq}\epsilon_{abr}\sigma_N^q \tau_N^r\right) \times \frac{1}{6}\left(\frac{10}{3}\delta_{ij}\delta_{ab} - 2\epsilon_{ijs}\epsilon_{abt}\sigma_N^s \tau_N^t\right), \tag{3.9}$$

according to rule 11. Since

$$\sum_{ij} \epsilon_{ijq}\epsilon_{ijs} = 2\delta_{qs}, \tag{3.10}$$

one arrives at a spin-isospin operator on the two nucleons A and B,

$$\frac{25}{9} + \frac{4}{9}(\tau_A\cdot\tau_B)(\sigma_A\cdot\sigma_B). \tag{3.11}$$

The presence of the factor $\frac{1}{6}$ is because rules 5 and 11 involve a summation over all six possible quark pair combinations.

## 3.2 Spin–Isospin Structure of QOPEP

Applying the rules in table 1, one obtains the spin-isospin structure for the *direct* part (that without the factor $-P$) of eight matrix elements in eqs.(3.4).

$$V_{36}^{(dnqc)} = \frac{1}{N}\frac{25}{81}\tau_A\cdot\tau_B(R_{36}^S\sigma_A\cdot\sigma_B + R_{36}^T S_{AB}) , \tag{3.12a}$$

$$V_{36}^{(dqc)} = \frac{Q_{36}^S}{N}\left[9 - \frac{1}{3}(\tau_A\cdot\tau_B + \sigma_A\cdot\sigma_B) + \frac{25}{81}(\tau_A\cdot\tau_B)(\sigma_A\cdot\sigma_B)\right] + \frac{Q_{36}^T}{N}(\frac{2}{9} - \frac{50}{243}\tau_A\cdot\tau_B)S_{AB} , \tag{3.12b}$$

$$V_{14}^{(dqc)} = \frac{Q_{14}^S}{N}\left[\frac{25}{9} + \frac{1}{27}(\tau_A\cdot\tau_B + \sigma_A\cdot\sigma_B) + \frac{61}{81}(\tau_A\cdot\tau_B)(\sigma_A\cdot\sigma_B)\right] + \frac{Q_{14}^T}{N}(\frac{1}{81} + \frac{7}{243}\tau_A\cdot\tau_B)S_{AB} , \tag{3.12c}$$

$$V_{34}^{(dqc)} = \frac{Q_{34}^S}{N}\left[5 + \frac{1}{9}(\tau_A\cdot\tau_B + \sigma_A\cdot\sigma_B) + \frac{85}{81}(\tau_A\cdot\tau_B)(\sigma_A\cdot\sigma_B)\right] + \frac{Q_{34}^T}{N}(\frac{1}{27} - \frac{5}{243}\tau_A\cdot\tau_B)S_{AB} , \tag{3.12d}$$

$$V_{12}^{(dnqc)} = \frac{5}{N}R_{12}^S , \tag{3.12e}$$

$$V_{12}^{(dqc)} = \frac{Q_{12}^S}{N}\left[5 + \frac{13}{9}(\tau_A\cdot\tau_B + \sigma_A\cdot\sigma_B) + \frac{205}{81}(\tau_A\cdot\tau_B)(\sigma_A\cdot\sigma_B)\right] , \tag{3.12f}$$

$$V_{23}^{(dqc)} = \frac{Q_{23}^S}{N}\left[5 + \frac{1}{9}(\tau_A\cdot\tau_B + \sigma_A\cdot\sigma_B) + \frac{85}{81}(\tau_A\cdot\tau_B)(\sigma_A\cdot\sigma_B)\right] + \frac{Q_{23}^T}{N}(\frac{1}{27} - \frac{5}{243}\tau_A\cdot\tau_B)S_{AB} , \tag{3.12g}$$

$$V_{12}^{(s)} = 5R_{12}^S , \tag{3.12h}$$

where R's and Q's are radial integrals depending only on the distance $R$ between two nucleons. $R's$ are non-quark-exchange and $Q's$ involve quark-exchange. The radial integrals will be calculated later in this section and we will also see that $V_{23}^{(dqc)} = V_{34}^{(dqc)}$.

The above expressions do not include the nucleon exchange part (signified by operator $-P$) of the matrix element. But due to the symmetry of the nucleon wave function, the corresponding nucleon exchange counterparts of eqs.(3.12) have the same spin–isospin structures as the above but multiplied by a phase factor $(-1)^{1+S+T}$ or the operator

$$-P^{\sigma\tau}_{AB} = -\tfrac{1}{2}(1+\sigma_A\cdot\sigma_B)\tfrac{1}{2}(1+\tau_A\cdot\tau_B). \tag{3.13}$$

The forms of the radial integrals $R's$ and $Q's$ are in general different with or without the nucleon exchange. In the case of nucleon exchange the radial integrals are denoted by $R^{eS}$, $Q^{eS}$ and $Q^{eT}$, whose evaluation is explained in the next subsection.

One can see from eqs.(3.12) that the simple OPE interaction between quarks is able to generate an $NN$ potential with richer structure than the simple OPEP for point nucleons. Central, isoscalar spin–spin and isoscalar tensor terms are present. But there is no spin–orbit interaction. Most of the terms affect the short range part of the $NN$ interaction as they involve quark exchange. One observes that eqs.(3.12) always contain the combination $\tau_A\cdot\tau_B + \sigma_A\cdot\sigma_B$. The consequence of this symmetry and the absence of the spin orbit interaction is that the radial dependence of singlet–even and triplet–even $NN$ potentials are the same.

## 3.3 Evaluation of the Radial integrals

There are two types of radial integrals, the *direct integrals* are those that do not include the nucleon exchange operator $(-P^x)$ but may have a quark exchange operator $P^x_{36}$, the *exchange integrals* are those that have the nucleon exchange operator $(-P^x)$. The direct integrals are defined as,

$$R^S_{ij} = <\phi_A(x)\phi_B(x)|G_0 v_s^{ope}(r_{ij})|\phi_A(x)\phi_B(x)>, \tag{3.14a}$$

$$Q^S_{ij} = <\phi_A(x)\phi_B(x)|-\frac{3}{4}G_0 v_s^{ope}(r_{ij})P^x_{36}|\phi_A(x)\phi_B(x)>, \tag{3.14b}$$

$$R^T_{ij}S_{AB} = <\phi_A(x)\phi_B(x)|G_0 v_t^{ope}(r_{ij})S_{AB}(r_{ij})|\phi_A(x)\phi_B(x)>, \tag{3.14c}$$

$$Q^T_{ij}S_{AB} = <\phi_A(x)\phi_B(x)|-\frac{9}{4}G_0 v_t^{ope}(r_{ij})S_{AB}(r_{ij})P^x_{36}|\phi_A(x)\phi_B(x)>, \tag{3.14d}$$

The exchange integrals are defined similarly to the direct integrals but with an extra nucleon exchange operator $-P^x$,

$$R_{ij}^{cS} =< \phi_A(x)\phi_B(x)|G_0 v_s^{ope}(r_{ij})(-P^x)|\phi_A(x)\phi_B(x) >, \tag{3.15a}$$

$$Q_{ij}^{cS} =< \phi_A(x)\phi_B(x)| - \frac{3}{4}G_0 v_s^{ope}(r_{ij})P_{36}^x(-P^x)|\phi_A(x)\phi_B(x) >, \tag{3.15b}$$

$$R_{ij}^{cT}S_{AB} =< \phi_A(x)\phi_B(x)|G_0 v_t^{ope}(r_{ij})S_{AB}(r_{ij})(-P^x)|\phi_A(x)\phi_B(x) >, \tag{3.15c}$$

$$Q_{ij}^{cT}S_{AB} =< \phi_A(x)\phi_B(x)| - \frac{9}{4}G_0 v_t^{ope}(r_{ij})S_{AB}(r_{ij})P_{36}^x(-P^x)|\phi_A(x)\phi_B(x) >, \tag{3.15d}$$

where $S_{AB}(r_{ij})$ is the tensor operator with quark coordinates $r_{ij}$ and nucleon spin operators $\sigma_A$ and $\sigma_B$,

$$S_{AB}(r_{ij}) = 3(\sigma_A\cdot\hat{r}_{ij})(\sigma_B\cdot\hat{r}_{ij}) - \sigma_A\cdot\sigma_B. \tag{3.16}$$

The quark coordinates $r_{ij}$ in ${S_{AB}}^{ij}$ are transformed into internucleon separation $\mathbf{R}$ after integration.

Using the radial functions for nucleons A and B [5,16]

$$\phi_A(x) = \left(\frac{\beta^2}{\pi}\right)^{9/4} e^{-\frac{1}{2}\beta^2\left[\left(r_1-\frac{1}{2}R\right)^2+\left(r_2-\frac{1}{2}R\right)^2+\left(r_3-\frac{1}{2}R\right)^2\right]}, \tag{3.17a}$$

$$\phi_B(x) = \left(\frac{\beta^2}{\pi}\right)^{9/4} e^{-\frac{1}{2}\beta^2\left[\left(r_4+\frac{1}{2}R\right)^2+\left(r_5+\frac{1}{2}R\right)^2+\left(r_6+\frac{1}{2}R\right)^2\right]}, \tag{3.17b}$$

the radial integrals $R's$ and $Q's$ can be evaluated straightforwardly and expressed in terms of gaussians and complementary error functions. To simplify notation and systemize expressions, we define two functions, $F_S(x)$, for central terms, and $F_T(x)$, for tensor terms. All radial integrals can be expressed in terms of these two functions, with the argument $x$ being $R$, $R/2$, or 0. The functional form of $F_S(x)$ is given by

$$\begin{aligned} F_S(x) &= \left(\frac{\beta^2}{2\pi}\right)^{3/2} e^{-\frac{1}{2}\beta^2x^2}\int e^{-\frac{1}{2}\beta^2(r^2-2r\cdot x)}v_s^{ope}(r)d^3r \\ &= \frac{1}{6}e^{-\frac{1}{2}\beta^2x^2}\left[\mu^2F(x) - 2\beta^3\sqrt{\frac{2}{\pi}}\right], \end{aligned} \tag{3.18}$$

where $v_s^{ope}(r)$ is given by eq.(2.20). The first term comes from the Yukawa and the second term comes from the contact piece of the central potential $v_s$ in eq.(2.20). The function $F_T(x)$ is defined as

$$F_T(x)S_{AB}(x) = \left(\frac{\beta^2}{2\pi}\right)^{3/2} e^{-\frac{1}{2}\beta^2 x^2} \int e^{-\frac{1}{2}\beta^2(r^2-2r\cdot x)} v_t^{ope}(r) S_{AB}(r) d^3r$$

where $v_t^{ope}(r)$ is given by eq.(2.21). For the purposes of calculation, the quantity $v_t^{ope}(r)S_{AB}(r)$ can be replaced by

$$(\sigma_A\cdot\nabla)(\sigma_B\cdot\nabla)\frac{e^{-\mu r}}{r} - \sigma_A\cdot\sigma_B v_s^{ope}(r).$$

The final form of $F_T(x)$ is given by

$$F_T(x) = \frac{1}{6} e^{-\frac{1}{2}\beta^2 x^2}\left[(\mu^2 - \frac{3\mu}{x} + \frac{3}{x^2})F(x) + \frac{6\mu}{x}g(x) - \sqrt{\frac{2}{\pi}}(2\beta^3 + \frac{6\mu}{x^2})\right]. \qquad (3.19)$$

In eqs.(3.18) and (3.19), the functions $F(x)$ and $g(x)$ are defined by

$$F(x) = 2\left(\frac{\beta^2}{2\pi}\right)^{3/2} \int e^{-\frac{1}{2}\beta^2(r^2-2r\cdot x)} \frac{e^{-\mu r}}{r} d^3r\ , \qquad (3.20)$$

$$g(x) = \frac{1}{x} e^{\frac{(\mu-\beta^2 x)^2}{2\beta^2}} erfc(\frac{\mu-\beta^2 x}{\sqrt{2}\beta}). \qquad (3.21)$$

$F(x)$ can be expressed in terms of $g(x)$ as

$$F(x) = g(x) + g(-x)\ . \qquad (3.22)$$

Functions $F_T(x)$ and $F_S(x)$ are related by

$$S_{AB}(x)F_T(x) + \sigma_A\cdot\sigma_B F_S(x) = \left(\frac{\beta^2}{2\pi}\right)^{3/2} e^{-\frac{1}{2}\beta^2 x^2} \int e^{-\frac{1}{2}\beta^2(r^2-2r\cdot x)}\left[(\sigma_A\cdot\nabla)(\sigma_B\cdot\nabla)\frac{e^{-\mu r}}{r}\right] d^3r$$

$$= \tfrac{1}{2} e^{-\frac{1}{2}\beta^2 x^2}\left\{\beta^4(\sigma_A\cdot x)(\sigma_B\cdot x) - \beta^2\left[(\sigma_A\cdot x)(\sigma_B\cdot\nabla) + (\sigma_A\cdot\nabla)(\sigma_B\cdot x)\right] + (\sigma_A\cdot\nabla)(\sigma_B\cdot\nabla)\right\} F(x) \qquad (3.23)$$

where $S_{AB}(x)$ is the tensor operator in $x$

$$S_{AB}(x) = 3(\sigma_A\cdot\hat{x})(\sigma_B\cdot\hat{x}) - \sigma_A\cdot\sigma_B.$$

For simplicity we use the symbol $F_0$ to denote the quantity $F_S(x=0)$

$$F_0 = F_S(0) = \frac{1}{3}[-\mu^3 e^{\frac{\mu^2}{2\beta^2}} erfc(\frac{\mu}{\sqrt{2}\beta}) + \sqrt{\frac{2}{\pi}}(\beta\mu^2 - \beta^3)]. \qquad (3.24)$$

All radial integrals are expressed in terms of $F_S$ and $F_T$ and listed in table 2.

Before going on to the numerical results, an examination of the behavior of the functions $F_S(x)$ and $F_T(x)$ can give a feeling of how different terms contribute. As $x \longrightarrow 0$, $F_T(x)$ goes to zero as $x^2$,

$$F_T(x) \longrightarrow const. \times x^2$$

The constant can be obtained analytically and expressed in terms of the pion mass $\mu$ and nucleon size parameter $\beta$. But the expression is lengthy and not illuminating and hence not given here. For large $x$

$$F(x) \longrightarrow g(x) \longrightarrow \frac{2}{x} e^{\frac{(\mu-\beta^2 x)^2}{2\beta^2}}, \tag{3.25}$$

so that

$$F_S(x) \longrightarrow \frac{\mu^2}{6} e^{-\frac{1}{2}\beta^2 x^2} F(x) \longrightarrow \frac{\mu^2}{3} e^{\frac{\mu^2}{2\beta^2}} \frac{e^{-\mu x}}{x}, \tag{3.26}$$

which goes like a Yukawa, and

$$F_T(x) \longrightarrow \frac{\mu^2}{3} e^{\frac{\mu^2}{2\beta^2}} \frac{e^{-\mu x}}{x}(1 + \frac{3}{(\mu x)} + \frac{3}{(\mu x)^2}) \tag{3.27}$$

which goes like the tensor part of the OPEP. With the help of eqs.(3.26-3.27) one can see from table 2 that contributions to the long range central (tensor) part come from direct terms $R^S$ ($R^T$) as expected. Quark exchange terms of *direct integrals*, $Q^S$ and $Q^T$, have an cut-off factor $e^{-\frac{1}{2}\beta^2 R^2}$. But nucleon exchange terms $R^{eS}, Q^{eS}$ and $Q^{eT}$ have shorter ranges than any *direct integrals*, due to cut-off factors like $e^{-\beta^2 R^2}$ or $e^{-\frac{3}{2}\beta^2 R^2}$. Notice that integrals $Q_{34}$ and $Q_{23}$ have longer ranges than other quark exchange integrals due to the argument $R/2$ in $F_T$ and $F_S$.

The normalization $N$ , as in ref. [5], is given by

$$N = 1 - 3C_{ST}\, e^{-\frac{1}{2}\beta^2 R^2} + 3C_{ST}(-1)^{S+T}\, e^{-\beta^2 R^2} - (-1)^{S+T}\, e^{-\frac{3}{2}\beta^2 R^2}, \tag{3.28}$$

where the spin-isospin dependent constant $C_{ST}$ has the values

$$C_{00} = \frac{7}{9}, \quad C_{11} = \frac{31}{81}, \quad C_{01} = C_{10} = -\frac{1}{27}. \tag{3.29}$$

One can see that $N \longrightarrow 1$ for large $R$ as expected. But as $R \longrightarrow 0$ the behavior of $N$ depends on the $NN$ spin–isospin quantum numbers, namely,

$$N \xrightarrow{R\to 0} \frac{20}{9} \qquad for\ (S,T) = (0,1)\ or\ (1,0), \tag{3.30a}$$

and

$$N \xrightarrow{R\to 0} \begin{cases} \frac{1}{3}\beta^2 R^2 & for\ (S,T) = (0,0) \\ \frac{25}{27}\beta^2 R^2 & for\ (S,T) = (1,1). \end{cases} \tag{3.30b}$$

The $R^2$ divergence for singlet–odd and triplet–odd states is due to the antisymmetrization of the wave function, i.e., the Pauli principle. This divergence of the normalization function at small $R$ does not lead to a divergence in the $NN$ potential for odd parity states. In the matrix elements for the odd parity states, the nucleon exchange term and non nucleon exchange term cancel at small $R$ to give a $R^2$ behavior.

# 4 Results and Analysis

In this section we present and analyze the numerical results of the calculations discussed in sections 2 and 3. We first compare QOPEP with the traditional meson exchange potentials and then look at the detailed dynamics of QOPEP.

There are no free parameters to adjust in this model, because the quark–pion coupling constant $f_{q\pi}$ and the nucleon size parameter $\beta$ can all be derived from nucleon properties. We take $\beta^{-1} = 0.5\ fm$ which is a median value used in most of the literature[13,12,7]. Since this model is somewhat similar to the chiral bag model picture, one would expect the value of $\beta^{-1}$ to be smaller than that in the naive quark model. But here we are concerned mainly with the general behavior of the QOPEP and slight variation of $\beta$ does not alter the main features of the QOPEP. Corresponding to the choice of spatial wave functions for the nucleon in eqs.(3.17), the quark pion coupling constant $f_{q\pi}$ can be related to the nucleon pion coupling constant $f_{N\pi}$ by examining the asymptotic behavior of the QOPEP and that of the OPEP for point nucleons. For large $R$ only one term dominates in QOPEP, namely, $V_{36}^{(dnqc)}$ in eq.(3.12a). With the help of table 2 and eq.(3.26) one finds

$$f_{q\pi}^2 = \frac{9}{25} e^{\frac{-\mu^2}{2\beta^2}} f_{N\pi}^2 , \tag{4.1}$$

where $f^2_{N\pi} = 0.082$ and $\mu$ is the pion mass.

## 4.1 Comparison with meson exchange potentials

Fig.2 shows the total central and tensor potentials calculated from eqs.(3.4a) and (3.4b) for various $NN$ states. The QOPEP is compared with three forms of meson exchange potentials: 1) OPEP–FF which is OPEP with a monopole form factor, 2) OPEP–PN which is just the pure OPEP for point nucleons, and 3) the Paris potential[2]. As seen in fig.2, while all the long range results are the same as the well known OPEP–PN, the short range behavior of the QOPEP exhibits several interesting features.

First, the central potential is repulsive for $r < 0.5$ $fm$ in all $NN$ states. This is supportive of the phenomenological repulsive core used in all meson exchange potentials.

Secondly, the singlet–even (triplet–even) central and the tensor potentials behave much like an OPEP-FF with a cut–off mass of 700 MeV for $r > 1$ $fm$, which is in line with the use of a soft pion form factor in meson exchange potentials as proposed in ref.[4]. Inside 1 $fm$, however, the results are different, which is to be expected since the rich structure of the quark dynamical model can not be accounted for by a simple form factor. Another interesting feature with the singlet–even (triplet–even) central potential is that a medium range attraction of about 50 MeV is produced. This medium range attraction in the $NN$ system has traditionally been attributed to two pion exchange which is often represented as $\sigma$ meson exchange. In this model we find such a force as a result of the inclusion of nucleon substructure.

Thirdly, strong repulsion is found in singlet-odd and triplet–odd states. On the other hand OPEP-FF is attractive in these states. In view of the repulsive core used in meson exchange potentials, we think the short range attraction of the OPEP–FF is not a desirable feature. Indeed it is quite artificial, as the form factor should act to slightly suppress the OPEP at intermediate distances but cannot be expected to represent the complex physics in the region where nucleons physically overlap. In fact neither OPEP–PN nor OPEP–FF can give the short range repulsion for *all $NN$ states*, but QOPEP does. This repulsion may offer an explanation to the $N - \omega$ coupling in

the meson exchange models, where it is considered to be too large - about twice its SU(3) value.

It is also shown in fig.2 that the overall behavior of QOPEP very much resemble the corresponding components of the Paris potential[2] in the parametrized form for all $NN$ states.

## 4.2 Analysis of the dynamics of QOPEP

In order to reveal the detailed dynamics, we look into various terms of eqs.(3.4a) and (3.4b). Contributions from each individual term (figs.1a–1g) are shown in fig.3.

Contributions to the short range repulsion mostly come from the quark exchange terms which can be seen in fig.3a-3c. One also sees from figs.3d and 3e that *quark exchange terms have little effect on the tensor force* and the total tensor potential is determined by only one non-quark-exchange term $V_{36}^{(nqc)}$. This explains why the tensor force in QOPEP is so much similar to OPEP-FF. There are two reasons for this suppression of tensor force in quark exchange terms. The first is the cancellation in the spin–isospin coefficients which can be seen in eqs.(3.12). The second is the structure of the radial integrals. The function $F_T(R)$ peaks at about 0.8 fm and goes to zero for $x = 0$. But cut-off factors like $e^{-\beta^2 R^2}$ drop quickly to zero at intermediate ranges, making the whole integral small in both the short and medium ranges. This situation doesn't happen in the central terms since the function $F_S(x)$ is finite at $x = 0$.

The central singlet–even (triplet–even) potential gets contributions from many terms, most of which are repulsive. The medium range attraction for singlet–even and triplet–even states comes from the intracluster term $(V_{12}^{(nqc)} - V^{(s)})$. This term is neglected in some calculations[6,13] arguing that it cancels out exactly because it is a nucleon self energy term. But this is correct only if the total wave function $\Psi$ in eq.(2.7) is not antisymmetrized with respect to quark pairs from different clusters. This requires $A = 1$ in eqs.(2.8) and (2.7), which would leave out *all* the short range dynamics. With total antisymmetrization of the 6-quark wave function, *there is no exact cancellation*. Indeed one sees from eqs.(3.12h) and (3.12e) that at long distance this term cancels out, but at the short distance, the effects of quark exchange from

different nucleons in the normalization function make a significant contribution to the interaction process. We also find that the term $V_{14}^{(qe)}$ represented by fig.1c gives only a negligible contribution in any state.

One of the reasons for the repulsion in singlet-odd and triplet-odd states is the $R^2$ divergence in the normalization function $N$ for these states, which is due to the Pauli principle. For these states, QOPEP and OPEP-FF go in opposite directions at the short range. As mentioned earlier, OPEP-FF may not represent the complicated dynamics at very short ranges. The main reason for the QOPEP to be repulsive in these states is again because of the quark exchange. One can see that quark exchange is really the key in producing the short range repulsion.

## 4.3 Origin of the repulsion and effects of the pion size

In $NN$ OPEP the contact term is usually removed by the so called Poorman's procedure or smeared out by use of form factors. That problem does not arise in this calculation since the nucleon is treated as a composite particle. But since we treat the pion as a point particle, there is a contact term in the quark-quark potential $v_s$ of eq.(2.20). Therefore the problem of the pion size needs to be examined.

The effects of the contact term in $v_s$ and the pion size are studied in two ways: 1) by ignoring the contact piece in a way similar to the Poorman's procedure in $NN$ OPEP, and 2) by applying a form factor at the quark-pion vertex. The results are shown in fig.4, where the full QOPEP is compared with the no-contact-term and form factor calculations.

Dramatic changes in the behavior of QOPEP are found. Without the contact piece, the potentials become *very weak* and *attractive* at the short range. The contact force basically determines the central part of QOPEP. The importance of the $\delta$ function term indicates that in this model the short range repulsion depends heavily on the nucleon wave function overlap at short distances. The fact that the finite size effects of the nucleon dominate the $NN$ interaction at short ranges tells us that many body effects are large at these ranges. This may explain the need of phenomenological treatments required in many variations of meson exchange $NN$ potentials.

Two types of form factors used to incorporate the pion size are given by

$$F(q^2) = \frac{\Lambda^2 - \mu^2}{q^2 + \Lambda^2},$$

for the monopole form, and

$$F(q^2) = \sqrt{\frac{\Lambda^2}{q^2 + \Lambda^2}}.$$

for the square root form suggested in refs.[12,13] One can see from fig.4. that the form factors make the predominant contribution to the repulsion in the resulting $NN$ potential. Their role is very similar to the contact term in the central QOPEP. But unlike the contact force which affects the central part only, form factors weaken both the central and tensor parts. As the cut–off mass increases, the form factor results approach the contact term results, which is the limiting case for $\Lambda \longrightarrow \infty$. This is true for both the total potentials and individual terms in eqs.(3.4). Therefore the QOPEP with a point-like pion gives the *maximum repulsion*. It is known that $\omega$–exchange and gluon exchange are needed to get the spin–orbit force, which also provide a good part of the repulsion. The role of the repulsion from quark–pion coupling need be examined in conjunction with the $\omega$ and gluon exchanges.

On the other hand, if one takes the short range repulsion as an indication of the correct dynamics at the quark level, one can conclude from the usual phenomenology of the core that the quark–pion coupling must be almost point–like. This implies that the pion has a very small size.

At this point we would like to make a comment on the source of repulsion in the OGE calculations. The OGE quark–quark potential contains a color Coulomb term and spin–spin and central contact terms.

$$V_{ij}^{OGE} = \lambda_i \cdot \lambda_j \frac{\alpha_s}{4}\left[\frac{1}{r_{ij}} - \frac{2\pi}{3}\frac{\sigma_i \cdot \sigma_j}{m_q^2}\delta(r_{ij}) - \frac{\pi}{m_q^2}\delta(r_{ij}) + s.o. + tensor\right] \qquad (4.2)$$

Based on the results of the present calculation, one can conclude that the repulsion in OGE calculation is also from the contact piece, since at the short range the Yukawa term in OPE and the Coulomb term in OGE play similar roles.

# 5 Conclusions and discussion

Our study of the effects of the *quark one pion exchange* mechanism on the $NN$ interaction has led to several conclusions. We found that nucleon substructure has important implications on the $NN$ interaction process. In some cases meson exchange potentials with soft form factors generate similar dynamics to that given by the multiquark system in the subnucleon level. This happened for the singlet-even (triplet-even) central force and the tensor force in this calculation. For odd parity states the OPEP-FF gives a very different potential form. Therefore, the use of form factors may not be sufficient to describe the complex quark dynamics at short ranges. Many body effects may be responsible for the phenomenological parameters and even some coupling constants in meson exchange models. More investigation is needed to reveal the quantitative connection between multiquark dynamics and these parameters.

We also found several interesting features of the QOPEP. For all $NN$ states the QOPEP is repulsive at the short range, which agrees with the traditional picture of a repulsive core. The origin of the repulsion is the nucleon wave function overlap and quark exchanges. The medium range attraction is present in QOPEP, which is usually parametrized in term of $\sigma$ meson exchange. In this quark pion coupling model, the medium range attraction originates from exchange of quarks from the two different nucleons.

The qualitative characteristics of QOPEP are found to be very similar to the Paris meson exchange potential in both central and tensor channels.

Compared with the more sophisticated Resonating Group calculations, this local potential model sacrificed the non-local interaction effects for a more transparent view of the interaction process. Based on the success of the Heitler-London method in the prediction of the potentials between two hydrogen atoms[17], we hope the this average of non-localities does not affect the main conclusion of this study. One would expect that the $NN$ interaction is more complex than the exchange of a pion by a pair of quarks. But the present calculation shows that it could be a very important part of the $NN$ interaction process.

The authors wish to thank Drs. Benoit Loiseau, Manfred Gari for many valuable comments and a critical reading of the manuscript, and Dr. V.I. Kukulin for discussions. One of us (K.H.) would like to thank the Dept. of Physics and Math. Physics, University of Adelaide for the kind hospitality extended to him during several visits in the last years. This work was supported by the Australian Research Council.

# Appendix: Proofs for Substitution Rules 11–13

The proofs for rules 1–10 are given in ref. [5]. Here we give the proofs for rules 11, 12 and 13. This is done by comparing matrix elements in both quark and nucleon bases.

For rule 11, consider the spin–isospin matrix element in the quark level,

$$Q = < \chi_{m_s',m_t'} | \sigma_1^i \sigma_3^j \tau_1^a \tau_3^b | \chi_{m_s,m_t} >, \tag{A.1}$$

where $\chi_{m_s,m_t}$ is given by eq.(2.3). The products of singlet and triplet spin isospin parts w.r.t. the first pair of quarks are usually denoted as $\rho$ and $\lambda$ components of $\chi_{m_s,m_t}$. Hence eq.(2.3) can be rewritten as

$$\chi_{m_s,m_t} = \frac{1}{\sqrt{2}} \left[ \eta^\rho(m_s)\varphi^\rho(m_t) + \eta^\lambda(m_s)\varphi^\lambda(m_t) \right]. \tag{A.2}$$

where $\eta$ is the spin wave function and $\varphi$ the isospin wave function. The matrix element $Q$ can then be expressed as

$$\begin{aligned} Q = \tfrac{1}{2} \big[ & < \eta^\rho(m_s') | \sigma_1^i \sigma_3^j | \eta^\rho(m_s) > < \varphi^\rho(m_t') | \tau_1^a \tau_3^b | \varphi^\rho(m_t) > \\ & + < \eta^\lambda(m_s') | \sigma_1^i \sigma_3^j | \eta^\lambda(m_s) > < \varphi^\lambda(m_t') | \tau_1^a \tau_3^b | \varphi^\lambda(m_t) > \\ & + < \eta^\rho(m_s') | \sigma_1^i \sigma_3^j | \eta^\lambda(m_s) > < \varphi^\rho(m_t') | \tau_1^a \tau_3^b | \varphi^\lambda(m_t) > \\ & + < \eta^\lambda(m_s') | \sigma_1^i \sigma_3^j | \eta^\rho(m_s) > < \varphi^\lambda(m_t') | \tau_1^a \tau_3^b | \varphi^\rho(m_t) > \big]. \end{aligned} \tag{A.3}$$

Since spin and isospin wave functions have identical structures, it suffices to discuss the isospin matrix elements only. $Q$ involves four types of matrix elements

$$\begin{aligned} Q_1 &= < \varphi^\rho(m_t') | \tau_1^a \tau_3^b | \varphi^\rho(m_t) >, \\ Q_2 &= < \varphi^\lambda(m_t') | \tau_1^a \tau_3^b | \varphi^\lambda(m_t) >, \\ Q_3 &= < \varphi^\lambda(m_t') | \tau_1^a \tau_3^b | \varphi^\rho(m_t) >, \\ Q_4 &= < \varphi^\rho(m_t') | \tau_1^a \tau_3^b | \varphi^\lambda(m_t) > . \end{aligned} \tag{A.4}$$

To evaluate $Q_1 - Q_4$ it is helpful to express $\varphi$ as linear combination of products of the state of the pair (12) and that of the third quark. Let $\xi_{t_{12},m_{12}}$ denote the isospin states $(t_{12}, m_{12})$ of the quark pair (12), i.e.,

$$\xi_{0,0} = \tfrac{1}{\sqrt{2}}(ud - du),$$

$$\xi_{1,-1} = dd,$$

$$\xi_{1,0} = \frac{1}{\sqrt{2}}(ud + du),$$

$$\xi_{1,1} = uu. \tag{A.5}$$

Then $\varphi$ can be decomposed as the following

$$\varphi^{\rho}(\tfrac{1}{2}) = \frac{1}{\sqrt{2}}(|ud> - |du>)|u> = \xi_{0,0}|u>,$$

$$\varphi^{\rho}(\tfrac{-1}{2}) = \frac{1}{\sqrt{2}}(|ud> - |du>)|d> = \xi_{0,0}|d>,$$

$$\varphi^{\lambda}(\tfrac{1}{2}) = \frac{1}{\sqrt{6}}(|udu> + |duu> - 2|uud>) = \frac{1}{\sqrt{3}}(\xi_{1,0}|u> - \sqrt{2}\xi_{1,1}d>),$$

$$\varphi^{\lambda}(\tfrac{-1}{2}) = \frac{1}{\sqrt{6}}(|udd> + |dud> - 2|ddu>) = \frac{1}{\sqrt{3}}(\xi_{1,0}|d> - \sqrt{2}\xi_{1,1}u>). \tag{A.6}$$

Using these decompositions and the properties of $\tau_1^a$ acting on $\xi_{t_{12},m_{12}}$ and $\tau_3^b$ on $u$ or $d$, such as $\tau_1^x\xi_{0,0} = \frac{1}{\sqrt{2}}(\xi_{1,-1} - \xi_{1,1})$ and $\tau_3^x|u> = |d>$ etc., one gets

$$Q_1 = 0,$$

$$Q_2 = \frac{-2}{3}\delta_{ab},$$

$$Q_3 = \frac{1}{\sqrt{3}}(\delta_{ab} + i\epsilon_{abr}\tau_N^r),$$

and

$$Q_4 = Q_3^{\dagger} = \frac{1}{\sqrt{3}}(\delta_{ab} - i\epsilon_{abr}\tau_N^r). \tag{A.7}$$

Taking into account the spin part, one finds for $Q$

$$Q = \frac{5}{9}\delta_{ij}\delta_{ab} - \frac{1}{3}\epsilon_{ijq}\epsilon_{abr}\sigma_N^q\tau_N^r. \tag{A.8}$$

The extra factor of 6 in rule 11 comes from the summation over 6 quark pairs.

Rules 12 and 13 can be obtained by simple algebraic manipulations using rules 1-11. For rule 12 one can write,

$$\sum_{n\neq m\neq l=1}^{3} \sigma_n^i\sigma_m^j\sigma_l^k\tau_n^a\tau_m^b = \sum_{n\neq m=1}^{3} \sigma_n^i\sigma_m^j\tau_n^a\tau_m^b(\sigma_N^k - \sigma_n^k - \sigma_m^k), \tag{A.9}$$

and then uses rules 1-11 for the three terms. Similar procedure works for rule 13 but the algebra is more tedious,

$$\sum_{n\neq m\neq l=1}^{3} \sigma_n^i\sigma_m^j\sigma_l^k\tau_n^a\tau_m^b\tau_l^c = \sum_{n\neq m=1}^{3} \sigma_n^i\sigma_m^j\tau_n^a\tau_m^b(\sigma_N^k - \sigma_n^k - \sigma_m^k)(\tau_N^c - \tau_n^c - \tau_m^c). \tag{A.10}$$

Then rules 1-12 can be applied to the nine terms above.

Table 1. *Substitution Rules* for Spin–isospin matrix elements. Operators in the left column are on the quark basis, the right column are the corresponding nucleon operators. The indices $n, m, l$ denote quarks, $i, j, k$ and $a, b, c$ label the vector components of $\sigma$ and $\tau$ respectively.

| | *operators on quarks* | *operators on nucleon* |
|---|---|---|
| 1) | $\sum_{n=1}^{3} 1_n$ | $3$ |
| 2) | $\sum_{n=1}^{3} \sigma_n^i$ | $\sigma_N^i$ |
| 3) | $\sum_{n=1}^{3} \tau_n^a$ | $\tau_N^a$ |
| 4) | $\sum_{n=1}^{3} \sigma_n^i \tau_n^a$ | $\frac{5}{3}\sigma_N^i \tau_N^a$ |
| 5) | $\sum_{n\neq m=1}^{3} \sigma_n^i \sigma_m^j$ | $-2\delta_{ij}$ |
| 6) | $\sum_{n\neq m=1}^{3} \sigma_n^i \tau_m^a$ | $-\frac{2}{3}\sigma_N^i \tau_N^a$ |
| 7) | $\sum_{n\neq m=1}^{3} \sigma_n^i \sigma_m^j \tau_n^a$ | $\frac{2}{3}\delta_{ij}\tau_N^a$ |
| 8) | $\sum_{n\neq m\neq l=1}^{3} \sigma_n^i \sigma_m^j \tau_l^a$ | $-\frac{10}{3}\delta_{ij}\tau_N^a$ |
| 9) | $\sum_{n\neq m\neq l=1}^{3} \sigma_n^i \sigma_m^j \sigma_l^k$ | $-2(\delta_{ij}\sigma_N^k + \delta_{jk}\sigma_N^i + \delta_{ki}\sigma_N^j)$ |
| 10) | $\sum_{n\neq m\neq l=1}^{3} \sigma_n^i \sigma_m^j \sigma_l^k \tau_l^a$ | $-\frac{10}{3}\delta_{ij}\sigma_N^k\tau_N^a + \frac{2}{3}\delta_{jk}\sigma_N^i\tau_N^a + +\frac{2}{3}\delta_{ki}\sigma_N^j\tau_N^a$ |
| 11) | $\sum_{n\neq m=1}^{3} \sigma_n^i \sigma_m^j \tau_n^a \tau_m^b$ | $\frac{10}{3}\delta_{ij}\delta_{ab} - 2\epsilon_{ijq}\epsilon_{abr}\sigma_N^q\tau_N^r$ |
| 12) | $\sum_{n\neq m\neq l=1}^{3} \sigma_n^i \sigma_m^j \sigma_l^k \tau_n^a \tau_m^b$ | $\frac{2}{3}\delta_{ab}(5\delta_{ij}\sigma_N^k - \delta_{jk}\sigma_N^i - \delta_{ki}\sigma_N^j) - 2\epsilon_{ijk}\epsilon_{abr}\tau_N^r$ |
| 13) | $\sum_{n\neq m\neq l=1}^{3} \sigma_n^i \sigma_m^j \sigma_l^k \tau_n^a \tau_m^b \tau_l^c$ | $\frac{10}{3}(\delta_{ij}\delta_{ab}\sigma_N^k\tau_N^c + \delta_{jk}\delta_{bc}\sigma_N^i\tau_N^a + \delta_{ki}\delta_{ca}\sigma_N^j\tau_N^b)$ $-2\epsilon_{ijk}\epsilon_{abc} - \frac{2}{3}\left[\delta_{ab}\tau_N^c(\delta_{ik}\sigma_N^j + \delta_{kj}\sigma_N^i)\right.$ $\left.+\delta_{ca}\tau_N^b(\delta_{ij}\sigma_N^k + \delta_{jk}\sigma_N^i) + \delta_{bc}\tau_N^a(\delta_{ij}\sigma_N^k + \delta_{ik}\sigma_N^j)\right]$ |

Table 2. Radial Integrals. The definitions of the integrals are given in section 3.3, where the functions $F_S(x)$, $F_T(x)$ and $F_0$ are discussed in detail. The coupling constant $G_0$ is given in eq.(2.19).

| | *Direct Integrals* | *Exchange Integrals* |
|---|---|---|
| *Central* | $R^S_{36} = R^S_{14} = R^S_{34} = G_0 F_S(R)$<br>$R^S_{12} = R^S_{23} = G_0 F_0$ | $R^{eS}_{36} = R^{eS}_{14} = R^{eS}_{34} = -G_0 F_0\, e^{-\frac{1}{2}\beta^2 R^2}$<br>$R^{eS}_{12} = R^{eS}_{23} = -G_0 F_0\, e^{-\frac{1}{2}\beta^2 R^2}$ |
| | $Q^S_{36} = Q^S_{12} = -\frac{3}{4} G_0\, e^{-\frac{1}{2}\beta^2 R^2} F_0$<br>$Q^S_{34} = Q^S_{23} = -\frac{3}{4} G_0\, e^{-\frac{1}{2}\beta^2 R^2} F_S(\frac{R}{2})$<br>$Q^S_{14} = -\frac{3}{4} G_0\, e^{-\frac{1}{2}\beta^2 R^2} F_S(R)$ | $Q^{eS}_{36} = \frac{3}{4} G_0\, e^{-\beta^2 R^2} F_S(R)$<br>$Q^{eS}_{34} = Q^{eS}_{23} = \frac{3}{4} G_0\, e^{-\beta^2 R^2} F_S(\frac{R}{2})$<br>$Q^{eS}_{14} = Q^{eS}_{12} = \frac{3}{4} G_0\, e^{-\beta^2 R^2} F_0$ |
| *Tensor* | $R^T_{ij} = \begin{cases} = G_0 F_T(R), & i\epsilon(123) \text{ and } j\epsilon(456) \\ = 0, & (ij)\epsilon(123) \text{ or } (ij)\epsilon(456) \end{cases}$ | $R^{eT}_{ij} = 0$, *for all* $(ij)$ |
| | $Q^T_{36} = Q^T_{12} = 0$<br>$Q^T_{34} = Q^T_{23} = -\frac{9}{4} G_0\, e^{-\frac{1}{2}\beta^2 R^2} F_T(\frac{R}{2})$<br>$Q^T_{14} = -\frac{9}{4} G_0\, e^{-\frac{1}{2}\beta^2 R^2} F_T(R)$ | $Q^{eT}_{36} = \frac{9}{4} G_0\, e^{-\beta^2 R^2} F_T(R)$<br>$Q^{eT}_{34} = Q^{eT}_{23} = \frac{9}{4} G_0\, e^{-\beta^2 R^2} F_T(\frac{R}{2})$<br>$Q^{eT}_{14} = Q^{eT}_{12} = 0$ |

# References


[1] R.Machleidt, K.Holinde and Ch.Elster, Phys. Rep. 149(1987)1

[2] W.N.Cottingham, et al., Phys. Rev.D8 (1973) 800
M.Lacombe, et al. Phys. Rev.C21 (1980) 861

[3] M.M.Nagels, T.A.Rijken, and J.J. de Swart, Phys. Rev.D17 (1978)768, D15 (1977)2547, and D12 (1975)744

[4] A.W.Thomas and K.Holinde, Phys. Rev. Lett.63 (1989) 2025
K.Holinde and A.W.Thomas, Phys. Rev. C42 (1990) R1195
S.Deister et al., Few-Body Systems 10(1991) 1

[5] K.Holinde, Nucl. Phys. A415 (1984) 477

[6] C.S.Warke and R.Shanker, Phys. Rev. C21 (1980) 2643

[7] M.Oka and K.Yazaki, Int.Rev.Nucl.Phys. 1(1984)489, ed. W.Weise
S.Takeuchi et al., Nucl. Phys. A405 (1989) 777

[8] A. De Rújula, Howard Georgi, and S.L.Glashow, Phys. Rev. D12(1975)147

[9] R. Vinh Mau, C. Semay, B. Loiseau, and M. Lacome, Phys. Rev. Lett. 67 (1991)1392

[10] R.S.Willey, Phys. Rev. D18 (1978) 270

[11] A.W.Thomas, Advances in Nuclear Physics 13 (1983) 1
G.E.Brown and M. Rho, Phys. Lett. B82 (1979) 383

[12] A.Faessler and F.Fernandez, Phys. Lett. B124 (1983) 145
A.Faessler et al., Nucl. Phys. A402 (1983) 555
K.Bräuer et al., Nucl. Phys. A507 (1990) 599, Z.Phys. A320 (1985)609
F.Fernandez, Phys. Lett. B188 (1987) 314

[13] F.Fernandez and E.Oset, Nucl. Phys. A455 (1986) 720

[14] K.Shimizu, Phys. Lett. B148 (1984) 418

[15] I.T. Obukhovsky and A.M. Kusainov, Phys. Lett. B238 (1990) 142

[16] D.Liberman, Phys. Rev. D16 (1977) 1542

[17] J.C.Slater, *Quantum Theory of Molecules and Solids*, Vol.1 (McGraw-Hill, 1963)

[18] R.P.Feynman, M.Kislinger and F. Ravndal, Phys. Rev.D3 (1971) 2706

[19] F.E.Close, *An Introduction to Quarks and Partons* (Academic Press, 1979)

[20] D.Flamm and F.Schöberl, *Introduction to the quark model of elementary particles* (Gordon and Breach, 1982)

[21] M.Swift, Ph.D dissertation, University of Adelaide, 1992

[22] P.D.Morley, D.L.Pursey and S.A.Williams,Phys.Rev.C42(1990)2698

## FIGURE CAPTIONS

FIG.1. Diagrammatic representation of the seven terms in eqs.(3.4a) and (3.4b).

FIG.2. Total central and tensor potentials for various $NN$ states.
*solid line* : full QOPEP, *dashed line* : OPEP for point nucleons, *dotted line* : OPEP with a monopole form factors with a cut-off mass of 700 MeV. *dash dotted line* : the corresponding components of the Paris potential; where in fig.1b the *dash dot dot dot line* is for its (S=0, T=1) configuration.

FIG.3. Contribution from various terms of fig.1 (eqs.(3.4a) and (3.4b)).
*Solid line* : fig.1a ($9V_{36}^{(nqc)}$), *dotted line* : fig.1b ($V_{36}^{(qc)}$), *dashed line* : fig.1c ($4V_{14}^{(qc)}$), *dash dot line* : fig.1d,f ($4V_{34}^{(qc)}$), *dash dot dot dot line* : fig.1e ($4V_{12}^{qc}$), *long dashed line* : fig.1g $[6(V_{12}^{(nqc)} - V_{12}^{(\sigma)})]$.

FIG.4. Effects of finite pion size.
*solid line* : full QOPEP, *dashed line* : QOPEP with a square root form factor for quark-pion vertex with a cut-off mass 1.5 GeV, *dash dotted line* : QOPEP with a monopole form factor for quark-pion vertex with a cut-off mass 1.5 GeV, *dotted line* : QOPEP without the contact terms in $v_s$ in equation (2.20).

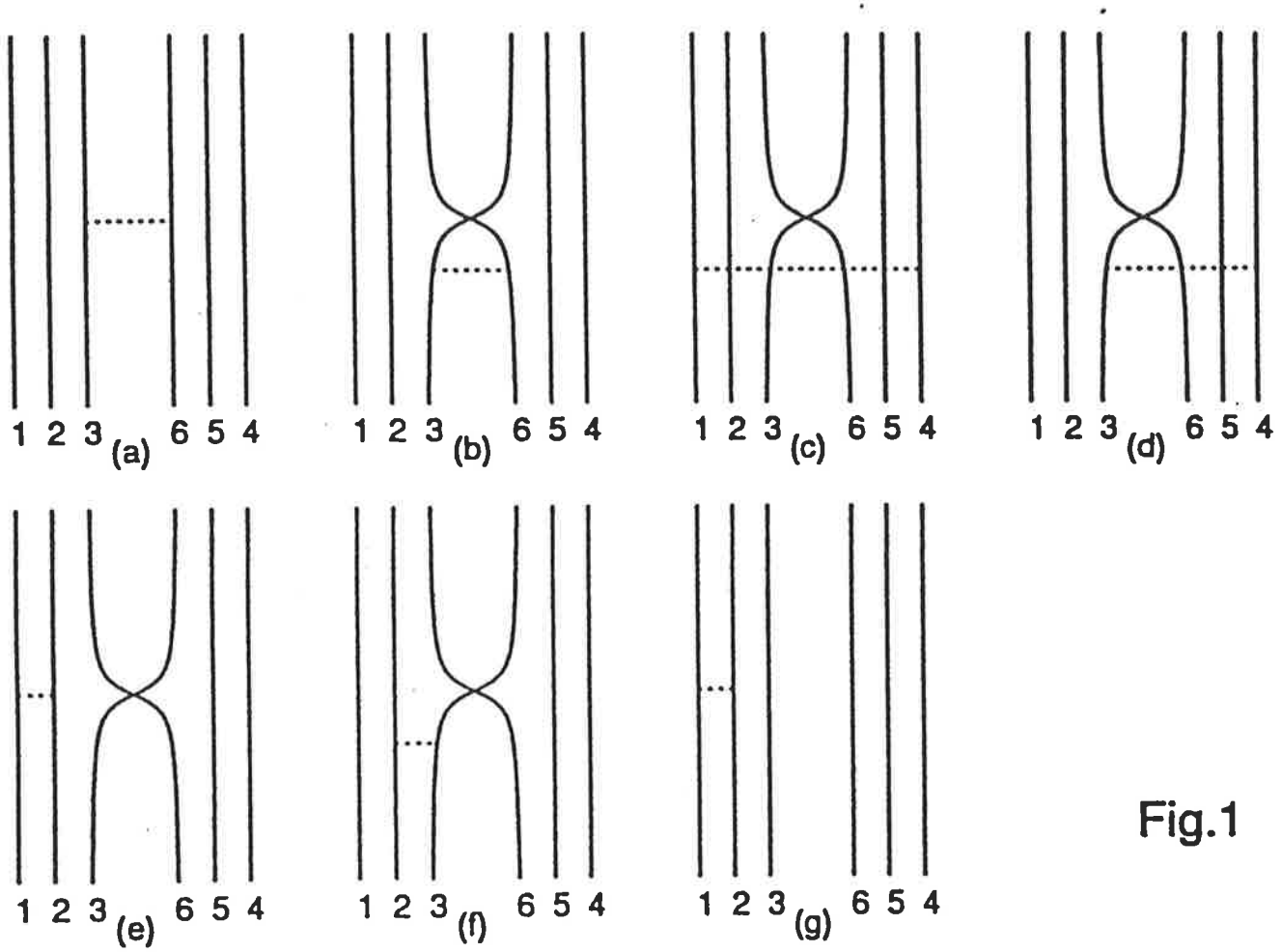


Fig.1

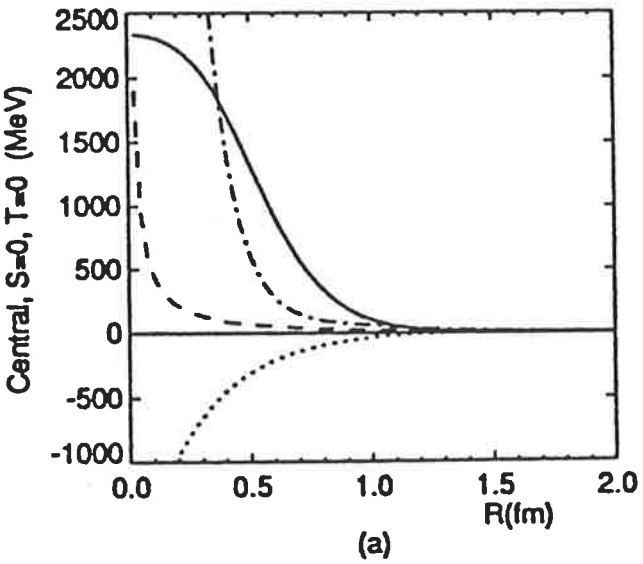
Central, S=0, T=0 (MeV)
2500
2000
1500
1000
500
0
-500
-1000
0.0
0.5
1.0
1.5
2.0
R(fm)

(a)

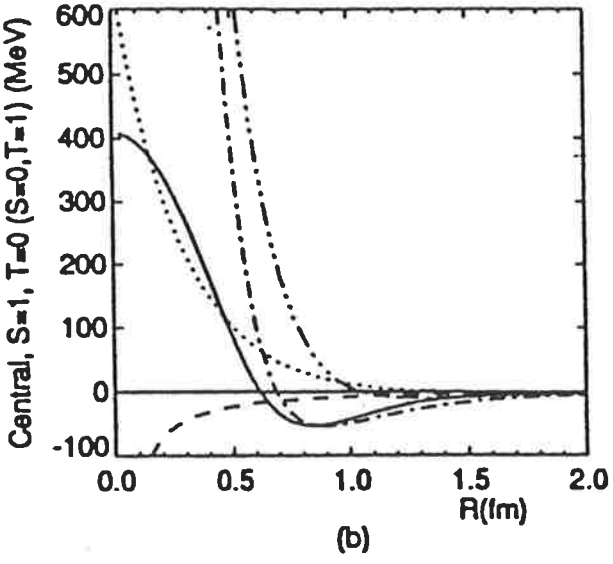
Central, S=1, T=0 (S=0,T=1) (MeV)
600
500
400
300
200
100
0
-100
0.0
0.5
1.0
1.5
2.0
R(fm)

(b)

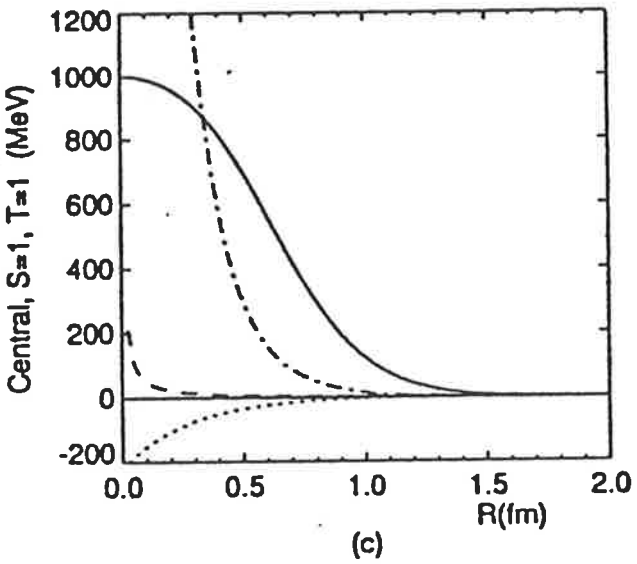
Central, S=1, T=1 (MeV)
1200
1000
800
600
400
200
0
-200
0.0
0.5
1.0
1.5
2.0
R(fm)

(c)

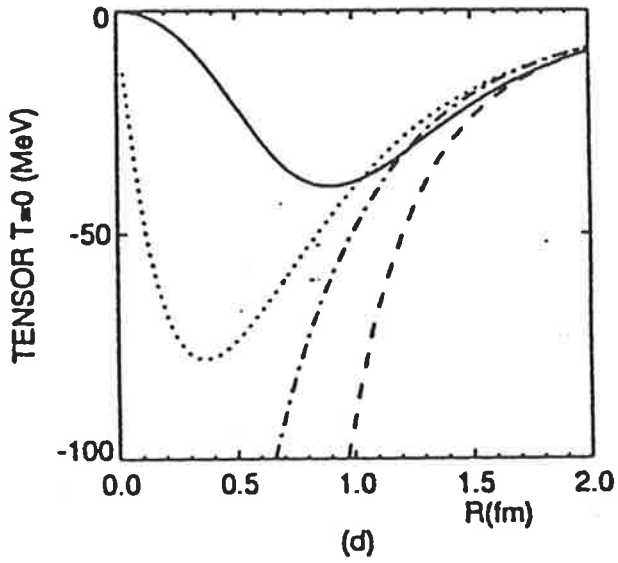
TENSOR T=0 (MeV)
0
-50
-100
0.0
0.5
1.0
1.5
2.0
R(fm)

(d)

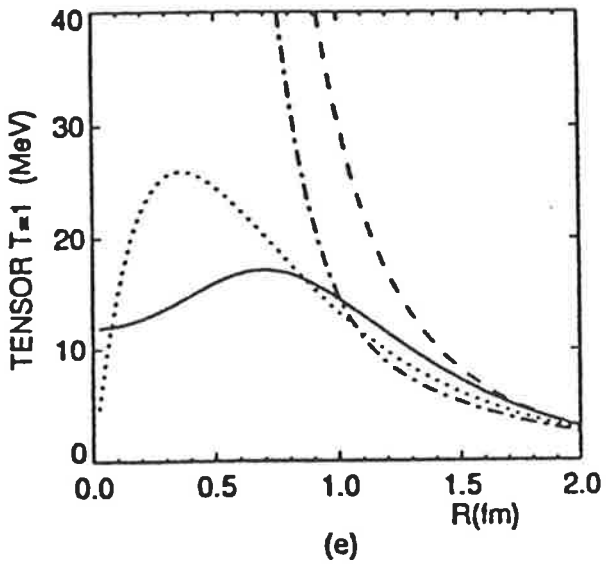
TENSOR T=1 (MeV)
40
30
20
10
0
0.0
0.5
1.0
1.5
2.0
R(fm)

(e)

Fig.2

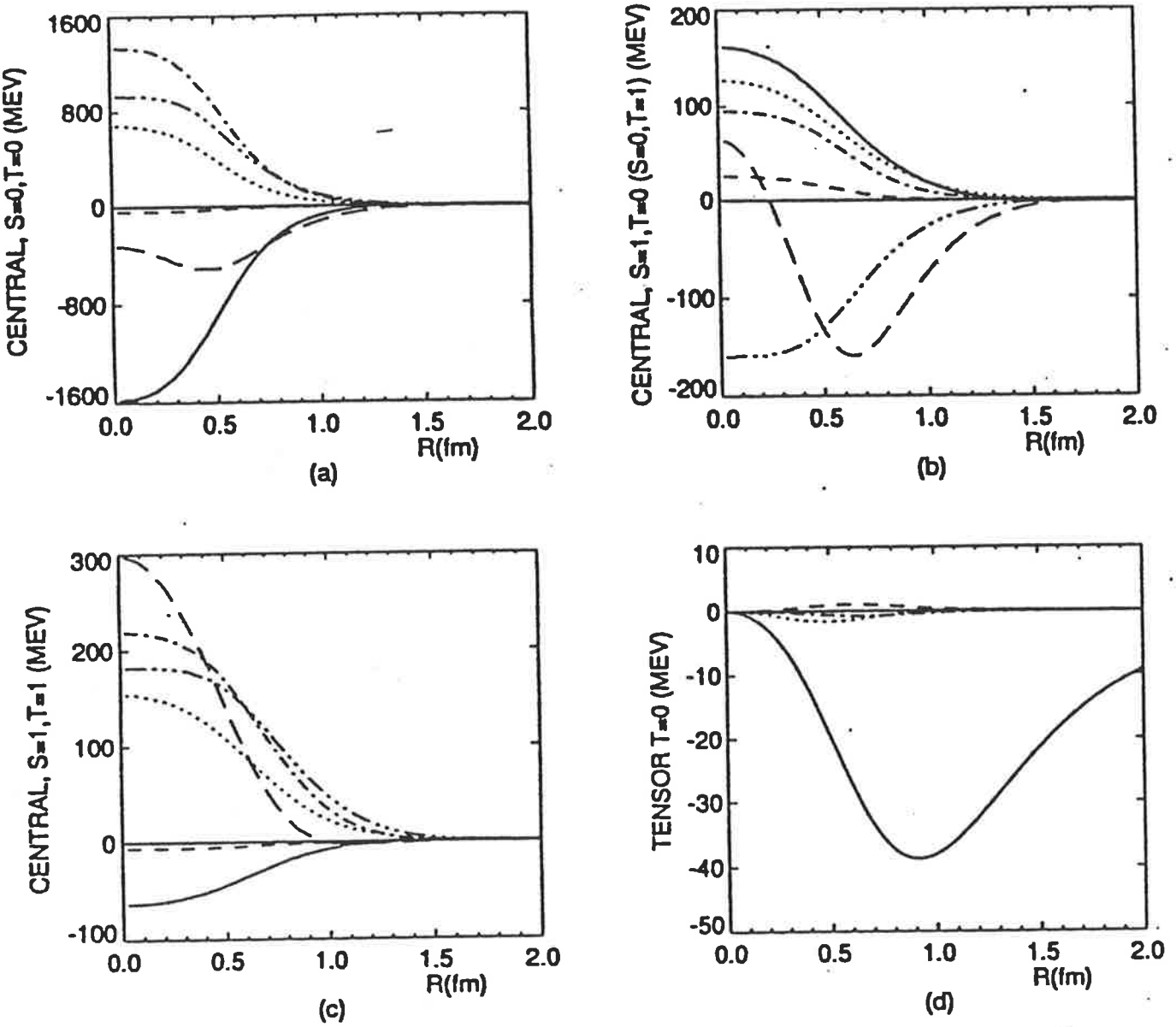
CENTRAL, S=0,T=0 (MEV)
1600
800
0
-800
-1600
0.0
0.5
1.0
1.5
2.0
R(fm)
(a)
CENTRAL, S=1,T=0 (S=0,T=1) (MEV)
200
100
0
-100
-200
0.0
0.5
1.0
1.5
2.0
R(fm)
(b)
CENTRAL, S=1,T=1 (MEV)
300
200
100
0
-100
0.0
0.5
1.0
1.5
2.0
R(fm)
(c)
TENSOR T=0 (MEV)
10
0
-10
-20
-30
-40
-50
0.0
0.5
1.0
1.5
2.0
R(fm)
(d)
TENSOR T=1 (MEV)
20
10
0
-10
0.0
0.5
1.0
1.5
2.0
R(fm)
(e)

Fig.3

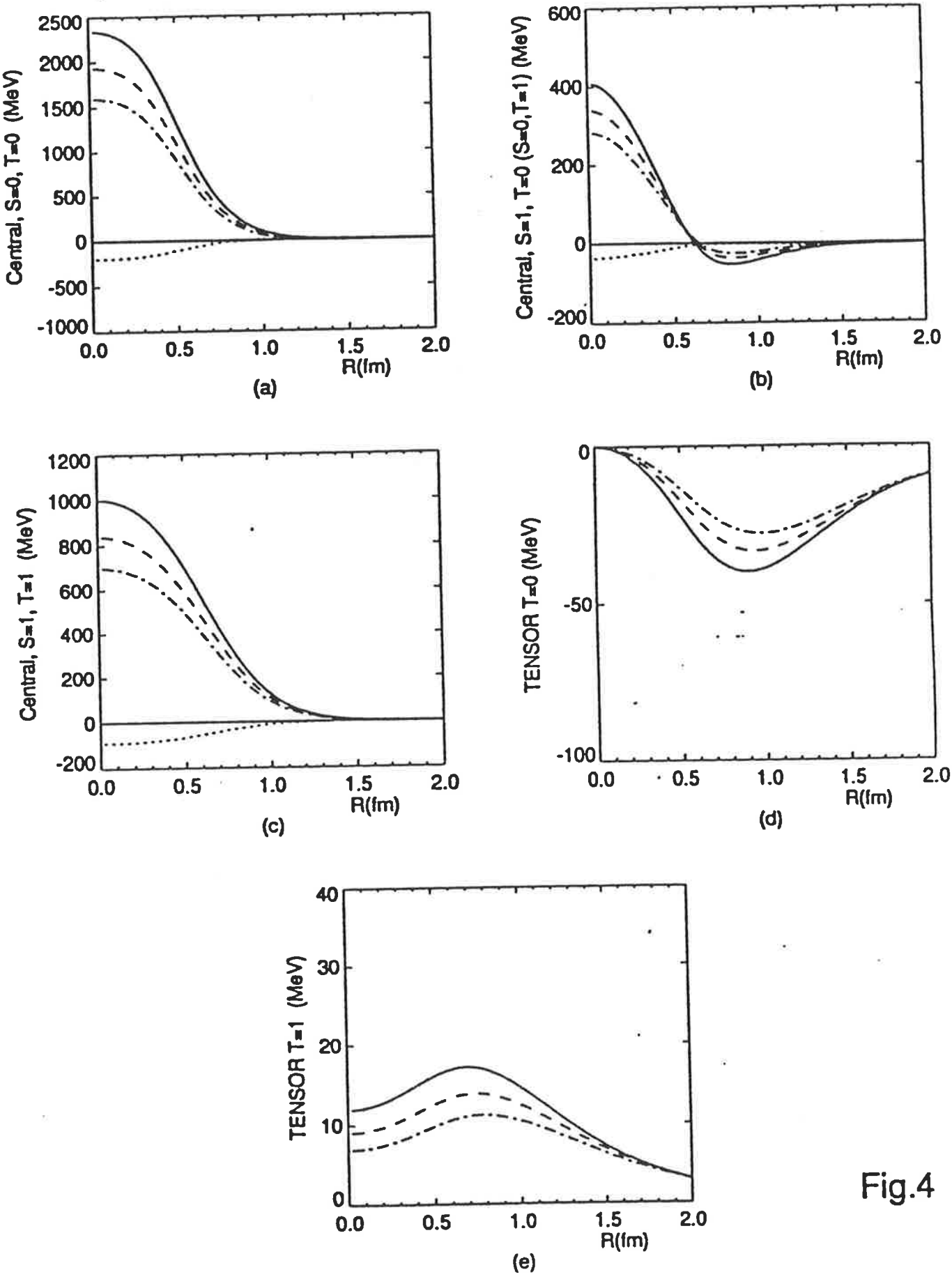
Central, S=0, T=0 (MeV)
2500
2000
1500
1000
500
0
-500
-1000
0.0
0.5
1.0
1.5
2.0
R(fm)
(a)
Central, S=1, T=0 (S=0,T=1) (MeV)
600
400
200
0
-200
0.0
0.5
1.0
1.5
2.0
R(fm)
(b)
Central, S=1, T=1 (MeV)
1200
1000
800
600
400
200
0
-200
0.0
0.5
1.0
1.5
2.0
R(fm)
(c)
TENSOR T=0 (MeV)
0
-50
-100
0.0
0.5
1.0
1.5
2.0
R(fm)
(d)
TENSOR T=1 (MeV)
40
30
20
10
0
0.0
0.5
1.0
1.5
2.0
R(fm)
(e)

Fig.4